Representation, Modeling, Data Development and Maintenance of Appropriate Protective Relaying Functions in Large Scale Transient Stability Simulations

Final Project Report

S-66

Power Systems Engineering Research Center

Empowering Minds to Engineer
the Future Electric Energy System

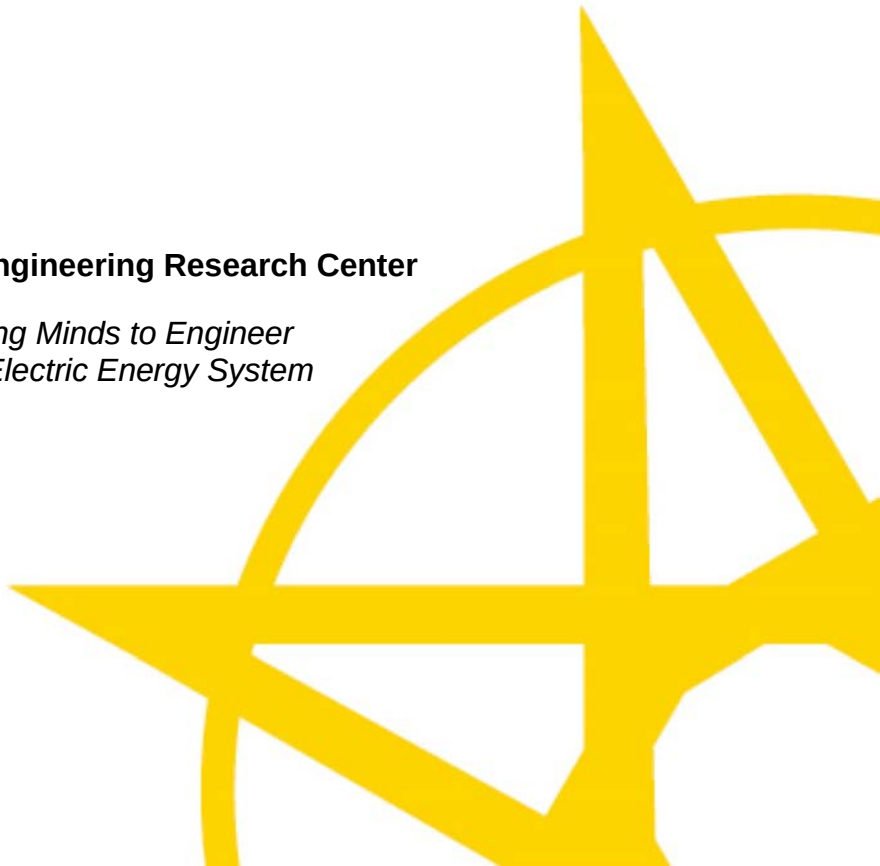

Representation, Modeling, Data Development and Maintenance of Appropriate Protective Relaying Functions in Large Scale Transient Stability Simulations

Final Project Report

Project Team
Vijay Vittal, Project Leader
Arizona State University

Saeed Lotfifard
Anjan Bose
Washington State University

Graduate Students
Mojdeh Khorsand
Arizona State University

Iman Kiaei
Washington State University

PSERC Publication 17-05

September 2017

For information about this project, contact

Vijay Vittal
Arizona State University
School of Electrical, Computer, and Energy Engineering
P.O. BOX 875706
Tempe, AZ 85287-5706
Phone: 480-965-1879
Fax: 480-727-2052
Email: Vijay.Vittal@asu.edu

Power Systems Engineering Research Center

The Power Systems Engineering Research Center (PSERC) is a multi-university Center conducting research on challenges facing the electric power industry and educating the next generation of power engineers. More information about PSERC can be found at the Center's website: http://www.pserc.org.

For additional information, contact:

Power Systems Engineering Research Center
Arizona State University
527 Engineering Research Center
Tempe, Arizona 85287-5706
Phone: 480-965-1643
Fax: 480-727-2052

Notice Concerning Copyright Material

Acknowledgements

The work described in this report was sponsored by the Power Systems Engineering Research Center (PSERC).

The authors thank industry collaborators including Mahendra Patel (EPRI, mpatel@epri.com), Anish Gaikwad (EPRI, agaikwad@epri.com), Brian Keel (SRP, brian.keel@srpnet.com), Jay Giri (Alstom Grid, jay.giri@ge.com), Daniel Houghton (APS, daniel.haughton@aps.com), Jianzhong Tong (PJM, jianzhong.tong@pjm.com), Alan Engelmann (ComEd alan.engelmann@comed.com), Bruce Fardanesh (NYPA, bruce.fardanesh@nypa.gov), Mike Koly (Exelon/PECO, john.koly@exeloncorp.com), Curtis Roe (croe@atcllc.com).

Executive Summary

After a major disturbance, the power system response is highly dependent on protection schemes and system dynamics. Improving power systems situational awareness requires accurate and simultaneous modeling of both protection schemes and dynamic characteristics in power systems analysis tools. Historical information and ex-post analysis of blackouts reaffirm the critical role of protective devices in cascading events, thereby reinforcing the necessity to represent protective schemes in transient stability studies. The primary goal of this report is to investigate and examine the importance of modeling protection systems during transient stability studies and to develop systematic techniques to identify and represent critical protective relays in large commercial transient stability software packages. In addition, this report proposes a method to identify the appropriate locations of out-of-step blocking schemes in order to prevent relay mis-operations during unstable power swings. The report is presented in two parts.

Part I: Analytical Approaches for Identification and Representation of Critical Protection Systems in Transient Stability Studies

Part I of the final report on PSERC project S-66 studies the importance of representing protective relays in power system dynamic studies. The results have clearly confirmed the critical nature of accurate protection system modeling within stability studies.

Moreover, Part I of this report proposes a novel method, the minimum voltage evaluation method, to determine the location of the mis-operating relays at the planning phase. Blocking these mis-operating relays, combined with an appropriate islanding scheme, helps avoid a system-wide collapse. The proposed method is tested on data from the Western Electricity Coordinating Council (WECC). A triple line outage of the California-Oregon Intertie (COI) is studied. The electrical center is determined and appropriate out-of-step blocking schemes are identified. The results of this test show that:

- The correct design of out-of-step protective relays and representing these relays in transient stability studies improve the dynamic performance of the power system and reduces the fluctuations in voltage and frequency throughout the system.
- The minimum voltage evaluation method is able to detect the potential mis-operating relays accurately.
- The minimum voltage evaluation method augments and enhances the remedial action scheme (RAS) associated with the California-Oregon Intertie outages. The out-of-step (OOS) blocking scheme based on the proposed method, along with the Northeast/Southeast (NE/SE) separation scheme, provides a proper controlled islanding scheme.
- Assessing the voltage drop is a reliable evaluation method to detect the electrical center of the system. Blocking only the relays, which experience their relay impedance trajectories intersecting their line impedances, is an insufficient strategy and may result in uncontrolled islanding.
- OOS relays have to be designed with great care. Failure to detect all mis-operating relays may result in failure of the islanding scheme and may lead to a system-wide collapse.

Furthermore, Part I of this report presents a systematic method to determine essential relays to be modeled in transient stability studies. Although modeling all of the protective relays within transient stability studies may result in a better estimation of system behavior, representing, updating, and maintaining the protection system data becomes an insurmountable task. Inappropriate or outdated representation of the relays may result in incorrect assessment of the system behavior. The desired approach should identify protective relays that are critical for various operating conditions and contingencies. The proposed strategy is verified as a viable technique based on results obtained from the WECC 179-bus and the IEEE 145-bus test cases while considering various operating states and contingencies. This report shows that:

- The proposed strategy is able to identify all mis-operating relays for various operating conditions and contingencies.
- Modeling only the identified critical protective relays is sufficient to capture system behavior and precludes the need to model all protective relays.

In summary, Part I of this report contributes to the challenges of this topic by studying and clarifying the importance of protective relays modeling in transient stability studies, by presenting a strategy to detect mis-operating relays during unstable power swings, and by proposing a strategy to identify critical protective relays.

Part II: Evaluation of Relay Dynamic Response by Utilizing Co-simulation Platform (PSS/E-CAPE) and a Loss of Excitation Detection Algorithm to Prevent LOE Relay Mis-operation during Power Swing Cycle.

The objective of the work at Washington State University is to assess the transient response of protection system. Based on the literature, most of the catastrophic blackouts in the United States were triggered by unwanted operations of protective relays. Calibrating and testing the relays based on the steady state condition cannot provide the realistic and appropriate vision of the protection system performance during the transient condition. In this project a co-simulation platform is utilized to evaluate the dynamic response of the protective relays. CAPE-Transient Stability (CAPE-TS) module provides an internal interface between CAPE software and PSS/E software.

Transient performance of distance relays and loss of excitation relays as the most utilized protection devices in the power grid are analyzed in the co-simulation platform. Conventional schemes of distance relays and loss of excitation relays are modeled and the mis-operation conditions are investigated. Moreover, the Western Electricity Coordinating Council (WECC) with more than 20000 buses and 3000 generators is modeled in the co-simulation platform. Distance relays are modeled based on the typical settings and their responses are studied during the triple line outage (TLO) of California-Oregon Intertie (COI). It is shown that appropriate modeling and settings of the distance relays equipped with blocking function can enhance the dependability and security of the protection system and prevent catastrophic cascading outages and stop initiating urgent operation of predetermined remedial action schemes (RAS) in the large scale power system.

Besides, some protection schemes were studied to discriminate faulted condition and power swing condition for distance and LOE relays. The wavelet transform method based on the signal

processing technique is studied. In this strategy, the voltage and current signals of the relay terminal are decomposed in to various detail coefficients and it is shown the power swing condition can be detected based on the remarkable difference between the magnitudes of these coefficients.

Furthermore, secure and reliable operation of the synchronous generator as one of the important component in the power system is vital for the entire power system. So the correct operation of LOE relays as the main machine protection relay is important. Thus, in the last section of part II of this report, a novel approach in detecting loss of field condition is proposed. In this technique, the rate of change of the generator angle is calculated in each sampling window. Based on the polarity of this variable and the slip frequency magnitude, LOE contingency is distinguished from power swing. The validation is obtained through different simulation test cases on single machine infinite bus system. The simulation results show that adding the proposed algorithm to the conventional LOE relay prevents mis-operation of the relay and unwanted tripping of the generators.

In summary, Part II of this report studies the transient relay testing in the more realistic environment by utilizing CAPE-PSS/E co-simulation platform. It is shown that transient evaluation of relay performance can provide better vision for system operators of large scale power networks such as WECC system. Then, new free-setting LOE detection scheme is presented and tested to identify LOE condition.

Project Publications:

[1] M. Abdi-Khorsand and V. Vittal, "Modeling Protection Systems in Time-Domain Simulations: A New Method to Detect Mis-operating Relays for Unstable Power Swings," *IEEE Transactions on Power Systems,* vol. 32, no. 4, pp. 2790-2798, Jul. 2017.

[2] M. Abdi-Khorsand and V. Vittal, "Identification of Critical Protection Functions for Time-Domain Simulations," *IEEE Transactions on Power Systems,* submitted Mar. 23, 2017.

[3] I. Kiaei, S.Lotfifard, A. Bose, "Evaluation of Protective Relay Dynamic Response Via a Co-simulation Platform," to be submitted to *IEEE Transactions on Power Delivery*.

Student Theses:

[1] Mojdeh Khorsand Hedman. *Analytical Approaches for Identification and Representation of Critical Protection Systems in Transient Stability Studies*. PhD Dissertation, Arizona State University, Tempe AZ, May 2017.

Part I

Analytical Approaches for Identification and Representation of Critical Protection Systems in Transient Stability Studies

Mojdeh Khorsand
Vijay Vittal

Arizona State University

For information about this project, contact

Vijay Vittal
Arizona State University
School of Electrical, Computer, and Energy Engineering
P.O. BOX 875706
Tempe, AZ 85287-5706
Phone: 480-965-1879
Fax: 480-727-2052
Email: Vijay.Vittal@asu.edu

Power Systems Engineering Research Center

The Power Systems Engineering Research Center (PSERC) is a multi-university Center conducting research on challenges facing the electric power industry and educating the next generation of power engineers. More information about PSERC can be found at the Center's website: http://www.pserc.org.

For additional information, contact:

Power Systems Engineering Research Center
Arizona State University
527 Engineering Research Center
Tempe, Arizona 85287-5706
Phone: 480-965-1643
Fax: 480-727-2052

Notice Concerning Copyright Material

Table of Contents

List of Figures

List of Tables

Nomenclature

Abbreviations

BPA	Bonneville Power Administration
COI	California-Oregon Intertie
FCM	Fuzzy c-means
MILP	Mixed-integer linear programming
NERC	North American Electric Reliability Corporation
NE/SE	northeast/southeast
OOS	Out-of-step
PG&E	Pacific Gas and Electric
PMU	Phasor measurement units
PSLF	Positive Sequence Load Flow
RAS	Remedial action scheme
SCV	Swing center voltage
TRV	Transient recovery voltage
TOWI	Trip on the way in
TOWO	Trip on the way out
UFLS	Under-frequency load shedding
UVLS	Under-voltage load shedding
WECC	Western Electricity Coordinating Council

Indices and Sets

i	Group index
K	Set of transmission lines
k	Transmission line index
k_{from}	*From* bus of line k
k_{to}	*To* bus of line k
m , n	Bus index
N	Set of buses

N_g	Set of generators' buses
r_i	Bus assigned as the reference bus for group i

Parameters

$C_{n,m}^{c}$	Penalty factor for allocation of bus n and m to different groups based on grouping of scenario c
h	Distance relay reach point
$LODF$	Line outage distribution factor
M	Large multiplier
$PTDF_{l,n}^{R}$	Power transfer distribution factor for line l with respect to an injection at bus n and withdrawal at bus R
R	Resistance of transmission line
$T1$	The slope representing *Rdot/R*
x	Reactance of transmission line
Z	Apparent impedance
Z_L	Line impedance
α, β	Scaling factors of objective function
ρ^c	Probability of contingency c

Variables

a	Fraction of length of transmission line
A_R	Acceleration; the rate of change of the slip frequency
E	Generator internal voltage
I	Current
I_x	Real part of current I
I_y	Imaginary part of current I
$I_{3\Phi-RS}$	Fault current over the line for a three-phase fault at bus S
$I_{3\Phi-S}$	Total fault current for a three-phase fault at bus S

l_k^i	Connectivity variable for line k and group i
P_e	Electric power output of the generators
P_m	Mechanical power input of the generators
S	Slip (degrees/second)
S_R	Slip frequency; the rate of change of the angle between the two measurements of the synchrophasor
V	Voltage
$\lvert V_{amin} \rvert$	Minimum voltage magnitude through the transmission line
V_a	Voltage at fraction a of length of transmission line
V_x	Real part of voltage V
V_y	Imaginary part of voltage V
X_n^i	Binary variable for allocation of bus n to group i; note that $X_{r_i}^i = 1$ as each group is assigned a reference bus and that reference bus, r_i, for group i must belong to group i
Z_t	Relay impedance at time t
Z_{Th-S}	The positive-sequence driving point impedance for a fault at bus S
δ	Generator rotor angle
$\delta_{n,m}$	Variable for allocation of buses to groups; $\delta_{n,m} = 1$: bus m and n can be in the same group
θ_L	Transmission line impedance angle
θ_R	Relay trajectory impedance angle
$\lambda_{n,m}$	Variable for allocation of buses to groups; $\lambda_{n,m} = 0$: bus m and n are in the same group

1. Introduction

1.1 Overview

Major blackouts are the result of a single initiating event combined with an inappropriate action or lack of action of essential protective equipment. The single initiating event or equipment failure generally involves aging equipment, a cyber-security attack, an environmental factor (lightning, earthquake, excessive heat, or tree contact), human error, or relay mis-operation. The North American Electric Reliability Corporation (NERC) mandates that the *N*-1 reliability requirement be maintained during power system operations and it must be accounted for during planning as well [1]. To meet this requirement in real-time, operators check system states for potential *N*-1 violations (post-contingency violations) at least once every thirty minutes; this process is known as real-time contingency analysis. If a contingency is detected, the operator must take appropriate action to regain *N*-1 reliability within thirty minutes. This process ensures that the system is able to move from a base-case, pre-contingency setting, survives a single contingency, and then regains *N*-1 reliability [2]-[3].

Ensuring that the system is *N*-1 and *N*-1-1 reliable is not easy as the actual operating state of the system is not always the same as predicted. Therefore, depending upon the state of the system and severity of the event, the system might face an emergency condition, especially during peak load hours. In this stage, if proper automatic control actions or appropriate operator response are not taken fast enough, the initiating failure may cause additional failures and could also result in a cascading outage. As an example, in the case of a transmission line outage, the alternative paths may become overloaded after the initiating contingency leading to dynamic and stability issues. These dynamic issues may cause further mis-operation of system elements resulting in additional outages and imbalance between load and generation. Without preventive and corrective actions, the imbalance between load and generation will lead to acceleration or deceleration of a generator or group of generators, which in turn may cause inappropriate islanding and, ultimately, a blackout. In addition, although in rare situations, two unrelated contingencies might happen sequentially (within a short time difference) or simultaneously. This simultaneous occurrence may increase the speed at which the cascading outage propagates and it is also likely to increase the severity of the outage.

For instance, the major 2003 Italian blackout started with a tree flash over on a tie line between Italy and Switzerland. The automatic breaker control did not reclose the tie line. This initial outage caused an overload on parallel tie lines. While the first outage was still not cleared, another 380 kV tie line connecting Italy and Switzerland, tripped out due to tree contact. This cascading trend continued and, finally, the Italian system lost synchronism with the rest of Europe. The tie lines between Italy and France tripped due to distance relay operation on these lines. The same happened for the 220 kV lines connecting Italy and Austria. In addition, a 380 kV tie line between Italy and Slovenia, tripped due to overload. With a shortage of 6400 MW of power, the frequency dropped rapidly resulting in operation of under-frequency relays of several generating units. Therefore, the entire Italian system collapsed, causing a nationwide blackout [4].

1.2 Instability during contingency conditions

Identifying the initiating events quickly and minimizing the impact of those events is the best way to avoid cascading outages. If the proper corrective actions are not taken quickly, the initial event may lead to system stability issues. The dynamic states leading to system wide collapse are categorized as follows:

Transient angular instability: The initial disturbance can cause load-generation imbalance in a region; due to differences in the rate of change of mechanical and electrical power, the generator rotor angles may deviate in response to the disturbance. This deviation might be followed by loss of synchronism between different groups of generators, which is also known as an out-of-step (OOS) condition. As the region loses synchronism, the relative rotor angles separate, which results in different groupings of generators. The voltage at the electrical center of these groups will then be depressed, resulting in protective relays detecting what is thought to be a fault and, thus, the protective relay systems will trip additional transmission lines. Therefore, all of the electrical paths between the groups of the generators may trip, which can result in islands. While it is preferred to form islands due to the loss of system wide synchronism and the result of generator groupings, those islands must be formed with an appropriate supply and demand balance. With the protective relay systems tripping lines that have depressed voltages at the electrical center, it is unlikely that the resulting islands will have the required load-generation balance. Without taking proper actions, these separations result in unintentional islands with load-generation imbalances that will cause additional generators to trip leading to a cascading outage. These outages happen in the order of a few seconds [4]. Proper OOS protection schemes are essential to avoid system separation at undesired locations. This issue is explained in more detail in section 2.

Small signal instability: In a weakened power system, large power transfers lead to uncontrollable growing electromechanical oscillation on the tie lines. This event also results in the separation of the system into different generator groups. This event takes several to tens of seconds [4].

Voltage instability and collapse: Transient voltage instability is a very fast phenomenon that may result in voltage collapse, especially during peak load conditions.

Without implementing proper control actions, any of these initiating events may lead to separation of the system into several islands. Then, the situation exacerbates due to load-generation imbalance and unforeseen frequency response in the uncontrolled islands. Finally, a point of no return is reached and the cascading events are not manageable. This series of unmanageable failures ultimately leads to a major blackout [4]. Figure 1.1 provides a generic description of grid operations during and after contingencies.

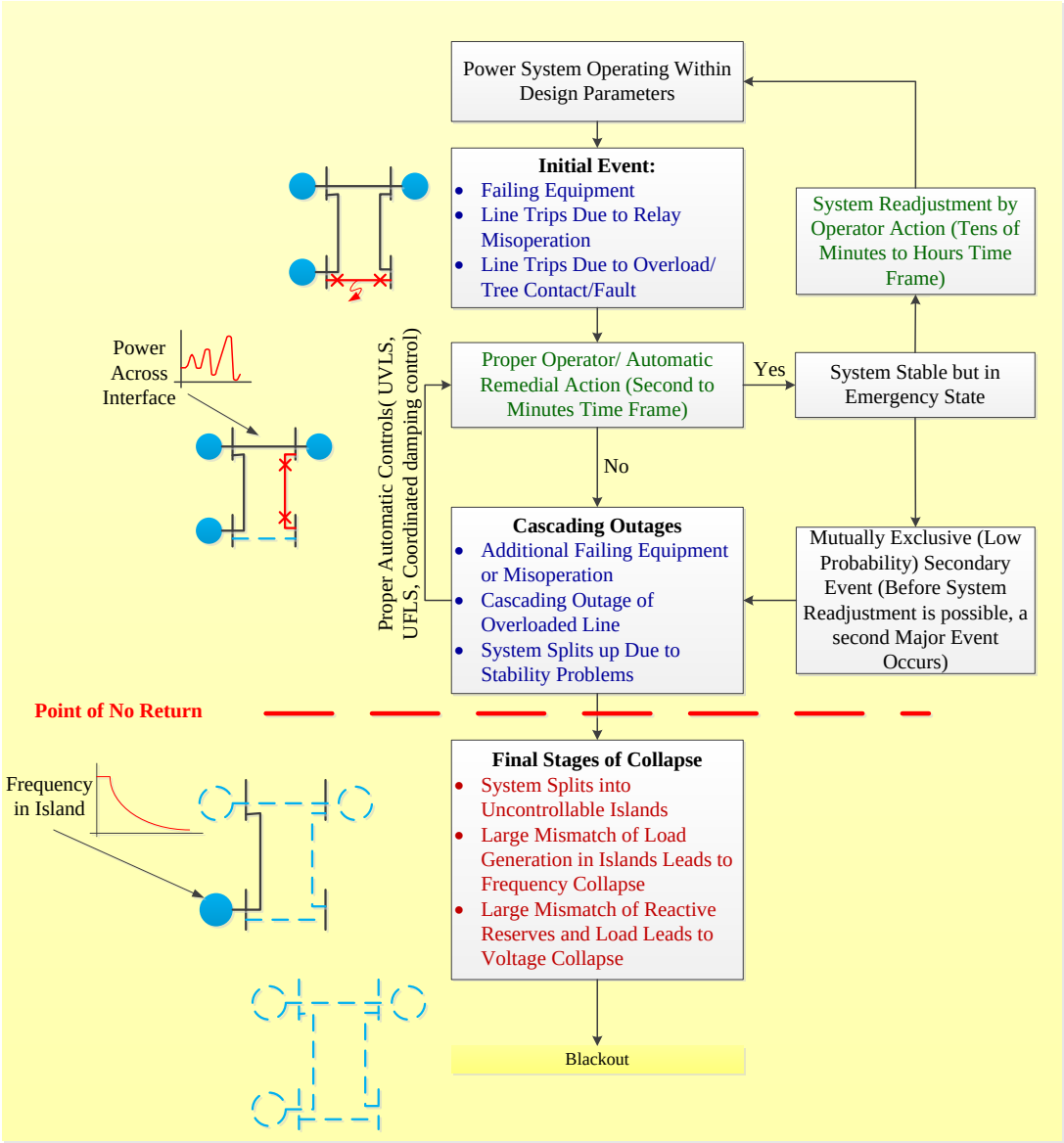

Figure 1.1 General Sequence of Events Leading to Blackout [4]

1.3 Relay mis-operation

Historical information from outages shows that a significant percentage of disturbances are caused by relay mis-operation (also known as hidden failures) [5]-[6]. Although blackouts involve various factors (such as human error, weather related events and device failure), protection systems failure is a critical factor. Hidden failures may occur when the system is under stress after an initial event and may exacerbate the power system state.

Heavily loaded transmission lines cause the apparent impedance characteristic to fall inside zone 3 of the relay setting. Therefore, the relays trip the lines. This tripping happens while no fault is

actually present. As a result, the alternative transmission paths will be overloaded. This process continues, weakens the system, and potentially leads to blackout.

Furthermore, the initiating event may result in a power swing, which can cause the apparent impedance to locate inappropriately within the distance relay characteristic, resulting in a relay mis-operation. Reference [7] discusses relay apparent impedance trajectory during unstable power swing.

Therefore, performing a proper and precise stability study, while modeling protective relays, is essential to find the potential mis-operating relays; using the result of such a study, an appropriate OOS protection scheme can be designed to prevent relay mis-operations.

While modeling all of the protective relays within transient stability studies may result in a better estimation of system behavior, mis-representation of relays or outdated relay models may result in a false assessment of the system behavior. Thus, there is a pressing challenge to not only model protection systems within stability studies in order to get better assessments of system behavior but also identify which subset of protection systems are the most critical to model in order to maintain a practical limitation.

1.4 Scope of work

This project aims to address these real and challenging questions. First, this research proposes a method that accurately finds the potential relay mis-operation locations during a power swing. The proposed method can be implemented during power systems planning studies. Using the results of transient stability planning studies, the proposed method is able to successfully identify the essential locations of OOS blocking relays.

Second, this research introduces a network partitioning method, which successfully identifies the essential distance relays to be modeled in transient stability studies. This network partitioning model uses the result of transient stability studies for identified critical contingencies to specify the most vulnerable distance relays to the unstable power swing in the system. These relays are considered as the critical relays to be modeled in a transient stability study.

The proposed strategies of this research mainly focus on preventing undesirable operations of the protective relays during unstable power swings. Similar strategies can be developed for identifying potential protective relays mis-operations of transmission lines and generators during stable swings.

The rest of this report is organized as follows. A literature review on power swings, protection systems, and stability analysis is presented in section 2. The importance of modeling protective relays within transient stability studies is discussed in section 3. A method to locate electrical centers of the system is presented in section 4. Section 4 also illustrates the results of this proposed method. Section 5 presents the proposed network partitioning model for identifying critical protective relays. Section 5 also demonstrates the results of the proposed network partitioning method. Section 6 is allocated to the conclusions of this report.

2. Power Swings and Out-of-step Protection

Sudden changes in the state of a power system, such as a change in power generation, a large change in load, faults, or transmission line switching, can cause an imbalance between mechanical power input and electrical power output of generation units since the change in mechanical power input is much slower than the change in electrical power output. This mismatch causes an acceleration or deceleration of the generation units. Such disturbances may lead to a change of the generators' rotor angles relative to each other. These changes or oscillations in generator rotor angles impose stable or unstable power flow swings on transmission lines. Power swings might be observed by protective relays as three-phase faults and cause unwanted system wide separation as a result of relay mis-operation. The potential load-generation imbalance in these unintentional islands may lead to frequency drop situations and, eventually, a system wide blackout. Ideally, the system should be separated at the desired points in order to maintain the load-generation balance in each island. To accomplish this separation scheme, out-of-step blocking relays should block the tripping of the transmission lines in which power swings occur. In addition, the out-of-step tripping protective scheme should trip the transmission lines at the proper locations. Although maintaining load-generation balance in each island might seem unrealistic, this goal can be achieved by implementing a proper load-generation shedding plan. This research is aimed at studying the impact of power swings in various protective relays, the importance of including various protective relays in power system dynamic studies, and determining the critical protective relays for power system dynamic studies. Moreover, this research proposes a method that can be implemented to determine the appropriate location for installing OOS blocking relays. Relevant literature is reviewed in this chapter.

2.1 Rotor angle stability and loss of synchronism

A simple two-machine system, which is shown in Figure 2.1, is considered in this subsection in order to study generator behaviors after a disturbance. It is very common to reduce a power system to this two-machine system representation; while such an approximation is frequently useful to replicate the system behavior and performance, it is important to keep in mind such an approach is not an exact equivalent in general. Figure 2.2 shows the electric power-angle curve of one of these equivalent generators. Moreover, the mechanical power input of this equivalent generator, P_m, is shown in this figure.

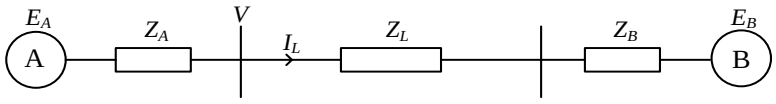

Figure 2.1 One-Line Diagram of a Two-Machine System

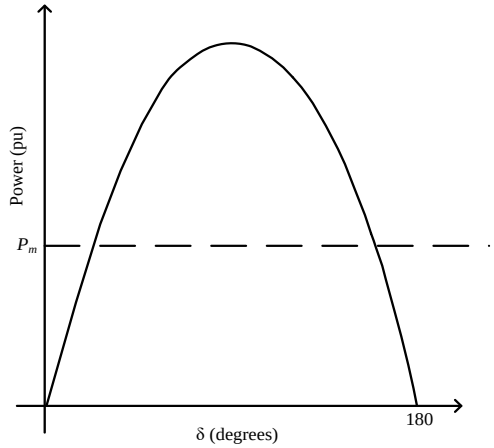

Figure 2.2 Power Angle Curve

After occurrence of a contingency, the transfer capability of the system reduces while the rotor angle remains the same (δ_1) due to inertia. This is shown in Figure 2.3 as the transition between point A and point B. At point B, the electric output power is lower that the mechanical input power (power from the prime mover). This imbalance causes the rotor angle to accelerate till it reaches δ_2, shown by the transition between point B and point C. In Figure 2.3, A_1 represents the kinetic energy of the generator. After the clearing of the fault by the protection system, the transfer capability is improved, which allows the machine to transfer more power at angle δ_2 (shown as the transition between point C and point D in Figure 2.3). At this point, the electric power output is higher than the mechanical power input, which causes the rotor to decelerate. However, the rotor angle continues to increase due to the rotor inertia. If the excess energy (represented by A_1 in Figure 2.3) is not used up before electric power output decreases below the prime mover input, the rotor angle will keep increasing and the machine will lose synchronism with the rest of the system.

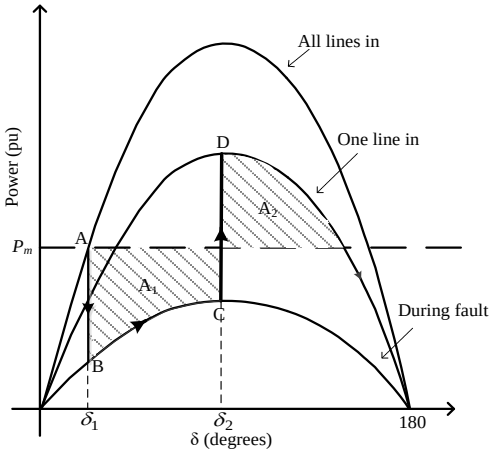

Figure 2.3 Power Angle Curve for Various Network Conditions

In prior literature [8]-[9], it is explained that if the angle reaches the critical value for maintaining stability (commonly considered as 120 degrees) and is still increasing, it is most likely that the

system will not reach the equilibrium (area A_1 is equal to area A_2) and will lose synchronism. The critical angle for maintaining stability changes based upon the system condition and the contingency. However, [8] and [10] explain that the likelihood of recovering from swing, which has exceeded 120 degrees, is marginal. Therefore, 120 degrees is usually accepted as a proper basis for setting out-of-step protection.

2.2 Stable and unstable power swings

In a stable power swing, the power system finds a new stable operational condition with a balance between load and generation. In an unstable swing, the generators' relative rotor angles continue to separate; this almost surely results in no new balance condition being found. Unstable power swing leads to loss of synchronism between different groups of generators in different areas of the system. During loss of synchronism, a generator or group of generators slip poles, which is also referred to as an out-of-step condition. Pole slipping is a condition whereby terminal voltage angles of a generator or a group of generators exceed 180 degrees relative to the rest of the interconnected power system. After loss of synchronism, the areas should be separated quickly to avoid a possible collapse of the entire system. The system should be separated at some locations such that each of the separated areas can maintain a power balance considering the appropriate generation or load shedding plan [8].

Power swings can result in desired or undesired relay operation in the network. The swing impedance characteristic might enter relay impedance zones during a dynamic swing condition of the system resulting in an undesired relay operation. The unwanted relay operation may exacerbate the power system operating conditions and cause unwanted tripping of power system elements and deteriorate the system operating conditions leading to a cascading outage. Therefore, protective relays should be temporarily prohibited from unintentional tripping during stable or unstable dynamic conditions in order to avoid the system being separated at random locations and producing undesired islands. Modern distance relays are usually equipped with blocking functionality to prevent unintentional distance relay operations during stable or unstable power swings. A well-designed protective relaying scheme should differentiate between faults and power swings and block the tripping operation during power swings. In addition, faults occurring during power swings should be recognized by distance relays [11].

The transmission line protection system is required to distinguish line faults from power swings and operate appropriately. The rate of change of the swing impedance is usually used as a metric to differentiate between faults and power swings. During a fault condition, the voltage, current, and load characteristics change from their normal value to the value capable of triggering the relay instantly. However, for a power swing, these values change slowly from the normal value [12]. The basis for this slow change is the fact that it takes time for the rotor angle to advance due to inertia. Therefore, the rate of change of the swing impedance is slow.

There are also several other approaches presented in the literature with the purpose of distinguishing between a power swing and a fault condition. Some of these methods are presented in this chapter.

Relay mis-operations during unstable power swings can cause uncontrolled separation of parts of power systems. Uncontrolled separation during an OOS condition might result in equipment damage, pose a safety concern for utility personnel, and cause cascading outages and the interruption of electricity in larger areas of the power system. Thus, a properly controlled separation scheme is essential to reduce the impacts of the disturbance. A well-designed separation (islanding) scheme should successfully recognize stable swings from unstable swings and initiate the process of separation at predetermined locations at proper values of voltage angle differences.

OOS protection prohibits mis-operation of relays and separates the system at appropriate locations with the goal of minimizing loss of load and maintaining maximum service continuity. Therefore, blocking and tripping are two main functions related to power swings. Blocking prohibits the relays, which are prone to operate during stable or unstable swings, from operating. The OOS blocking function should be accompanied by OOS tripping schemes. This is accomplished with the application of a transfer trip scheme. Moreover, line reclosing should be blocked after the OOS tripping function is invoked [11].

An OOS condition imposes many risks to power systems if the OOS protection is not designed appropriately or malfunctions. In order to maintain system security, OOS conditions should be recognized and mitigated properly. Some of the associated risks of a stable and an unstable power swing are as follows [11]:

- Transient recovery voltage (TRV) causing breaker failure: an OOS condition may impose a TRV challenge to the circuit breaker. The worst case occurs when the voltage angles across the breaker are 180 degrees apart. It is very important for the OOS tripping function to avoid tripping when the angle difference between islands is close to 180 degrees. Tripping during this condition imposes a high amount of stress on the circuit breakers and can cause breaker damage. Appropriate caution should be taken in designing the OOS tripping to avoid breaker failure. There are two different methods of out-of-step tripping: trip on the way in (TOWI) and trip on the way out (TOWO). TOWI trips the line when the swing impedance enters the OOS tripping characteristic. This approach imposes breaker stress as it issues the line tripping signals when the phase angle difference approaches 180 degrees. TOWO trips the line when the swing impedance exits the OOS tripping characteristic. TOWO has the advantage of tripping when the system is close to being in-phase (i.e., the angle difference is reducing). However, TOWI is necessary in some systems in order to prevent intense voltage dips and loss of load [8]. Reference [8] also explains that TOWI is helpful for large systems where the relative movement of the two systems is slow. Moreover, TOWO has the risk of transmission line thermal damage.
- Isolating load and generation: without proper OOS protection scheme, the system may sectionalize into uncontrolled islands. Load-generation imbalance in each island might result in a widespread outage. Therefore, appropriate OOS function and methods to coordinate load and generation shedding should be implemented.
- Equipment damage: transmission disturbances might result in pole slipping of a synchronous generator, which creates thermal and mechanical stress on the generator. These phenomena may cause physical damage and reduce the life of the machine.

- Cascading line tripping: unintentional tripping of transmission lines during stable power swings should be blocked by protective relays equipped with power swing detection features. Undesired line breaker tripping weakens the system and may result in additional line tripping; this series of tripping may cause cascading outages of lines. The NERC standards do not allow such cascading tripping [13]. Therefore, protective relays with proper power swing detection features should be implemented.
- Unwanted generator tripping: the proper separation scheme should be implemented during unstable swings. Failure to trip a line may result in pole slipping of the generator and may cause cascading outages in the system.

Out-of-step protection schemes should be designed to avoid these risks. The fundamental objectives of out-of-step protection systems are [9] and [14]:

- Block tripping at all locations for stable power swings.
- Separate the system during out-of-step conditions.
- Controlled separation in order to maintain the load-generation balance at each separated area considering proper load/generation shedding.
- Block tripping or reclosing at one end of any line, which has tripped because of an out-of-step condition.
- Initiate tripping while the two systems are less than 120 degrees apart in order to reduce breaker stress.
- Minimize detrimental impacts of out-of-step condition by considering the following alternatives:
  - Utilize high-speed relaying.
  - Utilize high-speed excitation system on generators.
  - Equip all generators with loss-of-field relays.
  - Provide sufficient transmission capability.
  - Trip generators on the loss of critical lines.
  - Apply generator braking resistors or insertg series capacitors for critical faults.
  - Utilize fast valving of turbines to control over-speed properly.
  - Utilize independent pole tripping to increase power flow through the fault point and reduce the separation during the fault.

These out-of-step protection requirements are difficult to achieve. Some tradeoffs may be necessary to avoid a blackout. For instance, the system operator may need to curtail some portion of load or generation in order to avoid frequency drop leading to a cascading outage. The utility practice for out-of-step protection is listed in [9], [14], and [15]:

- Implementation of the line relays to initiate out-of-step protection.
- Utilization of generators loss-of-field relays to trip generators during out-of-step conditions.

- Restriction of relay trip sensitivity at higher power factor.
- Blocking the relay tripping at selected locations.
- Blocking the line reclosing after out-of-step tripping.
- Initiating tripping using relays designed for out-of-step tripping.

2.3 Out-of-step protection

Power swings are classified to have a local mode or an inter-area mode. A local mode power swing represents a generator swinging with respect to the rest of the system. Inter-area power swings are the oscillations of a group of generators against other groups. During an inter-area power swing, the protective relays of the transmission lines observe the power swing. During a local mode power swing, the local protective relays, e.g. protective relays of the out-of-step generator and its step-up transformer, observe the power swing. The protective relays, which are involved in local and inter-area power swings, are reviewed separately in the remainder of this section.

2.3.1 Impact of inter-area mode power swings on protection systems

Pole slipping of groups of generators, i.e., 180 degree separation, causes a zero magnitude voltage at the electrical center of the system. At the electrical center, conditions identical to a three-phase short circuit will be observed by the nearby relay, which will trip unless it is blocked from tripping. These relays are the potential locations for OOS blocking relays.

As mentioned before, the separation of the accelerating and decelerating parts of the system should take place at the proper points in order to maintain load-generation balance as much as possible. Figure 2.4 shows a simple system. Although breaker 1 might observe the power swing, this is not a proper separation point; this unintentional separation will cause at least 5 MVA of load shedding due to the lack of available generation capacity. This breaker should be blocked from tripping and the system should be separated at breaker 2 or breaker 3; in this situation, generator B needs to increase its output by 1 MVA and generator A needs to reduce its output by 1 MVA to serve the demand properly.

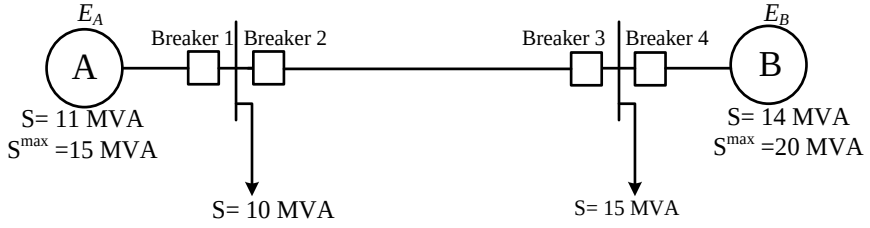

Figure 2.4 Generation and Load Balance during Out-of-Step Protection

Loss of synchronism affects the protective relays of the system. Some of the relays do not respond to the loss of synchronism, while others, such as distance relays, may trip. The out-of-step condition is a balance phenomenon; therefore, the main focus is on phase relaying. In the following

subsections, different types of protective relays are described briefly and the impacts of power swing on these relays are studied.

2.3.1.1 Effects of power swings on overcurrent relays

Overcurrent relays operate if the current measured at the relay location exceeds a predefined value. These relays will be affected by out-of-step conditions. This condition is explained here for the system of Figure 2.5.

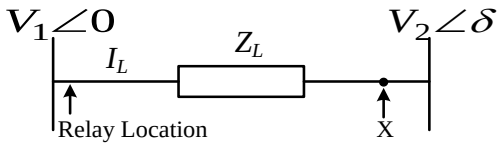

Figure 2.5 Impacts of Out-of-Step Condition on Overcurrent Relay

The overcurrent relay located at the point shown in the Figure 2.5 is designed to protect this line during a fault. The fault current, in case of fault at X, can be calculated as $I_L = V_1 / Z_L$. In the case of a power swing, $\delta = 180$, this current can be calculated as $I_L = 2V_1 / Z_L$ (assuming $V_1 = V_2$). This current is twice of the fault current. Therefore, it can be concluded that the current during the out-of-step condition exceeds the pickup settings of these relays, which causes the relays to respond to the out-of-step condition. In addition, the current during a stable power swing is higher than the normal current; therefore, these relays may trip during a stable power swing. In fact, one of the shortcomings of these protective relays is their potential tripping during a stable power swing [14].

2.3.1.2 Effects of power swings on differential relays

Differential relays respond to the difference between the input and output values of the protected device. These relays measure and compare the quantities (e.g., current) at two points; if these value are different, a fault condition would be detected and the tripping signal will be sent. Existing differential relaying is used for the protection of generators, transformers, buses, and lines. These protective relays do not respond to power swings. During a power swing, the current flows through the power element; therefore, these relays are not triggered by the power swing. If the swing locus is passing through the element, which is protected by differential relays, and tripping is desired, a backup or supplementary relay should be used.

2.3.1.3 Effects of power swings on distance relays

A distance relay measures the electrical distance between the relay location and the fault point. These relays respond to voltage, current, and angles between voltage and current. These quantities can be evaluated in terms of relay impedance, which is proportional to the distance to the fault.

These relays are usually set to trip if a fault occurs within a fractional distance *h* of the line from the relay location (Figure 2.6). This fraction is referred to as the “reach setting”, which means that the relay will trip without any time delay if a fault occurs in this portion of the line. The relays will

trip with a programmed time delay in the case that the fault is beyond the reach point. If a fault occurs at the reach point, the impedance, which can be observed at the relay A, is as follows:

$$Z_R = \frac{V_1}{I_L} = hZ_L \tag{2.1}$$

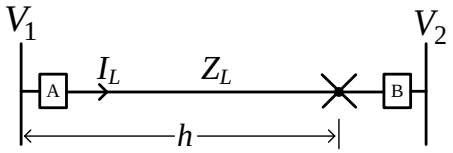

Figure 2.6 Reach Point of Distance Relay

The tripping threshold (without programmed time delay) of such a relay is expressed in (2.2). This equation confirms that if a fault occurs after the reach point, the relay A will not trip without a time delay.

$$Z_R \leq hZ_L \tag{2.2}$$

The tripping criteria of these relays are not dependent on the system operational condition or network structure changes (transmission maintenance scheduling or transmission switching). It is a common practice to set the reach point (distance h) at 80% to 90%. For the faults beyond this point, relay B trips first (relay A trips after a time delay). This practice leads to sequential tripping and helps with relay coordination. However, sequential tripping is slower than simultaneous tripping, which makes sequential tripping undesirable for some transmission lines. In particular, a distance relay may operate falsely depending on the fault impedance, the impedance behind the relay, and the external impedance. Distance relays can be designed with various characteristics, which are shown in Figure 2.7 (a)-(e) [16].

During a fault, the relay will trip the line if the impedance seen by the relay enters the relay impedance characteristic. These relays are one of the most common types of protection systems for the transmission network. The following features should be considered about various distance relay characteristics [16]:

- The impedance relay characteristic is not directional, i.e., trips for the fault behind the relay. If a directional characteristic is desirable, the supervision from a directional unit should be provided.
- The mho relay is inherently directional.
- The reactance characteristic defines the reach point clearly. However, these characteristics trip for faults behind the relay. Therefore, a supervision of a directional unit is required in order to achieve a directional behavior. Moreover, these types of relays may trip for normal load without implementing the supervisory directional unit.

- The blinder characteristic narrow down the relay operation area. However, these characteristics allow tripping for faults beyond the reach point. Therefore, supervision from a different characteristic is desirable.

The relay setting for distance relays is not difficult and relay coordination is practical. In addition, the response time of these relays are usually short (around 1 cycle).

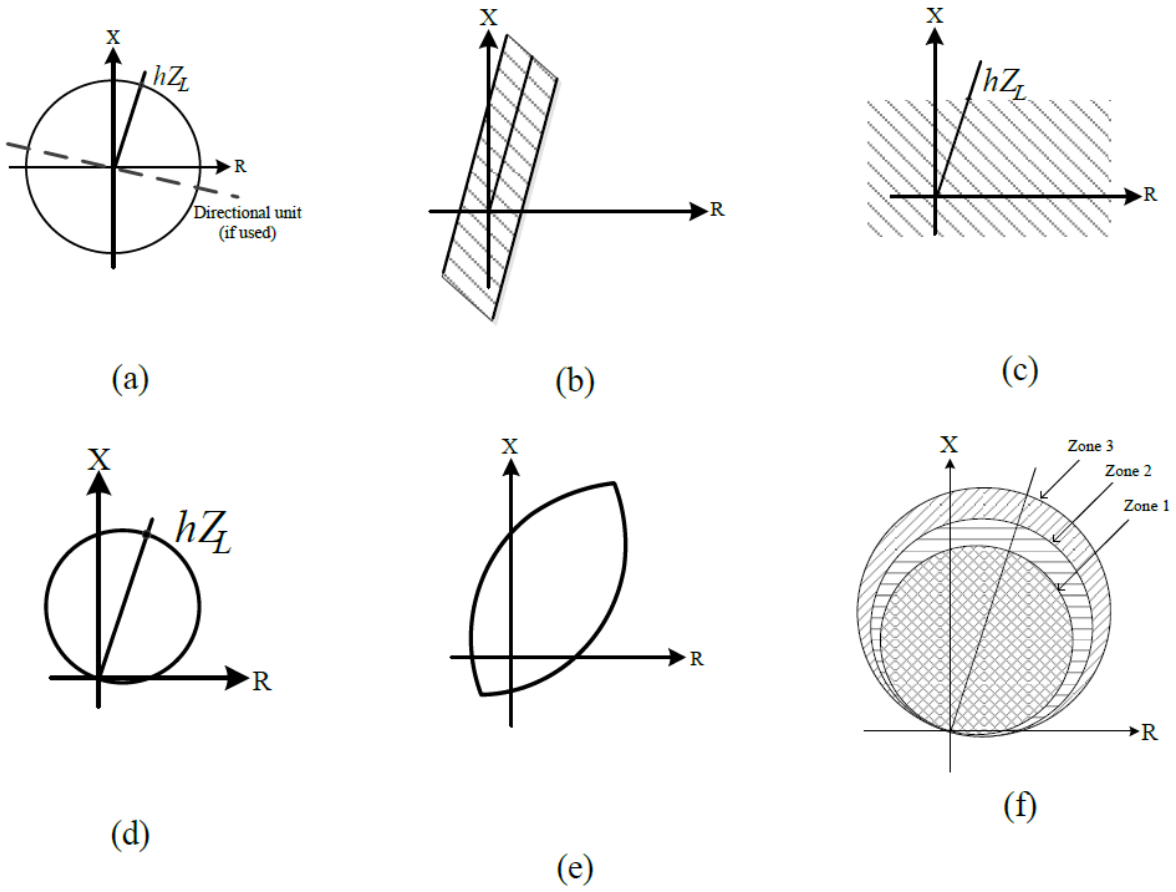

Figure 2.7 Various Distance Relay Characteristic and Zone:

(a) Impedance Characteristic; (b) Blinder Characteristic; (c) Reactance Characteristic; (d) Modified Impedance or Offset Mho Characteristic; (e) Lens Characteristic; (f) Mho Characteristic Zones

As mentioned before, distance relays are usually set to cover 80%-90% of the line length. These relays should also be equipped with another characteristic in order to cover the rest of the line as well as some portion of the neighboring line. Therefore, these relays are usually set as a package with 3 relaying zones. Figure 2.7 (f) shows the three zones of a mho characteristic. Figure 2.8 shows the coordination of these relaying zones. Zone 1 usually is set to respond without any time delay. This zone covers 80%-90% of the line length. The impedance setting of zone 2 protection

should be at least 120% of the protected line length. This setting should not overreach the zone of the adjacent downstream line. In Figure 2.8, zone 2 covers 100% of the first line as well as the 50% of the next line. The suggested time delay for this zone is 0.25 seconds plus the adjacent breaker opening time. Zone 3 is a back-up for the relay on the adjacent line; if the relay of the adjacent line fails to open, this zone responds. In Figure 2.8, this zone covers the adjacent line and reaches 25% of the second adjacent line. The time delay of this zone is usually set at 1-2 seconds. Occasionally, zone 3 settings are set to observe faults in the backward direction instead of the forward direction [16].

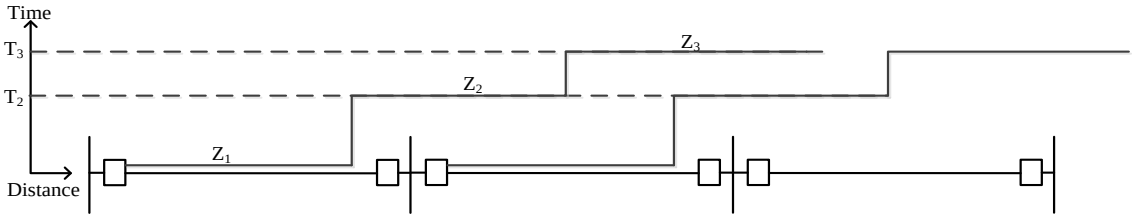

Figure 2.8 Transmission Lines Protected by Distance Relays

When the swing impedance enters the distance relay characteristic during a power swing, the relay will operate. Whether these relays will complete their operation and trip the line depends on the amount of time it takes for the swing locus to traverse the relay characteristic and the length of the line. If the power swing is stable and the system will recover, the swing locus may leave the relay impedance characteristic before the breaker or relay characteristic time delay is exhausted. Moreover, the length of the line and its impedance with respect to the system impedance are other important terms. If the line impedance is small in comparison to the system impedance, the system will trip during a power swing that the system would not recover from. In order to depict this fact graphically, the system of Figure 2.9 is considered. Figure 2.10 shows the relay impedance and swing characteristic while line impedance is small in comparison to the system impedance. In this case, the swing locus enters the relay impedance characteristic when the system angular difference is well passed 120 degrees [10]. In this case, the relay will operate due to any of the zones depending on the time delay of zone 2 or zone 3 as well as the operating time of the breaker. System separation at this point may not be desirable; therefore, the protective relays should be blocked from tripping. Reference [14] specifies that the likelihood of the system recovering from a power swing is almost zero after the angular difference passes 90 degrees.

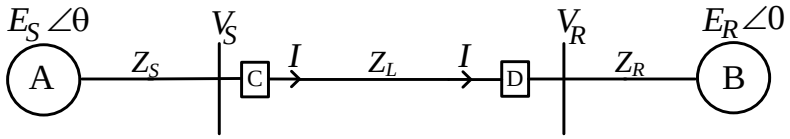

Figure 2.9 Equivalent System used to Study Loss of Synchronism Characteristic

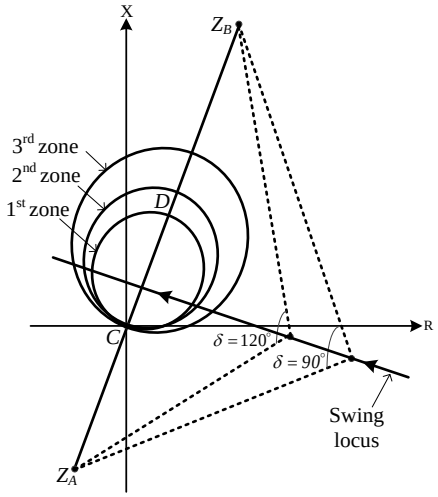

Figure 2.10 Effect of Loss of Synchronism on Distance Relays: Small Line Impedance in Comparison to System Impedance [10]

If the line impedance is large in comparison to the system impedance, the relay may trip for any stable power swing. Figure 2.11 shows such a case; two zones are shown in this figure for the sake of clarity. The swing locus enters zone 2 of the relay before the system angle difference reaches 90 degrees. The swing impedance enters zone 1 before the angular difference reaches 120 degrees. In this case, either the relay should be blocked from tripping the line or if desired to permit tripping, the relay characteristic area should be restricted using a supplementary characteristic such as blinders [10].

The traverse time of a swing locus inside a relay zone can be calculated as (2.3). If this traverse time is greater than the relay zone time delay plus the circuit breaker time delay, the system relay will trip the line. δ_2 and δ_1 are shown in Figure 2.12 and S represents slip in degrees per second [10].

$$T = \frac{\delta_2 - \delta_1}{S} \tag{2.3}$$

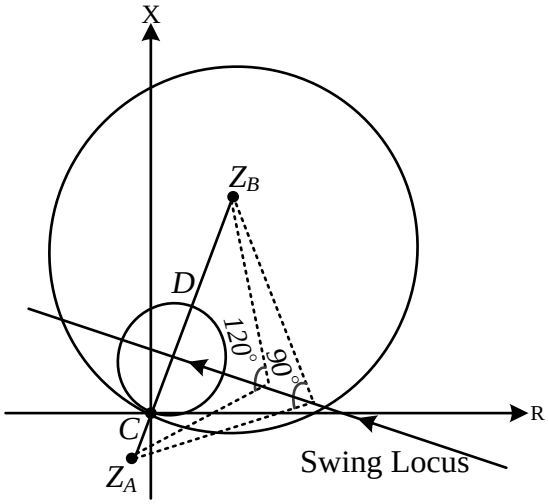

Figure 2.11 Effect of Loss of Synchronism on Distance Relays: Large Line Impedance in Comparison to System Impedance [10]

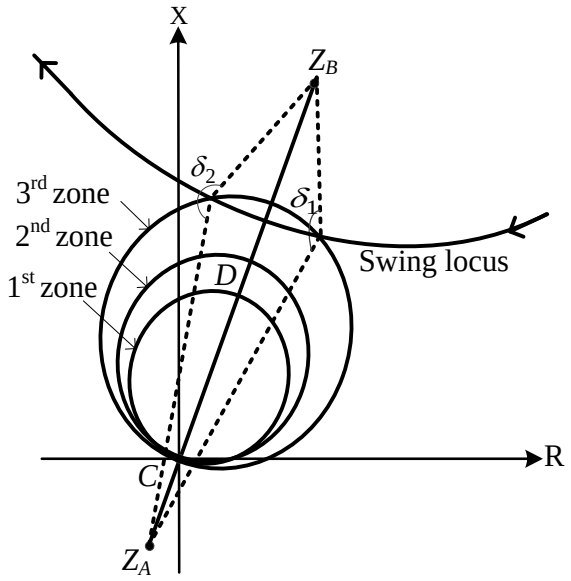

Figure 2.12 Method for Determining Relay Operation Tendency during Loss of Synchronism [10]

2.3.1.4 Under-frequency and under-voltage load shedding relays during power swings

Unlike most of the previously discussed relays, under-frequency load shedding and under-voltage load shedding relays do not get engaged in power swings. However, in case of unintentional islanding, under-frequency load shedding and under-voltage load shedding relays may operate due to the potential imbalance in each island. These relays would shed pre-defined blocks of loads

when the voltage drop or the frequency drop exceeds the set points of these relays. These pre-defined blocks of load may not be suitable for the uncontrolled islands, e.g., the block of load shedding may be more than the amount of load-generation imbalance. Therefore, the operation of these relays may exacerbate the system condition and result in more tension during emergency conditions. The impacts of modeling these relays during a transient stability study are shown in section 3 of this report.

2.3.2 Impact of local mode power swings on protection systems

2.3.2.1 Out-of-step tripping of generators

The OOS protection of transmission lines started before OOS protection for generators. After the United States 1965 northeast blackout, the necessity of protecting generators via OOS protection schemes was acknowledged [17]. Most of other generators' protective schemes are unable to protect the generators during out-of-step conditions. The loss-of-excitation relays provides some degrees of protection for the generators during out-of-step condition; however, these protective relays are not able to detect out-of-step conditions for all operational conditions.

In [14], the impact of using loss-of-field protection for out-of-step sensing is explained; [14] then concludes that using other protection schemes for detecting OOS conditions is less appropriate than those specifically designed for out-of-step relaying for generators. Loss-of-field relays are not equipped with proper out-of-step detection schemes. Furthermore, the responses required for these two different conditions are dissimilar, which leads to instability. This reference further explains that the easiest location to detect out-of-step condition is at generators' locations. However, the appropriate transfer trip signal should be sent to the desired separation location.

The OOS protective relays for generators observe and initiate when the electrical center of a power system disturbance passes through the generators' unit step-up transformers or the generators. These protective relays may also be essential if the electrical center is through the transmission system and transmission system relays are slow or unable to detect the out-of-step condition [18]. Figure 2.13 shows the relay characteristic of these relays. X_T, X_S, and X'_d represent generator step-up transformer reactance, system reactance, and generator transient reactance respectively. θ_c represents the critical switching angle. This critical angle should be calculated via stability studies. Without performing a stability study, θ_c is usually assumed to be around 120 degrees.

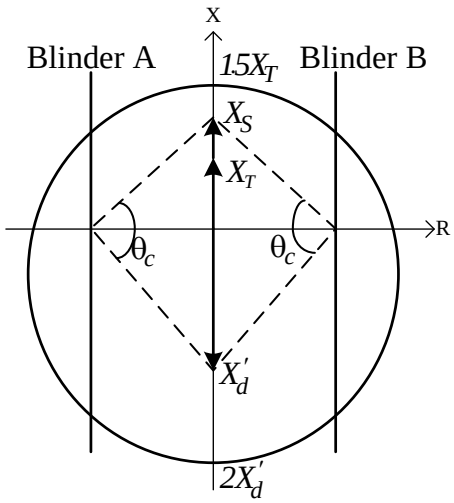

Figure 2.13 Generator Out-of-Step Tripping Scheme

Reference [10] specifies that, as a rule, it is not a recommended practice to perform out-of-step tripping for generators. Instead, it is more desirable to separate the system at appropriate locations in order to keep the load-generation balance. The generators are preferred to remain connected and be ready to resynchronize the system in each island after separation. This reference explains that there are definite exceptions to this rule and the consequences of this tripping should be thoroughly studied.

2.3.3 Power swing detection methods

Early detection of a power swing is very important due to two reasons. First, a power swing may lead to mis-operation of several protection schemes: generation protection, directional comparison schemes, distance relays, phase overcurrent, and/or phase overvoltage. Therefore, a power swing should be detected soon and appropriate out-of-step blocking schemes should be implemented. Second, in case of an out-of-step condition, a network separation scheme is needed in order to avoid a system wide collapse. Thus, an out-of-step tripping scheme should be implemented [19]. Several power swing detection methods are presented in literature. Each of these methods has their own advantages and drawbacks [19]. Some of these methods are reviewed here.

2.3.3.1 Conventional rate of change of impedance method

As mentioned earlier in this chapter, the swing impedance locus travels in the impedance plane slowly. This feature distinguishes the power swing from fault during which the impedance changes from a typical load level to the fault level instantly. The conventional power swing detection methods are based on this rate of change of impedances.

Blinder Schemes:

Figure 2.14 shows a single-blinder scheme. The time interval between right blinder and left blinder is recorded; if this time interval is greater than the time setting, a power swing is detected. This

method is functional for the trip on the way out scheme. A power swing blocking scheme cannot be achieved by this method as the swing locus passes the relay impedance characteristic before it meets the left blinder. In order to overcome this flaw, the dual-blinder scheme, which is shown in Figure 2.15, can be used. In this case, the time interval, between the inner and outer blinders, is measured and compared with a time-setting. If this time interval (ΔT) is larger than the time setting, the power swing is detected. This scheme also allows tripping on the way in.

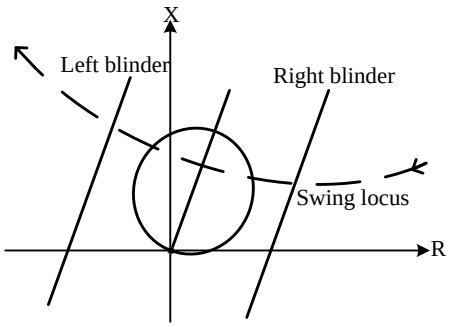

Figure 2.14 Single Blinder Characteristic

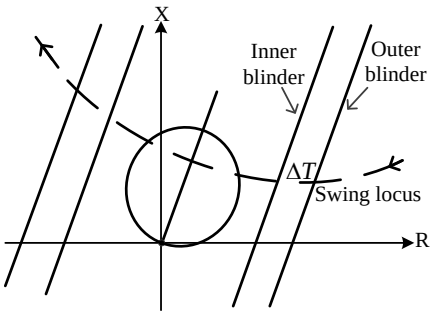

Figure 2.15 Dual Blinder Characteristic

Concentric characteristic scheme:

The concentric scheme works the same as the dual-blinder scheme. A timer will be triggered after the swing impedance locus crosses the outer characteristic. If the swing impedance locus crosses the inner characteristic after a set time delay, a power swing will be detected. Figure 2.16 shows some of these characteristic.

However, it is not easy to determine the appropriate settings for either the dual-blinder or the concentric scheme. In order to guarantee a proper out-of-step blocking scheme, the inner blinder must be located outside of the largest relay impedance characteristic for which the blocking is required. In addition, the outer blinder should be set outside of the load region in order to avoid incorrect blocking operation caused by heavy load. It is difficult to achieve such a proper setting when the line impedance is large in comparison to the network impedance.

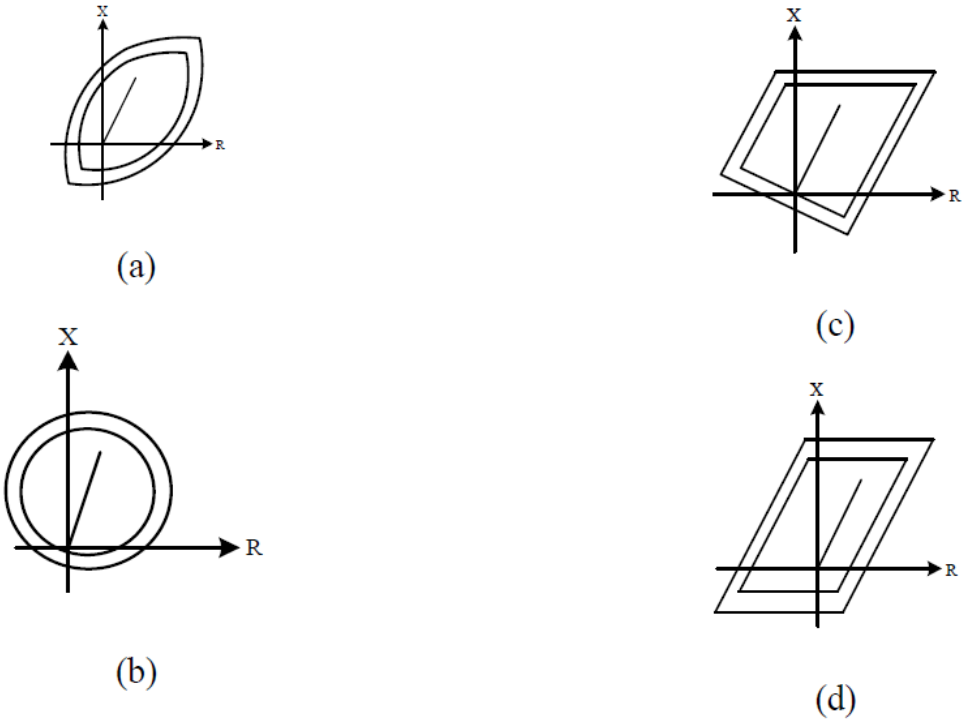

Figure 2.16 Concentric Characteristic of Various Shapes

In order to set these protective relays correctly, several stability studies are required. The fastest power swing should be determined and the blinder time delay should be set accordingly. The rate of slip between two individually synchronized systems is a function of the acceleration torque and system inertia. A relay cannot recognize the slip analytically due to the complexity of the system. By performing stability studies and analyzing the results, an average slip can be determined. However, the slip usually changes after the first slip cycle. Therefore, a fixed impedance separation between the blinders and a fixed time delay might not be adequate for an appropriate setting of the out-of-step blocking. Moreover, for a complex power system, it is very hard to calculate the source impedances in order to establish the blinder and out-of-step blocking scheme. These impedances change with network topology, commitment of an additional generation unit, or other network elements. The source impedances can also change during a disturbance. If the source impedance were to stay constant, the blocking and tripping scheme setting would have been trivial. Usually, very detailed stability studies for various contingencies are needed in order to find the best fit for equivalent source impedance and out-of-step protection settings.

2.3.3.2 Non-conventional power swing detection method

Continuous impedance calculation:

Continuous impedance calculation is presented in [20]. This method is based on monitoring impedance progression in the complex plane. The criteria for detecting a power swing in this

method are: continuity, monotony, and smoothness. Continuity confirms the motion of the trajectory, i.e., the trajectory should not be motionless; ΔX and ΔR (in Figure 2.17) should be greater than a threshold. Monotony confirms that the trajectory does not change direction. Smoothness checks that there are no abrupt changes in the trajectory. If these criteria are fulfilled for six sequential calculations, a power swing suspicion is established. This method usually implements a concentric characteristic as complementary. This concentric characteristic is designed to pick the very slow impedance trajectory movements (<5 ohm/second) during a swing. After the trajectory enters the concentric characteristic, a timer is started. A power swing is detected if the timer elapses before the fault detection zone is reached [20]. The advantage of this method is that it does not require any settings. This method is also able to handle a slip frequency up to 7 Hz.

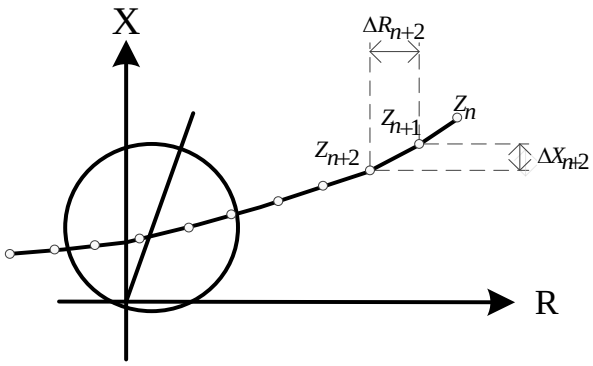

Figure 2.17 Continuous Impedance Calculation [20]

Continuous calculation of incremental current:

This method is based on the fact that current and voltage experience large variations during power swings. The difference between the present observed current value and the previous sampled value are used to detect power swing conditions. A power swing is detected if this difference is more than 5 percent of the nominal current and this condition is observed for 3 cycles. Figure 2.18 shows this scheme. This detection can trigger a power swing blocking scheme. An additional delta current detector is also used to detect a new step change of the current beyond the power swing. This additional detector is used to recognize the fault condition and remove the blocking scheme (Figure 2.19) [21].

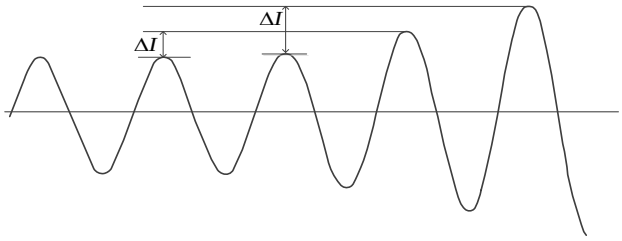

Figure 2.18 Continuous Calculation of Incremental Current [21]

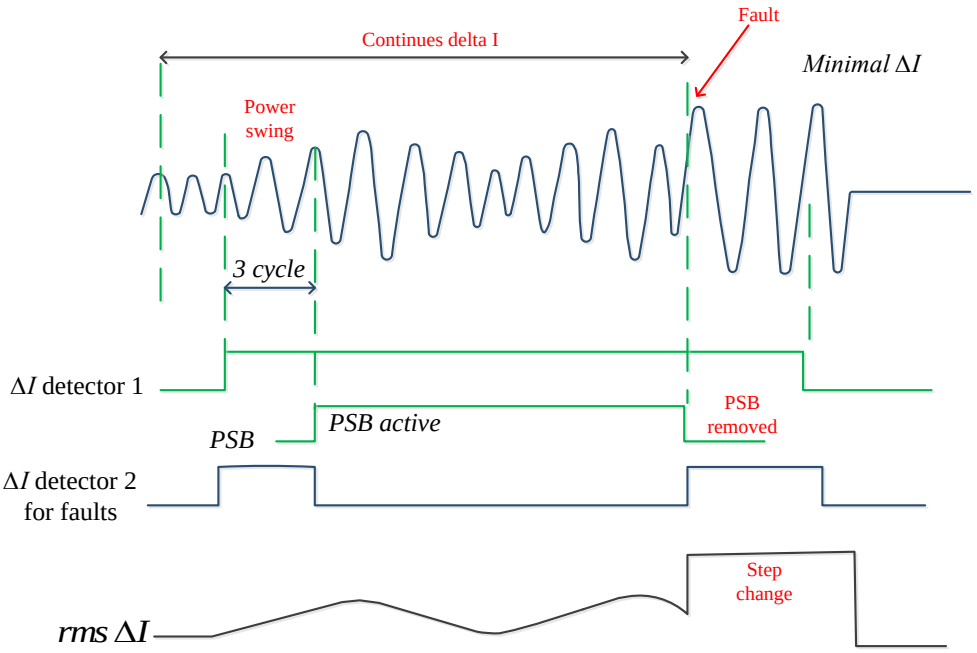

Figure 2.19 PSB and Removal of Blocking by Fault Detector 2 due to a Fault [21]

Continuous calculation of incremental current can detect very fast power swings that are difficult to detect using the traditional methods, specifically for heavy load conditions. However, the detection of a very slow slip (below 0.1 Hz) is hard since current may change less than 5% of the nominal current between two cycles [21].

R-Rdot out-of-step scheme:

This method was devised for the Pacific 500 kV intertie and installed in the early 1980s. The rate of change of impedance is used in order to detect an out-of-step condition. A control variable U is defined by (2.4) [22]-[23],

$$U = (Z - Z_1) + T_1 \frac{d_Z}{d_t} \tag{2.4}$$

where Z is the apparent impedance magnitude at the relay location. Z_1 and T_1 are two settings that are derived from system studies; Z_1 is the impedance of the swing that is to be tripped and T1 is the slope that represents Rdot/R. Out-of-step tripping relays will operate if U becomes negative. If we neglect the derivative part of (2.4), the control characteristic will be similar to the conventional method. Reference [19] explains that for a conventional out-of-step tripping, the relay will trip when the impedance observed at the relay location is less than a specified value. The Rdot/R method is a combination of this conventional method with a rate of change of the impedance observed at the relay location. Considering the derivative part of (2.4), the tripping

signal will be achieved faster when the impedance changes at a higher rate (when the derivative is negative). For a high separation rate, $\frac{d_Z}{d_t}$ would be a large negative value causing earlier separation. Therefore, a high $\frac{d_Z}{d_t}$ is used to anticipate instability. The amount of anticipation depends on T1 (a nominal value is generally the circuit breaker plus relay operating times). By drawing $\frac{d_Z}{d_t} - Z$ in a phase plane, (2.4) represents a switching line. Using (2.4), one can conclude that the control variable U will become negative when the switching line is crossed by the impedance trajectory from right to left. One modification of this method is to use the resistance and the rate of change of the resistance instead of impedance, which is shown by (2.5).

$$U = (R - R_1) + T_1 \frac{d_R}{d_t} \tag{2.5}$$

This switching line is shown in Figure 2.20. The benefit of this modification is that the relay becomes less sensitive to the location of the swing center with respect to the relay location [22]. For the conventional method, the switching line is a vertical line in the Rdot/R plane. For a low separation rate (small $\frac{d_R}{d_t}$), the control variable is similar to the conventional method. For a higher separation rate (large $\frac{d_R}{d_t}$), a larger negative value of U will be achieved and the tripping will be initiated much earlier. This method needs extensive simulation studies for various contingencies in order to set the relay characteristic properly.

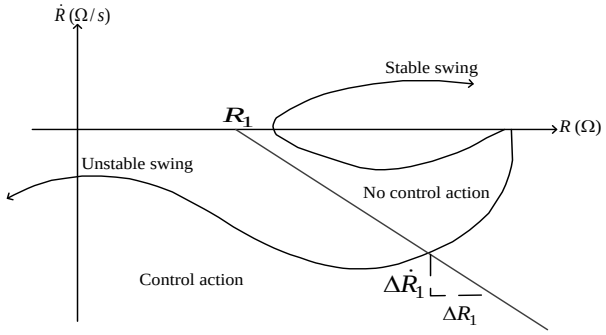

Figure 2.20 R-Rdot OOS Characteristic [8]

Rate of change of swing center voltage:

Swing center voltage (SCV) is the voltage at the location of the swing center. This method is based on tracking the voltage at the swing center. Considering a two-machine equivalent system similar to Figure 2.9, Figure 2.21 shows the phasor diagram of voltage and current in such a system.

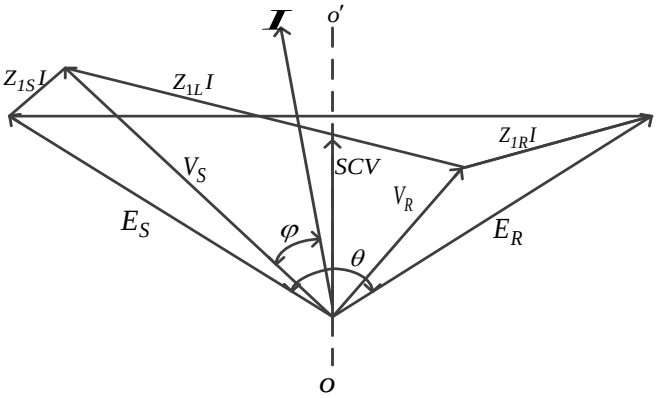

Figure 2.21 Voltage Phasor Diagram of a Two-machine System [8]

SCV becomes zero when the two equivalent systems are 180 degrees separated. When a two-source system loses synchronism, the angle difference between the two sources increases as a function of time. Assuming the equal voltage source magnitudes ($E = |E_R| = |E_S|$), SCV is represented in (2.6) [24].

$$SCV(t) = \sqrt{2}E \sin(\omega t + \frac{\theta(t)}{2}) \cos(\frac{\theta(t)}{2}) \tag{2.6}$$

The magnitude of SCV is between 0 and 1 pu. Under the normal load condition, the value of SCV stays constant. SCV can be also approximated by projection of $|V_S|$ into the current vector (Figure 2.21):

$$SCV \approx |V_s| \cos\varphi \tag{2.7}$$

This approximation can be considered valid as the rate of change of SCV provides the main information; therefore, the approximation of SCV magnitude has very little impact on power swing detection. Moreover, SCV can be approximated using the source voltage magnitude:

$$SCV1 \approx E_1 \cos(\frac{\theta}{2}) \tag{2.8}$$

where E_1 is the positive-sequence magnitude of the source voltage, E_S . SCV1 is used in the presented method in order to detect the power swing. The magnitude of SCV is maximum when the angular difference between the two sources is zero. When the angular difference is 180 degrees, this voltage magnitude is zero. This fact is used for the purpose of power swing detection. The rate of change of SCV, (2.9), is considered as an indicator for the swing condition.

$$\frac{d_{SCV1}}{d_t} \approx -\frac{E_1}{2} \sin(\frac{\theta}{2}) \frac{d_\theta}{d_t} \tag{2.9}$$

Equation (2.9) provides a relationship between the rate of change of the SCV and the two machines system slip frequency, $\frac{d_\theta}{d_t}$. When the machines go out-of-step (180 degrees separation), this slope is at a minimum (a large negative value). This method usually detects the power swing when the angle separation is close to 180 degrees.

Synchrophasor-based out-of-step relaying:

This method is based on approximating the system angle separation based on phase angle differences between synchrophasors measured at the lines extremities. A two-machine equivalent system similar to Figure 2.9 is considered. Assume that synchrophasors of positive-sequence voltages are measured at the sending and receiving ends of the line. The ratio of bus voltages measured by the synchrophasors are presented in (2.10),

$$\frac{V_{1A}}{V_{1B}} = \frac{\frac{Z_S}{Z_T} + (1 - \frac{Z_S}{Z_T})K_E \angle \theta}{\frac{Z_S + Z_L}{Z_T} + (1 - \frac{Z_S + Z_L}{Z_T})K_E \angle \theta} \tag{2.10}$$

where $Z_T = Z_S + Z_L + Z_R$ and $K_E = \frac{|E_A|}{|E_B|}$.

Assuming that the source impedances are small with respect to line impedance and $K_E = 1$, the magnitude of the right hand side of (2.10) becomes 1 with angle of θ. This result indicates that the angle differences between the two equivalent sources can be approximated by the phase angle of the ratio of the synchrophasors measurements at the line extremities. This property can be used for out-of-step detection [25].

Reference [25] represents a method based on the measurements of a positive-sequence voltage-based synchrophasors at two network locations. The slip frequency S_R, which is the rate of change of the angle between the two measurements of the synchrophasor, and the acceleration A_R, which is the rate of change of the slip frequency, are derived from the measurements. A network separation is initiated if the followings are asserted:

- If S_R is not zero and is increasing, which means that A_R is positive.
- Separation will be asserted if:

$$A_R > slope \times S_R + A_{Offset} \tag{2.11}$$

This is shown in Figure 2.22. This characteristic identifies unstable swings before the OOS condition occurs, allowing the system protection scheme to take immediate remedial actions.

- The absolute value of the angle difference between the two synchrophasors becomes greater than a threshold.

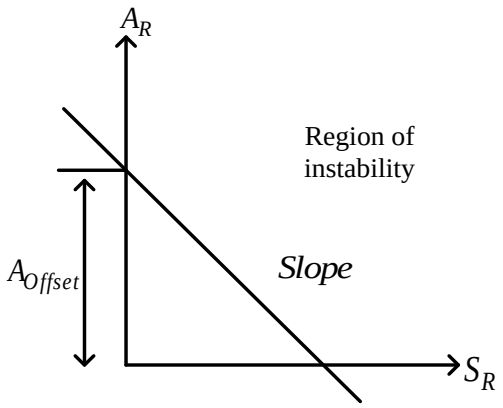

Figure 2.22 Synchrophasor-based Out-of-Step Detection

Using state-plane trajectories analysis for out-of-step detection:

Reference [25] suggests the analysis of the state-plane trajectory to check for the out-of-step condition. This method finds a single-machine equivalent of the system and performs the analysis on this equivalent network. The state planes (relative rotor speed versus relative voltage angle) during the fault and after the fault are used to distinguish stable power swings from unstable power swings. The critical clearing angle and time are found based on the maximum potential energy of the system. The critical clearing time is used as a criterion in order to predict stable or unstable power swings. The authors claim that the proposed method is faster, more efficient, and more accurate than previous methods. The disadvantage of this method is the use of a network equivalent, which may lead to inaccuracy.

Using decision tree technique for out-of-step condition detection:

References [27]-[28] explain the practice of using a decision tree algorithm for out-of-step detection. These methods implements training algorithms using the results of transient stability analysis for various contingencies. The achieved strategy can be used to recognize stable power swings from unstable power swings in unseen samples.

Frequency deviation of voltage:

In [29], a discrete Fourier transform is used in order to calculate the angular velocity of the bus voltage and the angular acceleration of the generator rotor angle. A criterion for out-of-step detection is developed in this reference by showing these two parameters (angular velocity of the bus voltage and the angular acceleration of the generator rotor angle) in the same plane. This method just needs voltage measurements without the need for current measurements.

Out-of-step detection using swing impedance trajectory circles:

Reference [30] proposes a new method based on power swing trajectory for power swing detection. This method describes the impedance locus as a circular characteristic during the swing and the fault. It is described that, during power swings, the center of the impedance trajectory is outside the relay impedance characteristic. However, during a fault, this center is located outside the relay impedance characteristic but shifts to a location inside the relay impedance characteristic. This identity is used in this reference for power swing detection.

Various methods for power swing detection have been explained. When an unstable power swing is detected, the proper OOS tripping and blocking action should be performed in order to avoid a system collapse. The location of OOS tripping and blocking should be determined in the planning phase. This report covers the issue of determining the proper location that OOS blocking functions should be performed.

2.3.4 Electromechanical relays

Electromechanical relays are a mature technology, which has been widely used for many years and still applied for many purposes. These devices are usually known for their reliable performance and low cost. Most of these devices are based on the presence of sufficient torque in order to overcome the restraining spring and rotate the induction disk [9]. Both OOS blocking and tripping functions can be performed by electromechanical relays. These two types of functions are explained in the following subsections.

2.3.4.1 Out-of-step blocking relays

Reference [10] explains that the standard out-of-step blocking relay is an offset mho characteristic in conjunction with mho-type tripping unit used for line protection during fault. These relays provide blocking of tripping during stable power swings, OOS conditions, or blocking from reclosing after OOS tripping at the desired separation location.

A dual-concentric characteristic similar to Figure 2.16-(b) is used for this type of relay. The traverse time between inner and outer characteristics is used for out-of-step detection. Reference [10] also specifies that it is a common practice to block zone 1 and zone 2 of the distance relays by OOS blocking relays. Zone 3 is usually not blocked in order to capture if a fault were to occur on that or a nearby line, which may occur during the blocking of zone 1 and zone 2. However, [4] specifies that most North American major blackouts since 2003 happened due to distance relay mis-operation of zone 3.

2.3.4.2 Out-of-step tripping relays

Reference [10] explains these relays as two modified reactance type units (Figure 2.23). When a loss of synchronism occurs, the impedance trajectory passes characteristic A and characteristic B and will be evaluated by an auxiliary unit in order to ascertain that a loss of synchronism has occurred. These relays either trip the local lines or send a transfer trip signal to the appropriate separation location. An overcurrent relay is utilized to allow operation only if the current is higher or equal to the magnitude of load current.

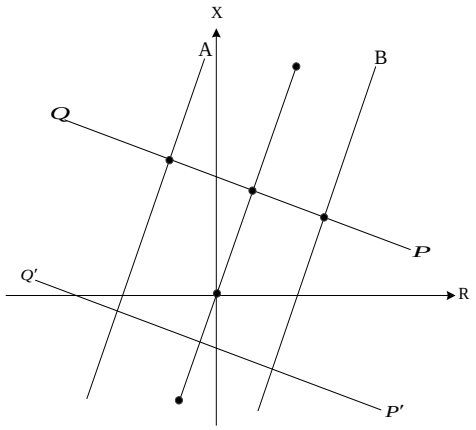

Figure 2.23 Characteristic of Out-of-Step Tripping Relay [10]

In general, the desired point of separation changes from time to time. Therefore, the system operator will have to transfer the trip to another location of the network based on system operational condition [10].

2.3.5 Static relays

Static relays are referred to relays in which there is no armature or other moving elements. The design response is usually developed by electronic, solid state, magnetic, or other components without mechanical motion [9]. Static relays usually provide more flexibility and desired relay operation characteristics. With these relays, two functions of out-of-step blocking and tripping can be achieved in one package. Figure 2.24 (a) and (b) show two characteristics for these relays. The characteristic presented in Figure 2.24 (a) is similar to the offset mho used to describe electromechanical relays. Figure 2.24 (b) shows a lens characteristic supervised by a directional mho characteristic; an outer lens characteristic is involved in order to differentiate a fault from a power swing. In this scheme, tripping is restricted to the shaded area.

(a) (b)

Figure 2.24 Static Out-of-Step Relay Characteristic [10]

The blocking scheme is achieved with the similar logic as electromechanical relays, which is based on the traverse time between the outer layer, e.g. mho out-of-step blocking (MOB) in Figure 2.24

(a), to the inner layer, e.g. mho tripping (MT) in Figure 2.24 (a). A logic circuit for this operation is shown in Figure 2.25. When the impedance locus passes MOB or lens out-of-step blocking (LOB), and no output from MT or lens tripping (LT), AND1 will produce an input to the A/16 timer. “A” milliseconds later, the timer provides an output, which blocks tripping or reclosing. The pick-up time “A” is adjustable between 2-4 cycles (32 to 64 milliseconds).

Similarly, the tripping will be initiated if the following sequence of events occurs:

1. The swing impedance enters MT of LT more than “A” milliseconds later than MOB or LOB.
2. The swing impedance exits MOB or LOB 1 cycle or later after MT or LT.

The tripping function initiates the local tripping or sends a transfer trip signal to other locations based on the schedule. Please note that the relay logic may be different from Figure 2.25 based on the desired relay characteristics [10].

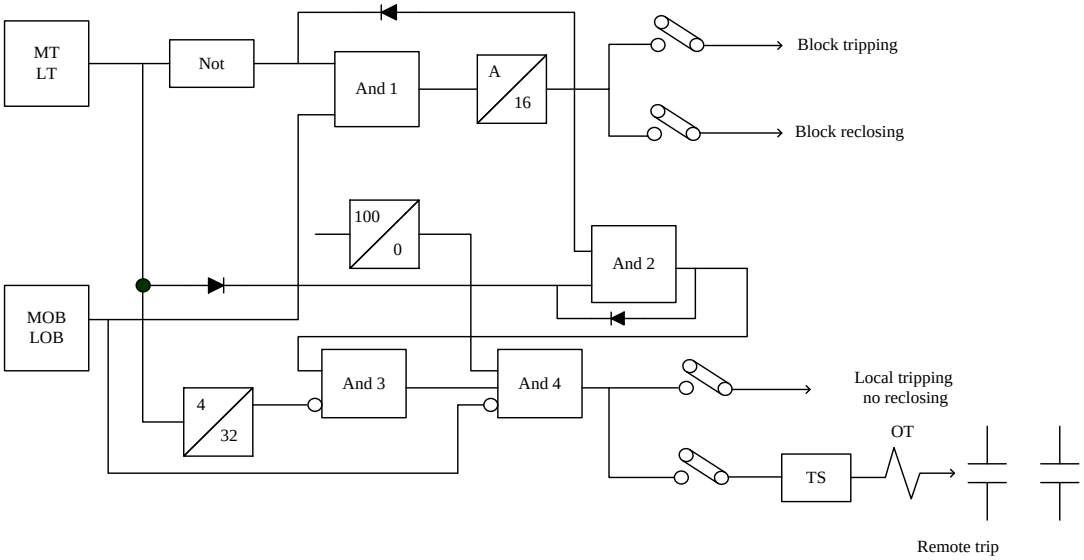

Figure 2.25 Static Out-of-Step Relays Logic [10]

2.4 Summary

This section describes issues associated to power swings and out-of-step conditions. The impacts of a power swing on the system and various protective relays are studied. Various out-of-step detection methods from previous research are presented and analyzed. In addition, the OOS protective relaying is explained. This chapter forms the foundation for this report by explaining the details of OOS conditions and OOS protection function.

3. Modeling Protection Systems in Time-Domain Simulations

Improving situational awareness is one of the key concerns of utilities, which can be achieved by enhancing the representation of protection mechanisms in analysis tools. One important analysis tool where this would be required is positive sequence time domain analysis for transient stability. The proper representation of protection functions in stability software has been a long term goal for utilities. The records from previous blackouts confirm the necessity of representing protective devices within transient stability studies. The actual representation of protection functions and the identification of which protection functions/systems are important to include in a transient stability study will greatly enhance the capabilities of the transient stability studies. This report is aimed at specifying the important protective relays to be modeled in transient stability studies. The impacts of modeling distance relays, OOS relays for generators, under-frequency load shedding relays, and under-voltage load shedding relays in transient stability studies are analyzed in this chapter. The results of transient stability studies with and without modeling protective relays are compared in this chapter. Section 4 proposes the proper design of OOS blocking schemes. Section 5 suggests a method to identify the important distance relays to be modeled in a transient stability study.

3.1 Test case

The WECC system data representing the 2009 summer peak load case is used to perform the analysis. The system includes 16,032 buses, 3,217 generators, 13,994 transmission lines, and 6,331 transformers. The overall generation capacity is roughly 238 GW and the load is roughly 167 GW.

The data includes nine existing OOS tripping relays. These are defined by a lens and a tomato shape. The lens characteristic is the intersection of two circles shown in Figure 3.1. The tomato characteristic is the union of the two circles [31]. A summary of these nine OOS relays for transmission lines are presented in Table 3.1. Moreover, no distance relays are modeled in this dataset. However, several under-voltage load shedding (UVLS) and under-frequency load shedding (UFLS) relays are included. In the remaining sections of this report, the term “base case” will be used in reference to the results pertaining to the original dataset.

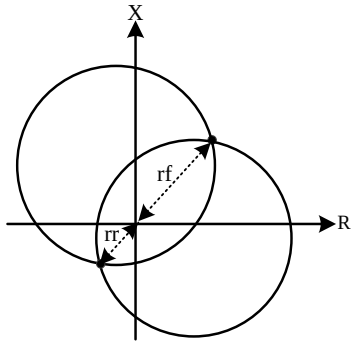

Figure 3.1 Relay Characteristic of Type Lens or Tomato

Table 3.1 Existing OOS Relays in the WECC System

No.	kv	Relay zone 1 type
1	25	Lens
2	25	Lens
3	230	Lens
4	120	Lens
5	120	Lens
6	345	Lens
7	345	Tomato
8	60	Tomato
9	120	Lens

3.2 Impact of modeling distance relays in transient stability study

In order to perform this study, distance relays are added on all transmission lines with the voltage level higher than or equal to 138 kV. These distance relays are modeled using the *zlinw* model from the Positive Sequence Load Flow (PSLF) library [31]. This model considers two zones for each distance relay. Please note that there exist other distance relay models in PSLF, which are able to model three zones of distance relays. However, implementation of these distance relay models are avoided due to the large-scale test case and software limitations. The zone 1 and zone 2 of the modeled distance relays are considered to be 0.85 and 1.25 times the transmission line reactance respectively. The zone 2 of the distance relays operate with a time delay of 0.25 seconds. Zone 1 initiates tripping without any time delay. However, the breaker operation time is modeled to be 0.03 seconds. While the relay settings for various transmission lines will vary across a system, these settings are considered to be similar for all transmission lines in this study due to the lack of available data for protection systems across the entire WECC. No additional OOS relays are modeled in this case (all originally provided OOS relays are included here). In order to have a realistic estimate of system behavior, OOS tripping, OOS blocking, and remedial action schemes (RAS) should be modeled within the transient stability study; these protection schemes are modeled in the study performed in Chapter 4. Please note that the results, which are presented in this chapter, are simply showing the importance of modeling distance relays during a transient stability study.

The outage of the California-Oregon Interface (COI) is studied in this section. The COI includes three 500 kV transmission lines transferring about 3800 MW from north to south during this hour and they are very critical tie lines. The result of the transient stability study while modeling distance relays are compared with the base case.

Figure 3.2 and Figure 3.3 show the generators' relative rotor angles for the base case and with modeling distance relays respectively. While modeling distance relays, 9 relays operated, which caused the different behavior between Figure 3.2 and Figure 3.3.

Modeling distance relays does not impose computational complexity to the transient stability study. However, preparing the relays model, data preparation, and data maintenance for all high voltage transmission lines are exhaustive tasks. Incorrect models, outdated data, or relay mis-representation may result in inaccurate estimation of system behavior.

Moreover, it is not essential to model the distance relays, which are not exposed to the power swing. For instance, the distance relays, which connect extremely coherent generators, may not be vulnerable to the power swing and do not need to be modeled within the transient stability study. Potentially mis-operating distance relays, OOS relays, and any other distance relays that influence the results of the transient stability study, should be modeled. An efficient approach needs to be developed in order to identify these critical distance relays. This report proposes two methods in section 4 and section 5, which identify the potential mis-operating and critical distance relays during the power swing.

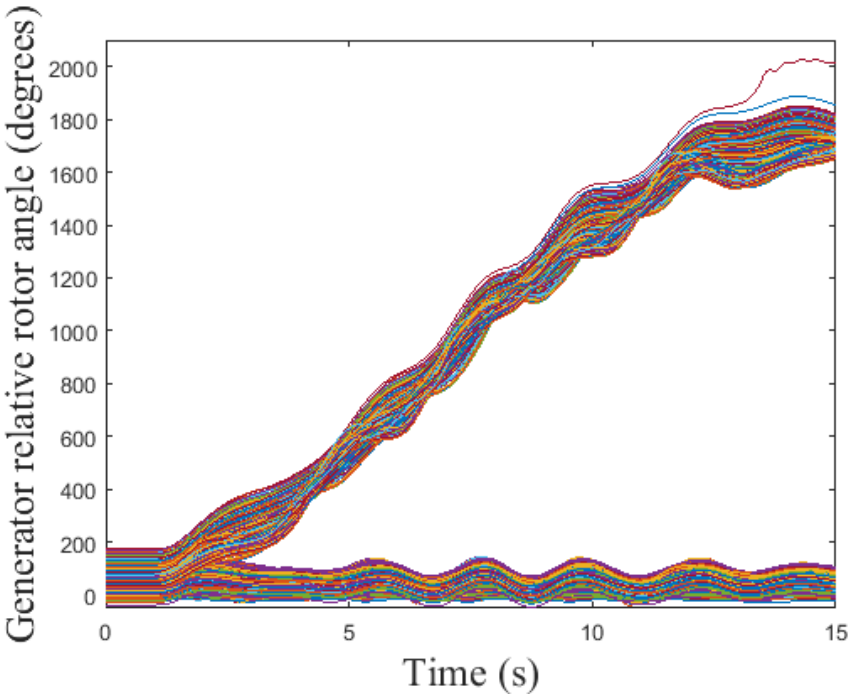

Figure 3.2 Generators' Relative Rotor Angles without Modeling Distance Relays

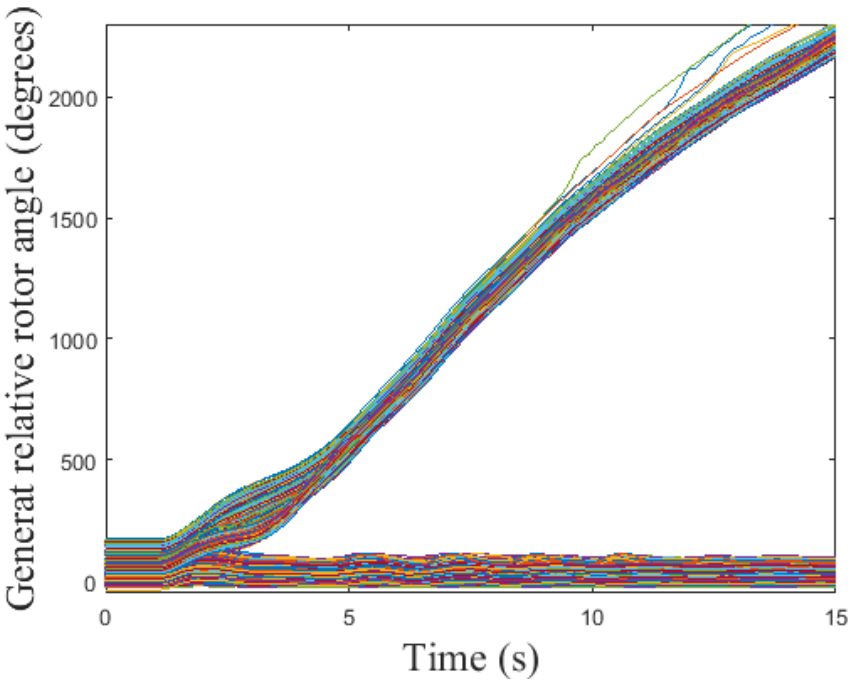

Figure 3.3 Generators' Relative Rotor Angles while Modeling Distance Relays

3.3 Impact of modeling under-frequency and under-voltage load shedding relays

The original test case includes 1881 UFLS relays and 47 UVLS relays. In this section, the same contingency as in Section 3.2 is studied. The transient stability studies are performed with and without UFLS and UVLS relays. Figure 3.4 and Figure 3.5 show the generators' relative rotor angle with and without modeling UFLS and UVLS relays respectively. From these two figures, both stability studies identify that two groups of generators will be formed due to the modeled contingency. Note that the two groups of generators in both figures are the same, i.e., the two coherent groups of generators in Figure 3.4 are identical to the two coherent groups of generators in Figure 3.5. While this qualitative result is the same between the two studies, there is more to be understood from these figures, which indicate that, indeed, the modeling of UFLS and UVLS is an important addition to stability analysis. As can be seen, the speed of the separation of the two groups of generators in Figure 3.4 is much faster than the speed of separation of the groups in Figure 3.5. By modeling UFLS and UVLS, the drop in frequency for the group that has more demand than supply capability will be slower since load shedding occurs. Therefore, the separation of the relative rotor angles is smaller in the case with UFLS and UVLS activated, which is to be expected. Finally, while the separation scheme and distance relays for this contingency are not modeled, the importance of this result remains. The speed by which the two groups separate largely impacts system dynamics and the ability to form controlled islands that are able to recover from the outage with minimal involuntary load shedding, thereby confirming the importance of modeling UFLS and UVLS.

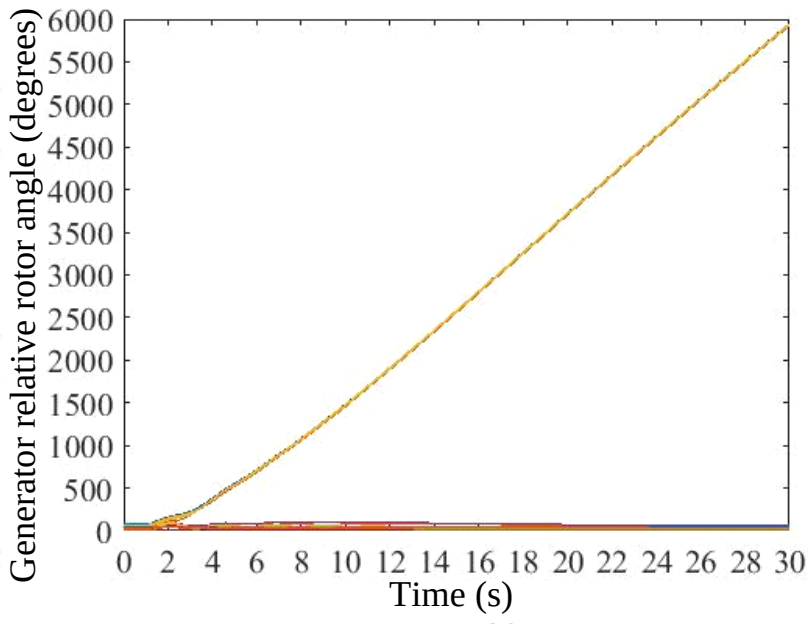

Figure 3.4 Generators' Relative Rotor Angles without Modeling UVLS and UFLS

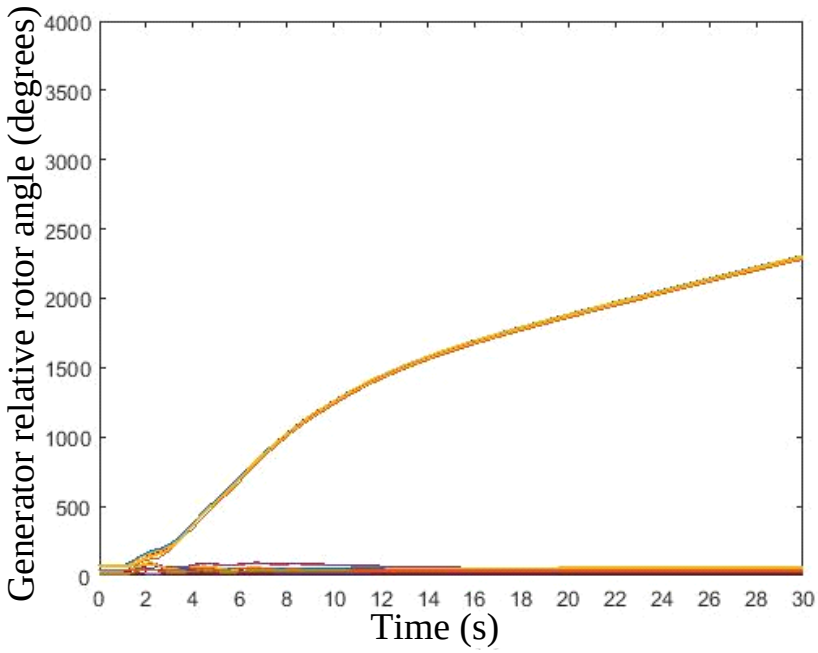

Figure 3.5 Generators' Relative Rotor Angles while Modeling UVLS and UFLS

This impact of the UFLS and UVLS can be further confirmed with the results in Figure 3.6 and Figure 3.7. As shown in Figure 3.7, the generators that drop in speed recover faster with the modeling of UFLS and UVLS; while there is still a separation of the two generator groups, the impact of the generators' rotor speeds is also important.

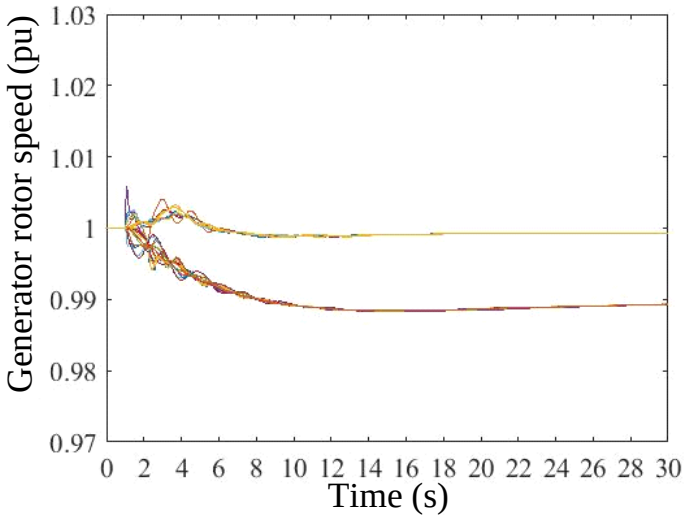

Figure 3.6 Generators' Rotor Speed without Modeling UVLS and UFLS

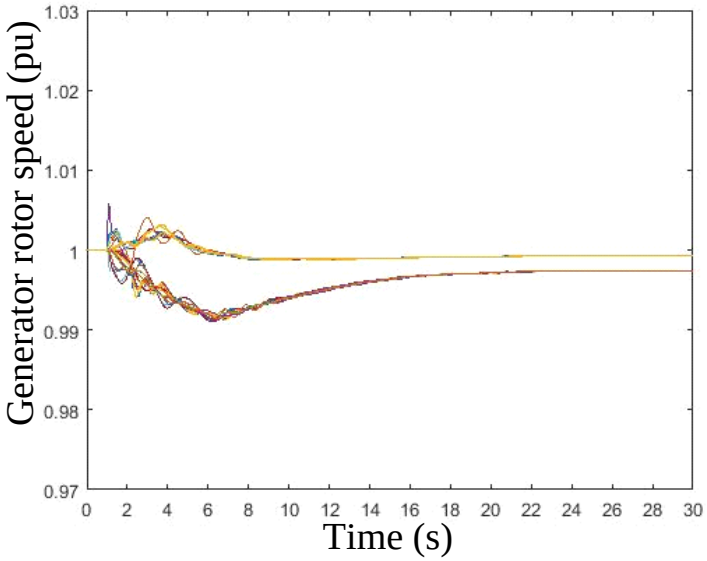

Figure 3.7 Generators' Rotor Speed while Modeling UVLS and UFLS

Similarly, Figure 3.8 and Figure 3.9 show the bus frequency with and without modeling UVLS and UFLS at the locations that UFLS relays triggered. Figures 3.4-3.8 prove the importance of modeling UVLS and UFLS relays during transient stability study.

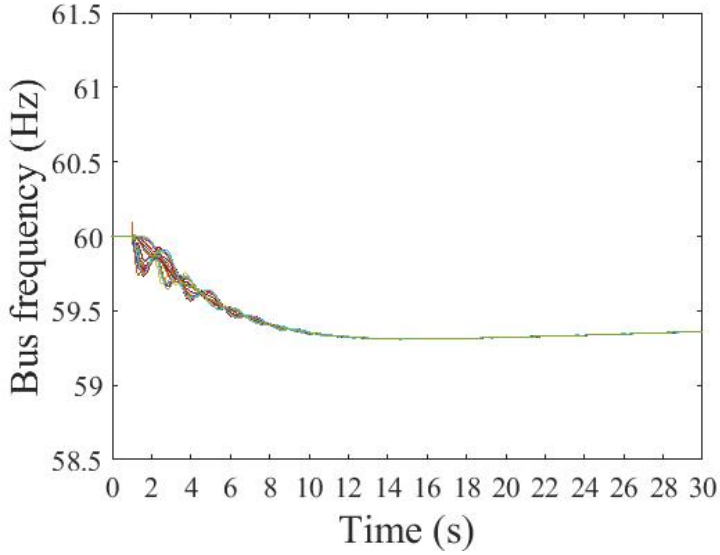

Figure 3.8 Bus Frequency without Modeling UVLS and UFLS

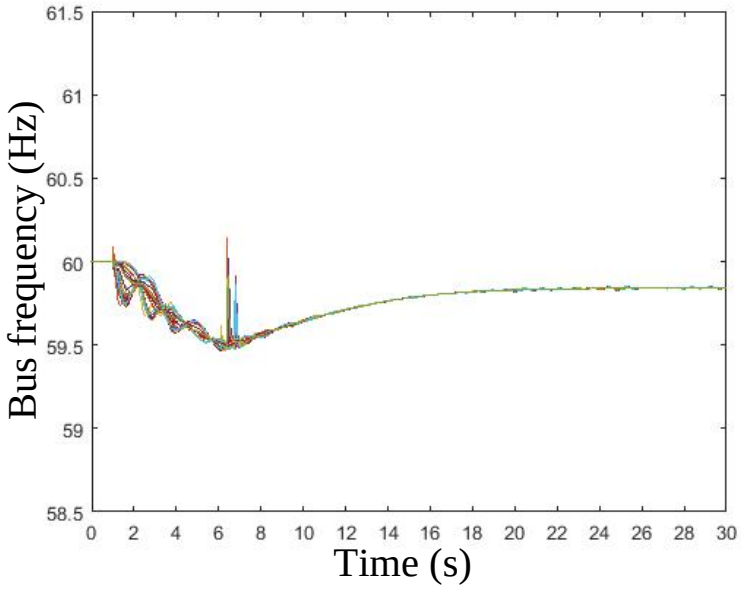

Figure 3.9 Bus Frequency while Modeling UVLS and UFLS

3.4 Impact of modeling OOS relays for generators

An out-of-step condition causes high currents and added pressure in the generator windings; out-of-step conditions also cause high levels of transient shaft torque. Pole slipping events can also result in abnormally high stator core end iron fluxes that can lead to overheating and shorting at the ends of the stator core. The step-up transformer will also experience very high transient winding currents. A proper OOS protection scheme should be designed for generators in order to

avoid severe damages to the generators and the step-up transformers. This section studies the importance of modeling generators' OOS relays during dynamic studies.

The WECC data set, which is discussed in Section 3.1, is used for this study. However, the contingency under study is different from Section 3.2 and Section 3.3. First, a three-phase fault at bus Navajo 500 kV is modeled. This fault is cleared after four cycles (0.067 seconds) by opening two transmission lines: Navajo-Crystal 500 kV and Navajo-Moenkopi 500 kV. Navajo-Crystal 500 kV transfers 978 MW from Navajo to Crystal in the pre-contingency operational state. Similarly, Navajo-Moenkopi 500 kV transfers 824 MW from Navajo to Moenkopi in the pre-contingency operational state.

Figure 3.10 shows the generators' relative rotor angles. As a result of this contingency, Navajo generators lose synchronism with the other generators. Transient stability studies are performed with and without modeling OOS relays for Navajo generators. These OOS relays are designed similar to the OOS relay settings, which is discussed in section 2.3.2.1. While modeling OOS relays for Navajo generators, these generators would be disconnected when they slip a pole; as a result, the impacts of their loss of synchronism will not be reflected on the other results of transient stability studies. Without modeling OOS protective relays for these generators, the impacts of their loss of synchronism would be shown in the other results of transient stability studies and cause inappropriate estimation of system behavior.

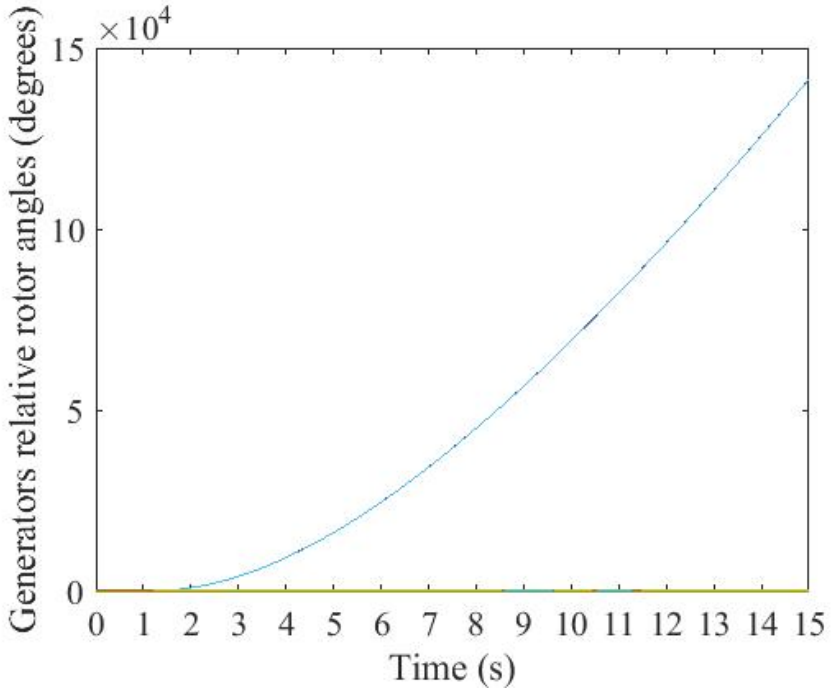

Figure 3.10 Generators' Relative Rotor Angles

In the study performed in this section, if the OOS protective relays are not modeled on Navajo generators, frequency oscillates and deviates more than the set points of 38 UFLS relays. These UFLS relays reduce the load at these locations. While modeling OOS relays for Navajo generators, frequency does not deviate from the set points of any of these UFLS relays. Figures 3.11-3.14

show the bus voltage magnitude and bus frequency at these 38 locations with and without modeling OOS relays for Navajo generators. Without modeling OOS relays for the Navajo generators, voltage and frequency show oscillatory behavior. These oscillations are results of pole slipping of Navajo generators as these generators are not disconnected in this case. In order to have a realistic estimate of system behavior, it is essential to model OOS relays for the involved generators.

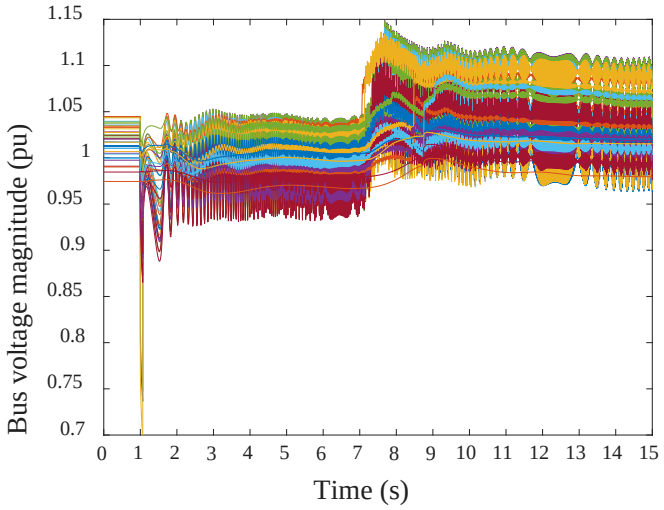

Figure 3.11 Bus Voltage Magnitudes without Modeling OOS Relays for Navajo Generators

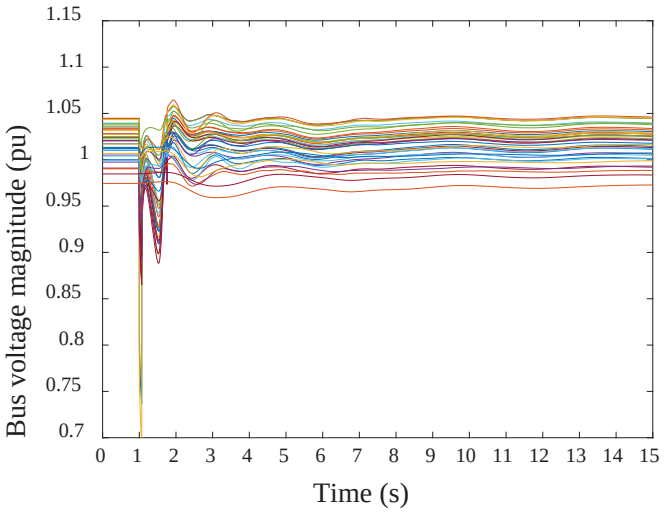

Figure 3.12 Bus Voltage Magnitudes without Modeling OOS Relays for Navajo Generators

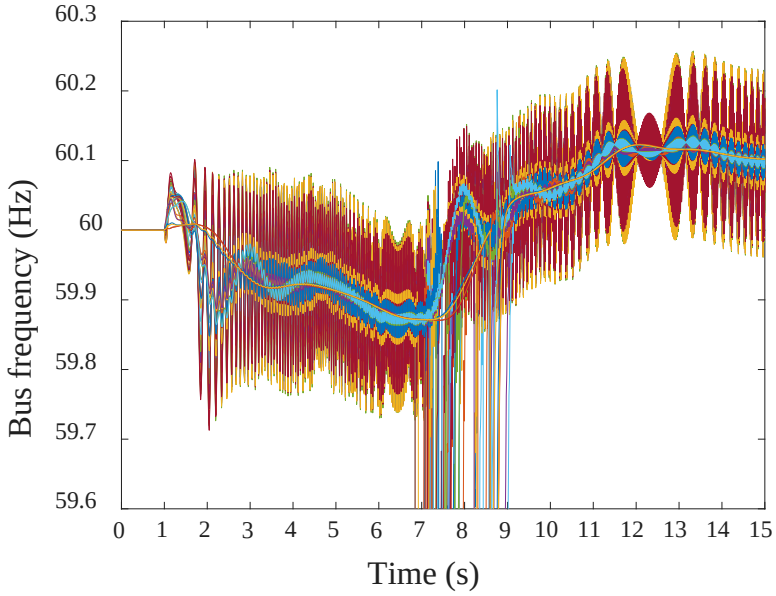

Figure 3.13 Bus Voltage Magnitudes without Modeling OOS Relays for Navajo Generators

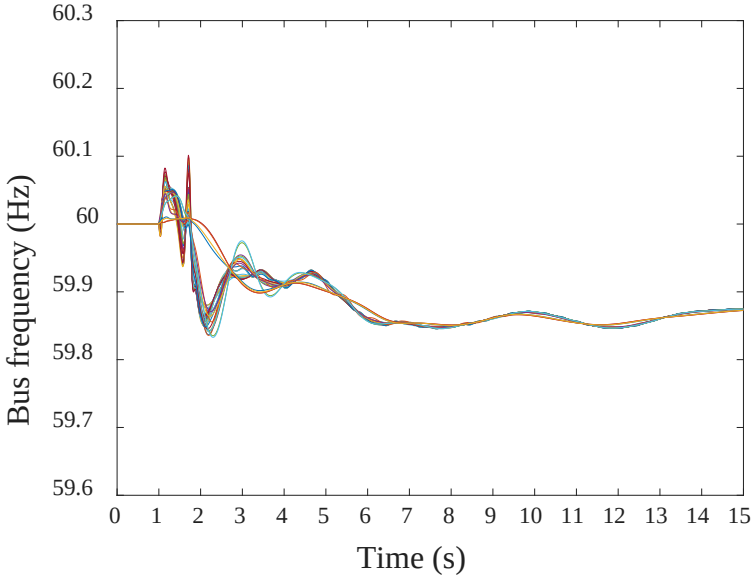

Figure 3.14 Bus Voltage Magnitudes without Modeling OOS Relays for Navajo Generators

3.5 Summary

This chapter shows the importance of modeling distance relays, OOS generation relays, UVLS, and UFLS relays within a transient stability study in order to achieve a realistic estimate of system behavior. Modeling OOS relays for transmission lines is explored in section 4, where an analytical method is presented that identifies the proper locations for OOS blocking functions. Modeling all

of the distance relays, data preparation, and data maintenance are exhaustive tasks. Therefore, this report proposes a methodology that can successfully identify critical distance relays to be modeled in transient stability studies.

4. Identifying Mis-operating Relays for Unstable Power Swings

Data from many blackouts in North America confirm that distance relay mis-operation is one key factor that may initiate a series of outages, which can cause a blackout. A power swing, triggered by initiating events, can cause protection system mis-operation. During an unstable power swing, the voltage magnitude at the electrical center will be depressed, resulting in protective relays detecting what appears to be a fault and, thus, the protective relays will trip additional transmission lines [4]. Undesirable operation (also referred to as mis-operation) of relays may lead to reduction of transfer capability, unwanted islanding, and/or load shedding and excessive generation. The load-generation unbalance can cause under-frequency relays to operate in each unintentional island leading to system collapse. In order to avoid cascading events, the distance relays, which are located at the electrical center, should be blocked from tripping.

This report proposes a methodology, minimum voltage evaluation method, that contributes to the challenge to detect mis-operating relays during unstable power swings and identifies essential locations for OOS blocking functions. The proposed minimum voltage evaluation method extends the empirical based approach of [8] with an analytical approach to determine the worst voltage dip along transmission lines. This approach is not only effective but it is straightforward, easy to implement, and computationally fast making it suitable for large-scale power systems. Furthermore, the simulation results demonstrate that the proposed approach is able to detect all transmission lines along the electrical center. Prior methods, such as the projected relay trajectory method in [32], do not detect all potential mis-operating relays, which can lead to further relay mis-operation and, thus, a cascading outage.

In the following sections of this chapter, the impedance observed by distance relays at relay location is studied first. Then, an overview of the previous methods for identifying electrical center is shown. The electrical center detection method proposed by [32] is described in detail. The proposed method of this research is explained in section 4.3.

4.1 Swing impedance locus seen by distance relay

A distance relay may recognize a power swing as a fault if the impedance observed by the relay enters the relay impedance characteristic. The impedance measured by the relay during an OOS condition is presented below. Figure 4.1 shows the one-line diagram of a two-generator equivalent system.

The location of the relay, whose behavior is studied here, is shown in Figure 4.1. Each generator may represent a generator or a group of generators, which remain in synchronism with respect to each other.

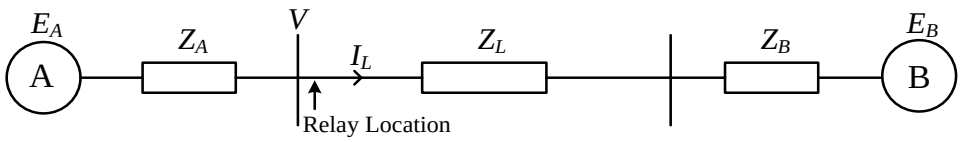

Figure 4.1 One-line Diagram of the System

The impedance observed by the relay is calculated as follows,

$$I_L = \frac{E_A - E_B}{Z_A + Z_L + Z_B} \tag{4.1}$$

$$V = E_A - I_L Z_A = E_A - \frac{(E_A - E_B)Z_A}{Z_A + Z_L + Z_B} \tag{4.2}$$

$$Z = \frac{V}{I_L} = \frac{E_A}{E_A - E_B}(Z_A + Z_L + Z_B) - Z_A \tag{4.3}$$

Considering E_B as the reference and that E_A advances in phase ahead of E_B by the angle θ and magnitude of nE_B,

$$\frac{E_A}{E_A - E_B} = \frac{n(\cos\theta + j\sin\theta)}{n(\cos\theta + j\sin\theta) - 1} = \frac{n[(n - \cos\theta) - j\sin\theta]}{(n - \cos\theta)^2 + \sin^2\theta}. \tag{4.4}$$

Reference [33] presents a figure (Figure 13 in chapter X of [33]) that shows a general impedance chart for various values of n and θ. For $n = 1$,

$$\frac{E_A}{E_A - E_B} = \frac{1}{2}(1 - j\cot\frac{\theta}{2}) \tag{4.5}$$

and, thus,

$$Z = \frac{Z_A + Z_L + Z_B}{2}(1 - j\cot\frac{\theta}{2}) - Z_A. \tag{4.6}$$

Point *P* in Figure 4.2 shows the value of Z for a particular θ and for $n = 1$. Moreover, various components of Z ($\frac{Z_A + Z_L + Z_B}{2}$, $(-j\cot\frac{\theta}{2})\frac{Z_A + Z_L + Z_B}{2}$, and $-Z_A$) are shown in Figure 4.2. Using the vector addition rule for these components, the relay impedance values (Z) lies on the dashed line through OP for any value of θ. The impedance observed by the relay (line OP in this case) during an OOS condition is referred to as loss of synchronism characteristic or power swing locus. Line OP is the perpendicular bisector of the line connecting points A and B.

During power swing, the generators slip poles, i.e., $\theta = 180$. Calculating (4.6) for $\theta = 180$,

$$Z = \frac{Z_A + Z_L + Z_B}{2} - Z_A. \tag{4.7}$$

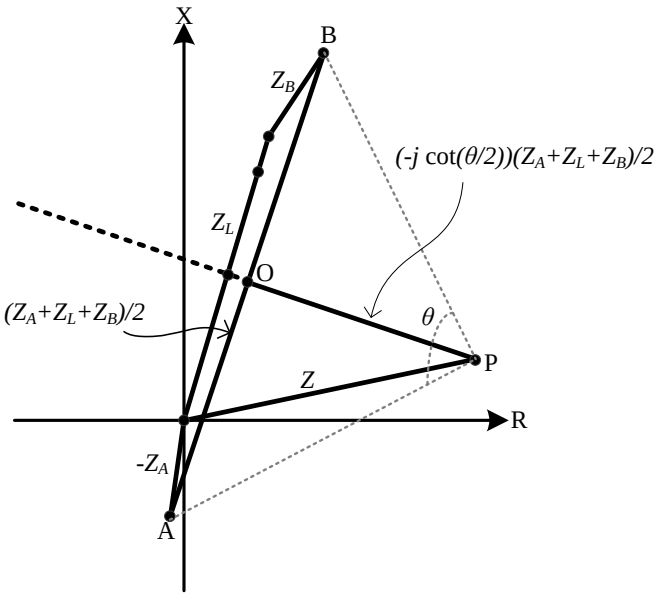

Figure 4.2 Relay Impedance Trajectory [15]

Using (4.7) and the vector addition rule in Figure 4.2, the relay observes the impedance at point *O* for $\theta = 180$. Therefore, loss of synchronism characteristic intersects impedance characteristic in OOS condition, i.e., $\theta = 180$. At this point the relay observes conditions identical to a three-phase fault. This point is electrically approximately midway between the ends of the line and indicates the "electrical center" of the system. At the point where line AB intersects the relay impedance, generator A has advanced generator B by 180 degrees [10]. In other words, at the electrical center, the two generators are 180 degrees apart. When a generator relative rotor angle reaches 180 degrees, the machine is said to have lost synchronism, reached an OOS condition, or have slipped a pole.

Figure 4.3 shows the locations of P for various values of θ. This location can be found by drawing straight lines from either A or B at an angle of $(90 - \theta/2)$ to AB and determines its intersection with the perpendicular bisector of line AB.

Figure 4.4 shows loss of synchronous characteristic for various values of *n*. When the transmission line is long (200-300 miles), the impedance locus is similar to $n > 1$ or $n < 1$ [10].

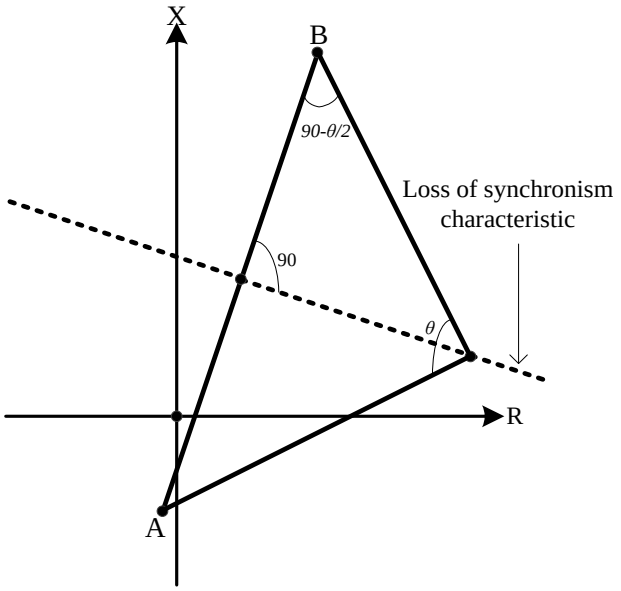

Figure 4.3 Loss of Synchronism Characteristic

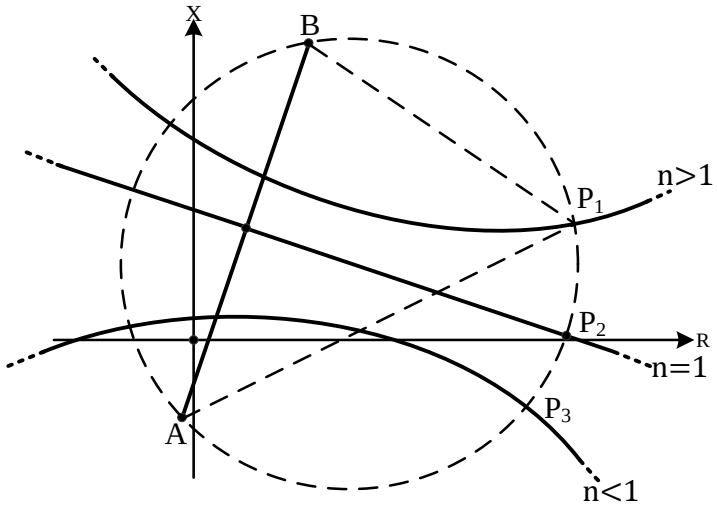

Figure 4.4 Loss of Synchronism Characteristic for Various Values of n

As shown in this figure, the electrical center may not be located electrically midway of a line impedance for $n \neq 1$. An interesting observation is the dashed circle. This circle intersects the loss of synchronism characteristic for various value of *n* for the same value of θ. In other words, P1, P2, and P3 occur at the same value of angle difference but for different values of *n*. Another interesting fact is that the ratios of lengths of lines drawn from A and B to any of these points is equal to *n*. For instance, AP1/BP1=*n* in Figure 4.4 [15].

Figure 4.5 shows the relay characteristic with the loss of synchronism characteristic displayed in the same R-X plot. It can be seen that the loss of synchronism characteristic enters the relay

characteristic when there is an increase in the value of θ. When generator A advances generator B by θ_2, the loss of synchronism characteristic enters the zone 2 characteristic of the distance relay. Similarly, for the angle difference of θ_3, the synchronism characteristic enters the first zone of the relay. Furthermore, if the angle difference increases to 180, the relay will observe a zero magnitude voltage at the electrical center. As mentioned previously, at the electrical center, conditions identical to a three-phase short circuit will be observed by the relay and swing impedance locus intersects the line impedance. For this unstable case, the relay will trip unless it is blocked from tripping by the use of an OOS blocking scheme. In order to obtain a proper OOS scheme, the separation should take place considering load and generation balance in each island and the stability of each island. Thus, it is usually required to block the lines, which observe the electrical center, from tripping. This requires the operator to perform sufficient studies and recognize the electrical centers properly.

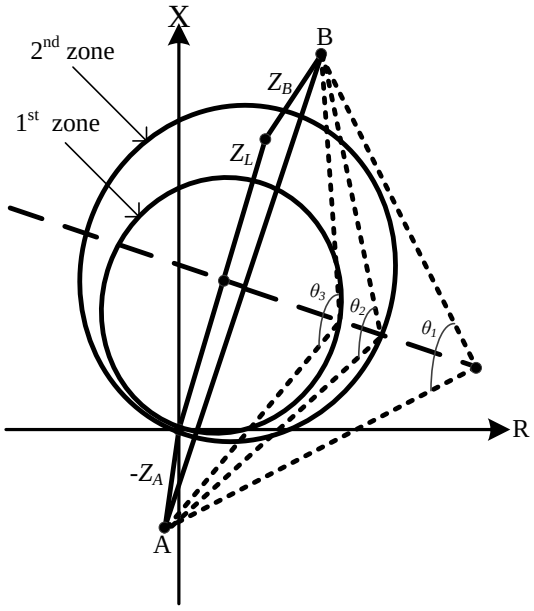

Figure 4.5 Relay Mho and Loss of Synchronism Characteristic

In the following section of this chapter, various different electrical center detection methods are reviewed. The method presented in section 4.2.3 is based on the intersection of swing impedance locus with line impedance. This method is presented in reference [32]. This report proposes the method explained in section 4.3, which is based on voltage properties of the electrical center.

4.2 An overview of electrical center detection methods

4.2.1 Traditional methods

In the literature, some approaches have been proposed to determine whether a loss of synchronism characteristic traverses a specific line. Most of these methods are based on reduction of the complex power system to a two-source equivalent system (Thévenin equivalent model similar to

Figure 4.1). IEEE PSRC WG D6 [11] presents two different processes for reducing a complex power system to a two-source equivalent system connected by a transmission line parallel to the line of interest. One of these methods utilizes the output of an equivalent network from a commercial short circuit program while the other method uses three-phase short circuit currents from a short circuit program. These two models are explained here.

4.2.1.1 Finding equivalent models from commercial short circuit program

This method uses the output of a commercially available short circuit program in order to find the equivalent models. The under-study line is deleted from the system and an equivalent two-part network as seen from the two ends of the line of interest is calculated using the commercial short circuit program. This equivalent model is shown in Figure 4.6; (Z_S , Z_R, and Z_{TR}) are reported by the short circuit program. At this stage, the transmission line of interest is inserted back to the model and the total impedance (Z_T) is calculated:

$$Z_T = Z_S + \left[\left(Z_{TR} Z_L \right) \Big/ \left(Z_{TR} + Z_L \right) \right] + Z_R \qquad (4.8)$$

Z_T is used to study whether the line in along the system wide electrical center; this analysis is similar to the analysis of section 4.1. It is considered that the swing locus bisects Z_T, assuming the equal source voltage magnitude ($E_S = E_R$).

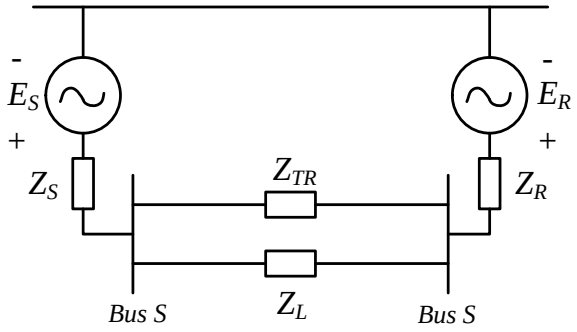

Figure 4.6 Two-Source System Equivalent [11]

4.2.1.2 Using three-phase short circuit currents from a short circuit program for finding equivalent model

The second method is based on the knowledge of the total three-phase fault current at the two ends of the under-study transmission line as well as the fault current flow on this line. Considering the following distribution factors,

$$K_S = \frac{I_{3\Phi-RS}}{I_{3\Phi-S}} \qquad (4.9)$$

$$K_R = \frac{I_{3\Phi-SR}}{I_{3\Phi-R}} \tag{4.10}$$

where $I_{3\Phi-RS}$ and $I_{3\Phi-SR}$ are fault currents over the line for a three-phase fault at bus *S* and *R* in per unit respectively. $I_{3\Phi-S}$ and $I_{3\Phi-R}$ are the total fault currents for a three-phase fault at bus *S* and bus *R* in per unit respectively.

Using (4.11)-(4.13), the wye equivalent network can be calculated; this network equivalent is shown in Figure 4.7.

$$X_1 = \frac{K_S Z_L}{1-(K_S + K_R)} \tag{4.11}$$

$$Q_1 = \frac{K_R Z_L}{1-(K_S + K_R)} \tag{4.12}$$

$$W_1 = Z_{Th-S} - X_1(1-K_S) \tag{4.13}$$

Z_{Th-S}, which is the positive-sequence driving point impedance for a fault at bus *S*, is shown in (4.14),

$$Z_{Th-S} = \frac{1}{I_{3\Phi-S}}. \tag{4.14}$$

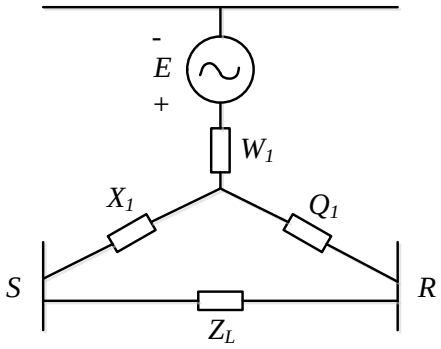

Figure 4.7 Wye System Equivalent with Line Reintroduced between Buses S and R [11]

By converting this wye model to a delta equivalent, the equivalent model is then similar to Figure 4.6. The reduction of a complex power system to a two-machine system can be considered as the traditional approach to determine the electrical center. Reference [8] specifies that these methods are applied to a northwest portion of the Eastern Interconnection of the United States. The system includes a ring of 345 kV transmission lines around an underlying 115 kV system. The equivalent

methods recognize that the swing center will pass through at least one of these 345 kV lines and most of 115 kV lines.

However, if any machine loses synchronism with their own group, this approach (two-machine equivalent model) cannot be used and a network-analyzer study is required [15]. The two-machine equivalent approach requires a-priori knowledge of the electrical center location since the two asynchronous groups of generators cannot be modeled as a single equivalent machine, i.e., the rotor oscillations are not in phase. In addition, [8] refers to [32] with regards to this two-machine equivalent method, "*When more than a line or two are to be analyzed, it is virtually impossible to use the method,*" [34]. It is explained that these methods are useful for identifying the electrical center between independent systems connected by limited number of tie lines.

4.2.2 Observing relay impedance characteristic method

Reference [10] expresses that the traditional method is not applicable for network type systems. It is explained that, it is necessary to perform a transient study on all possible combination of operating conditions; using a present-day advanced transient study program, the impedance locus at any or all transmission lines can be studied during the power swing. The intersection of this impedance locus and the line impedance can be studied in order to specify whether the line is along the electrical center. However, this approach is not applicable for large-scale test cases. An auxiliary method should be applied to find the intersection of the impedance locus and line impedance. One auxiliary method is explained in Section 4.2.3 below.

4.2.3 Projected relay trajectory method

Reference [32] provides a new approach, which is a more practical approach for the method in [10]. The technique suggested in [32] is innovative and advantageous in locating the electrical center for an unstable power swing. In this method, two sequential points on the relay impedance trajectory (corresponding to two sequential time intervals of transient studies) are projected to a perpendicular line of the transmission line impedance. If these projected values are of opposite algebraic signs, it is concluded that the relay impedance trajectory has intersected the line impedance characteristic between these two time intervals; therefore, the transmission line under study lies along the electrical center. Throughout the rest of this report, the term "*projected relay trajectory method*" will refer to the electrical center detection algorithm in [32].

Reference [32] explains that the following two criteria are two features of an electrical center:

- The ratio of the magnitude of relay impedance to the magnitude of line impedance is less than 1. This is referred to as the magnitude criterion.
- At an electrical center, the relay impedance angle (θ_R) is equal to the transmission line impedance angle (θ_L). This criterion is referred to as the angle criterion. As the transient stability study just simulates the snapshot of the system, achieving $\theta_R = \theta_L$ is not likely. One can use the sign changes in ($\theta_R - \theta_L$) between two consecutive snapshots to check for this criterion.

However, the authors of [32] have explained that using these two criteria may not be sufficient. They indicate that the proper method is to find the exact point of intersection of the loss of synchronism characteristic and transmission line impedance. This point should be in the first quadrant to represent an electrical center. For this purpose, trajectory sensitivity of the rotor angles to the branch impedance is implemented. Projected relay trajectory algorithm to locate the electrical center on a transmission line is as follows.

Let $Z_t\,(R_t, X_t)$ and $Z_{t-1}\,(R_{t-1}, X_{t-1})$ represent the relay impedance at instants t and $t-1$ respectively. $Z_L\,(R_L, X_L)$ represents the transmission line impedance.

1. In order to check if the electrical center is located on the transmission line between instants t and $t-1$ (the loss of synchronism characteristic intersects transmission line impedance (Z_L)), Z_t and Z_{t-1} are projected on to the axis perpendicular to the transmission line impedance. This is shown in Figure 4.8. Assume α and β are the projected points,

$$\alpha = -X_L \times R_t + R_L \times X_t \tag{4.15}$$

$$\beta = -X_L \times R_{t-1} + R_L \times X_{t-1}. \tag{4.16}$$

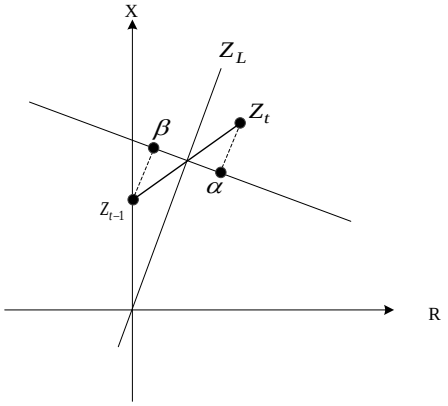

Figure 4.8 Projection of Swing Impedance on the Axis Perpendicular to the Transmission Line Impedance

2. If α and β have opposite signs, then Z_t and Z_{t-1} are located on the opposite side of the transmission line impedance, which indicates that the swing impedance locus intersects the line impedance characteristic between these two time steps. The intersection of the transmission line impedance and the loss of synchronism characteristic indicates the electrical center impedance, which is referred to as (R_E, X_E).

   Let $m_R = \dfrac{X_t - X_{t-1}}{R_t - R_{t-1}}$, $m_L = \dfrac{X_L}{R_L}$, and $c = X_t - m_R \times R_t$.

Then,

$$R_E = \frac{c}{m_L - m_R} \tag{4.17}$$

$$X_E = m_L \times R_E \tag{4.18}$$

If either α or β is zero, then the corresponding impedance (Z_t or Z_{t-1}) actually lies on the transmission line impedance. Therefore, the electrical center impedance is either Z_t or Z_{t-1}

3. If $0 \le R_E \le R_L$ and $0 \le X_E \le X_L$, then the electrical center exists on the transmission line of interest (R_E, X_E).

This method identifies the electrical center properly. However, there are other circumstances during the power swing when the relays may mis-operate; for instance, the swing impedance locus may enter zones of the relay characteristic and can cause mis-operation. This method is not able to recognize this situation as the swing impedance is not intersecting the line impedance characteristic. In addition, this method considers the transition of swing impedance between the two time steps as a line. However, this behavior may not be necessarily linear. This assumption impacts the accuracy of the result. This report proposed an electrical center detection method, which does not suffer from such shortcomings. The projected relay trajectory method [32] is implemented and compared with the method proposed in this report. Section 4.5 provides examples where the projected relay trajectory method fails.

4.2.4 Identification of coherent generators

Reference [35] presents a method to find the coherent groups of generators during a fault and at the post-fault stage. The coherent group of generators is found by comparing rotor angles of pairs of generators during the fault and at early stage of post-fault period. The unstable equilibrium point is studied to determine the coherency of the generators at an early post-fault stage. In order to make sure that each group stays coherent in the later stages, the admittance distances between the groups of generators are checked. The coherent groups of generators can also provide some information for the power swing center. The transmission lines connecting two different groups are potentially along the electrical center.

4.2.5 Voltage dip screening method

In [8], the system protection and control subcommittee of NERC suggests a voltage dip screening method in order to identify power swings and locate the system electrical center of a power swing. The voltage dip screening method in [8] can be used in transient planning studies. Such planning studies evaluate the power system operating condition, including voltages, for many contingencies in order to study the compliance of the system with various standards. The approach from [8] examines voltage drops during oscillations of the coherent groups of generators, i.e., inter-area oscillations. The transmission lines between these coherent groups of generators (at the electrical center) experience a condition similar to a three-phase short circuit, i.e., the line-to-line voltages become zero [33] and [36]. Using this attribute, the voltage dip screening method in [8] suggests

that monitoring the voltage magnitude throughout the system (at buses) can be considered as a flag for a power swing and can detect the electrical center. Empirical evidence shows that voltage magnitudes at buses, particularly at those buses connected to lines along the electrical center, drop to at least the range of 0.5 and 0.6 pu [8]. Moreover, an analysis is performed in [8] in order to show the correlation between the voltage dip and presence of the relay impedance trajectory in distance relay zones. This reference indicates that additional studies need to be conducted in order to establish voltage dip thresholds. Although the suggested method in [8] is based on empirical results and is intuitive, it sheds light on the application of voltage evaluation techniques for power swing conditions and system electrical center detection.

Reference [37] explains the voltage dip as the main problem of unstable power swings. It is explained that for voltage dips below 0.8 pu, some large industrial drives and motors may trip and cause unwanted situations. This reference has tried to find voltage dips by calculating the maximum potential energy.

4.3 Minimum voltage evaluation method for electrical center detection

This report proposes a method that provides a screening tool for OOS and electrical center detection during transient stability planning studies, which can be considered an extension of the voltage dip screening method [8] (section 4.2.5). While the method of [8] relies on a voltage drop only at buses, the proposed analytical approach can evaluate voltage magnitudes anywhere along all transmission assets. The proposed extension is critical since a voltage dip screening approach relying only on bus voltage magnitudes can be highly inaccurate since the electrical center can occur at a bus or along a transmission line. Terminal buses of the transmission lines along the electrical center may not experience extreme voltage drops. Note that [8] examines only stable power swings while the proposed approach also applies to unstable power swings.

The proposed method evaluates the voltage magnitude throughout the system using the outputs of the transient stability planning study. The voltage magnitude along each transmission line can be calculated based on the network solution, i.e., the value of bus voltages and transmission lines flows, at each time interval of the transient stability study. Therefore, the proposed model does not require any modification to existing transient stability study practices.

If the magnitude of the voltage along transmission lines (or at the terminal buses) reduces significantly, while no fault is present on the transmission line, it can be concluded that the system is experiencing an unstable power swing. In addition, the distance relays of the transmission lines with the depressed voltage are prone to operate. Therefore, these relays should be equipped with OOS blocking functions.

This method includes the following assumptions: 1) the shunt admittance of lines are considered to be negligible. Therefore, the current through the line is assumed to be same as the current at the ends of the line. 2) It is assumed that the line impedance is uniform throughout the length of the line.

First, a transient stability study for the critical contingency needs to be performed. Using bus voltages and transmission lines flows, which are known for each time interval from the results of

the transient stability study, the value of voltage along each transmission line can be evaluated using (4.19). Note that a represents the fraction of the length of the transmission line under study. This is shown in Figure 4.9.

$$\begin{aligned} V_a &= V_1 - a \times (R + jX) I_1 \\ &= \left(V_{1x} - aRI_{1x} + aXI_{1y}\right) + j\left(V_{1y} - aXI_{1x} - aRI_{1y}\right) \end{aligned} \tag{4.19}$$

where V_{1x}, V_{1y}, I_{1x}, and I_{1y} are real part of V_1, imaginary part of V_1, real part of I_1, and imaginary part of I_1 respectively. Moreover, R and X are resistance and reactance of the transmission line respectively. Therefore, the magnitude of V_a is as (4.20).

$$|V_a| = \sqrt{\left(V_{1x} - aRI_{1x} + aXI_{1y}\right)^2 + \left(V_{1y} - aXI_{1x} - aRI_{1y}\right)^2} \tag{4.20}$$

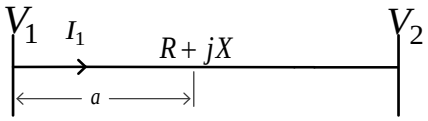

Figure 4.9 Evaluation of Voltage throughout the Transmission Lines

From the result of transient stability study, all of the variables on the right hand side of (4.20) (except a) at each time step are known. Therefore, the voltage magnitude through the line (for various values of a) can be calculated at each snapshot of time under study. Furthermore, the minimum voltage magnitude, which shows the worst voltage dip, through a transmission line can be calculated at each time interval using the minimization problem presented in (4.21). Evaluating this minimum voltage, it is possible to determine whether the protective relays of line would mis-operate during an unstable power swing. It is expected that the voltage magnitude reduces to zero at a point through the lines, which are located along the electrical center.

$$\begin{aligned} &Minimize \quad |V_a| = \sqrt{\left(V_{1x} - aRI_{1x} + aXI_{1y}\right)^2 + \left(V_{1y} - aXI_{1x} - aRI_{1y}\right)^2} \\ &Subject\ to: \quad 0 \le a \le 1 \end{aligned} \tag{4.21}$$

The minimization problem is a single variable optimization problem, i.e., a is the only unknown in this problem. There are three types of points that this non-liner problem can have a local minimum solution: 1) Points where $\frac{d|V_a|}{d_a} = 0$ for $0 \le a \le 1$. 2) End points, i.e., a=0, or a=1. 3) Points where $\frac{d|V_a|}{d_a}$ does not exists. The smallest value of $|V_a|$ among the local minimums is considered as the global minimum solution for minimization problem represented in (4.21).

This method calculates the minimum voltage through each transmission line and at each time step of the transient stability study. This minimum voltage then will be evaluated. If the minimum

voltage along a transmission line (in the absence of a fault) is zero, the contingency would lead to an OOS condition and the associated line is along the electrical center. However, the transient stability study monitors the system behavior in discrete time intervals. The voltage magnitude through the line may traverse to zero in between two discrete time intervals. In such cases, it is insufficient to search for a voltage magnitude of zero. Since power swings traverse slowly, a small threshold can be considered for this technique. Therefore, if (4.22) holds, the contingency would lead to an unstable power swing and the transmission line is located along the electrical center.

$$\left|V_{a^{min}}\right| \leq \varepsilon \tag{4.22}$$

where $\left|V_{a^{min}}\right|$ is the minimum voltage magnitude through the transmission line, which occurs at a^{min} fraction of the length of the line and ε represents the established threshold.

Note that the minimization problem, (4.21), and the evaluation of (4.22) should be performed for all time intervals of the transient stability study in order to detect all of the mis-operating relays.

4.4 Test case and contingency description

The WECC system data, which is explained in Section 3.1 and represents the 2009 summer peak load case, is used to perform the analysis. The California-Oregon Interface (COI) are very critical tie lines, which are transferring about 3800 MW from north to south during this hour.

First, an outage on two of the three COI ties is studied, which causes a stable power swing. The minimum voltage during this stable power swing is evaluated and the application of the minimum voltage evaluation method is explained in Section 4.5.1. Second, a fault on bus MALIN, located in the Northwest area, is modeled. It is considered that this fault leads to the outage of all three COI tie lines, which results in an unstable power swing; see Sections 4.5.2-4.5.4 for a discussion of this case. Both these contingencies fall under category D of the NERC standard [38].

In the dataset provided, no distance relays are modeled. As it is mentioned in Chapter 3, the term “base case” will be used in reference to the results pertaining to the original dataset. Transient stability analysis is first performed on the base case dataset considering the described contingencies (double and triple outages of the COI).

Additional studies are conducted where the triple line outage of the COI is studied with the modeling of distance relays for all lines at or above 100 kV. These distance relays are modeled using a model from the PSLF library [31]. This model, *zlinw*, just considers two zones for each distance relay. Please note that this specific distance relay model is chosen due to the large-scale test case and software limitation. The settings of these relays are similar to section 3.2. The zone 1 and zone 2 of the modeled distance relays are considered to be 0.85 and 1.25 times the transmission line reactance respectively. Zone 1 initiates tripping without any time delay. A time delay of 0.25 seconds is considered for zone 2. The breaker operation time is modeled to be 0.03 seconds. While the relay settings for various distance relays are different across a system, these

settings are considered to be alike for all transmission lines because of the lack of available data for protection systems across the entire WECC.

A controlled islanding scheme is tested using the designed OOS protection. The OOS tripping is based on the well-known northeast/southeast (NE/SE) separation scheme for the WECC [39]-[41]. This separation would be initiated after receiving a transfer trip signal from Bonneville Power Administration (BPA) and Pacific Gas and Electric (PG&E) [42]. An OOS blocking scheme is performed based on the minimum voltage evaluation method. In order to compare the proposed method with previous research, the OOS blocking function, based on the projected relay trajectory method [32], is also tested.

In order to test both the minimum voltage evaluation and the method in [32], a series of steps are carried out to replicate existing industry practices. Existing practices for conducting transient stability studies do not contain the modeling of protection systems particularly distance relays. Therefore, transient stability studies are conducted using the base case dataset, which does not include the distance relays. The transient stability results are used by these two approaches, the minimum voltage evaluation method and the method from [32], to determine appropriate OOS blocking schemes; Sections 4.5.3-4.5.4 present these results. Next, the protection systems and associated OOS blocking schemes are then modeled in transient stability analysis to determine if there are any relay mis-operations using these two approaches, the minimum voltage evaluation method and the projected relay trajectory method [32]. Note that the corresponding RAS of the described contingency (outage of COI interties) are modeled in all simulations, which includes the tripping of generators in the northwest, brake insertion at Chief Joseph, generator and pump load tripping in northern California, series capacitor bypassing in northern California, shunt reactor or capacitor insertion where needed, and the NE\SE Separation Scheme [43]. The NE\SE Separation Scheme initiates after the trip signal is received at Four Corners. In addition, all other RAS schemes in [43], which may be initiated as a result of relay mis-operation based on the system conditions, are modeled. More details are provided in section 4.5.3.

4.5 Numerical results and analysis

All transient stability studies are performed using PSLF. The minimum voltage evaluation method and the projected relay trajectory method [32] are programmed using MATLAB to locate the potential mis-operating relays. First, the application of the proposed method for OOS detection is described in Section 4.5.1. Then, the impacts of the simultaneous outage of three COI ties are studied using the base case data in Section 4.5.2. A transient stability study for the triple line outage of the COI is performed while modeling distance relays and OOS protection schemes in Sections 4.5.3-4.5.4. In section 4.5.3, the OOS blocking is implemented based on the projected relay trajectory method [32]. The proposed minimum voltage evaluation method is tested in section 4.5.4.

4.5.1 Out-of-step detection

The minimum voltage evaluation method determines whether a specific contingency would cause an unstable power swing. After conducting a transient stability study, the minimum voltage of each

transmission line can be calculated using the proposed method. This minimum voltage magnitude can be used as an indicator of stability of the power swing. In this section, the outage of two COI ties is studied. This contingency causes a stable power swing, i.e., all generators swing together. The proposed method estimates the minimum voltage magnitude through all transmission lines in the system to be 0.43 pu. Performing a similar study for an unstable power swing, i.e., initiated by triple outages of the COI tie lines, the minimum voltage magnitude is observed to be 0 pu. Therefore, a voltage magnitude of 0 (or near to 0) in the power system (in the absence of a fault) indicates an unstable power swing.

4.5.2 System behavior during COI tie lines contingency

A transient stability study for the base case dataset considering the simultaneous outage of all three COI ties has been performed. The generators' relative rotor angles are shown in Figure 4.10. As observed in Figure 4.10, the generators are split into two separate groups. Some of the generators lose synchronism within their own group and continue to slip poles. For this operating condition and in response to the described contingency, the generators located in the northern part of the system accelerate in comparison to the generators located in the southern part of the system. Figure 4.11 shows the accelerating and decelerating areas within the WECC system for this power swing.

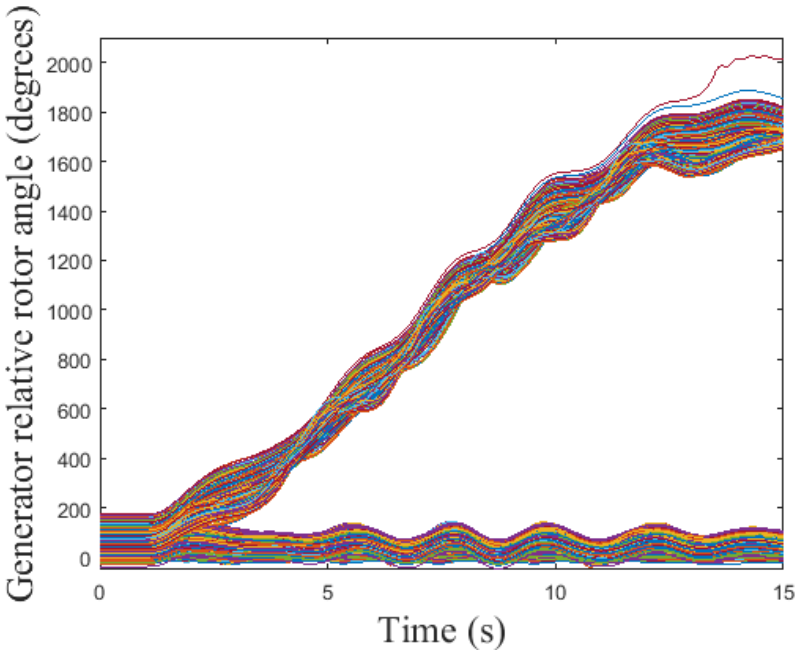

Figure 4.10 Generators Relative Rotor Angles for the Base Case.

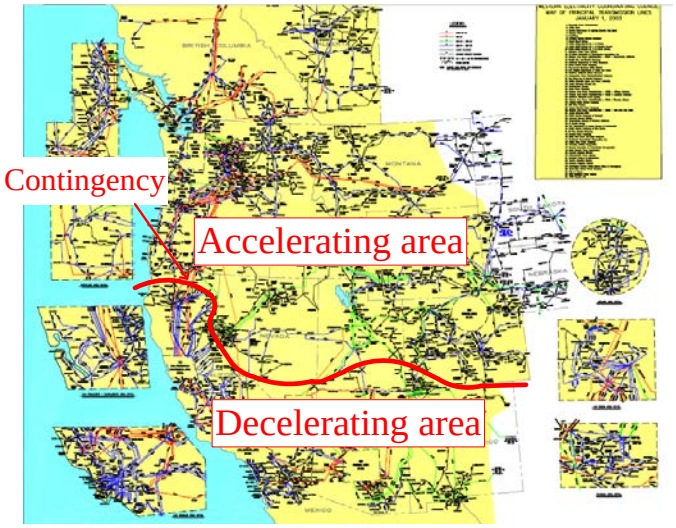

Figure 4.11 Acceleration and Deceleration Areas for the WECC System [39]

4.5.3 Out-of-step blocking using the projected relay trajectory method [32]

In this section, the simultaneous outage of all three COI ties, which results in an OOS condition, is studied. An OOS protection scheme is designed and modeled for the WECC system. The OOS blocking scheme is located on the transmission lines along the electrical center found by the projected relay trajectory method [32]. A separation scheme based on the slow coherency controlled islanding scheme is implemented [39]-[41]. This separation scheme is compatible with the NE/SE separation and splits the system into two islands. This split is implemented by tripping 15 transmission lines of the desired cutset during the OOS condition, which is initiated by the outage on the COI tie lines. In order to observe the impact of relay mis-operation, a delayed separation scheme is implemented. The time sequence of the actions is shown in Figure 4.12. Moreover, as mentioned in Section 4.4, the distance relays for all transmission lines at or above 100 kV are modeled.

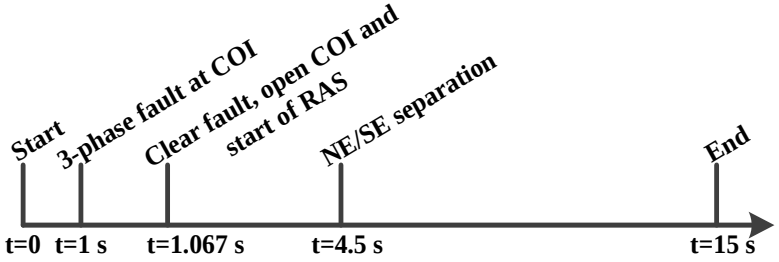

Figure 4.12 Time Sequence of the Contingency Under Study

When designing the OOS blocking functions based on the projected relay trajectory method [32], seven additional distance relays observe the relay impedance trajectory in their characteristic and mis-operate. These mis-operating relays protect three 345 kV, two 230 kV, and two 115 kV transmission lines. Mis-operation of one of the relays (namely Montrose-Hesperus 345 kV line) initiates a RAS action when the Nucla generators operate above 60 MW [43]: the Montrose-Nucla

115 kV line is automatically transfer tripped. This RAS action (TOT2A in [43]) is also modeled in this study. Please note that none of the other RAS actions, which are presented in [43], initiate during the performed study.

The relay impedance trajectory of one of the mis-operating relays located on a 345 kV line is shown in Figure 4.13. Zone 2 of this distance relay initiates tripping during this unstable power swing. The relay impedance trajectory enters and stays in the zone 2 characteristic of this relay for 0.316 s. This relay needs to be blocked from tripping. Blocking can be achieved using a dual blinder scheme. Unlike the projected relay trajectory method [32], the minimum voltage evaluation method is able to successfully detect this line as a necessary location to install OOS blocking function, such as a dual blinder scheme. All of the per unit (pu) values, which are specified in the figures, are calculated using the corresponding system base values.

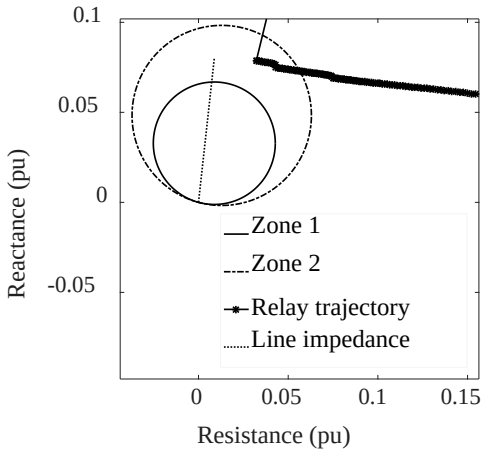

Figure 4.13 Relay Impedance Trajectory for a Mis-operating Relay on a 345 kV Transmission Line

The relay trajectory in Figure 4.13 is recorded while other distance relays have mis-operated and the network topology has been updated. As mentioned before, no distance relay is included while collecting the data input of the proposed method and the method of [32]. Therefore, the effects of mis-operation of relays are not captured in the initial study. In order to study the deficiency of the projected relay trajectory method [32], the relay trajectory should be studied without modeling the mis-operation of the other relays. Such a relay trajectory for the relay on the same 345 kV transmission line is shown in Figure 4.14. While the relay impedance trajectory passed very close to the line impedance, it does not intersect the line impedance; therefore, the projected relay trajectory method [32] is not able to predict mis-operation of this distance relay. It can be concluded that simply blocking the relay on the lines where their relay impedance trajectory intersects the line impedance is not sufficient; the protective relays on the other transmission lines, which connect two oscillating groups of generators, may mis-operate. A more generic approach needs to be implemented in order to recognize all of the mis-operating relays. These mis-operating relays need to be equipped with OOS blocking functions to prevent blackouts.

Similarly, the relay impedance trajectories of another mis-operating relay, which is located on a 115 kV line, are shown in Figure 4.15 and Figure 4.16. Figure 4.15 shows this relay impedance locus while including the modeling of distance relays and the OOS blocking function using method of [32], which results in other relays mis-operating as well. While in this figure the relay impedance trajectory intersects the line impedance, this transmission line is not detected by the method in [32] for a potential relay mis-operation.

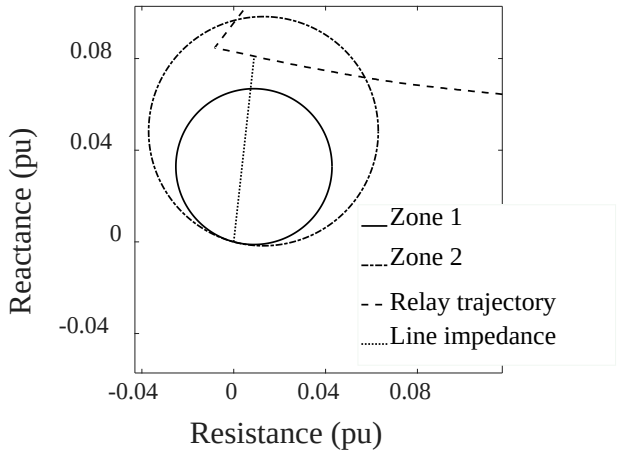

Figure 4.14 Relay Impedance Trajectory for a Mis-operating Relay on a 345 kV Transmission Line without Modeling any Distance Relay

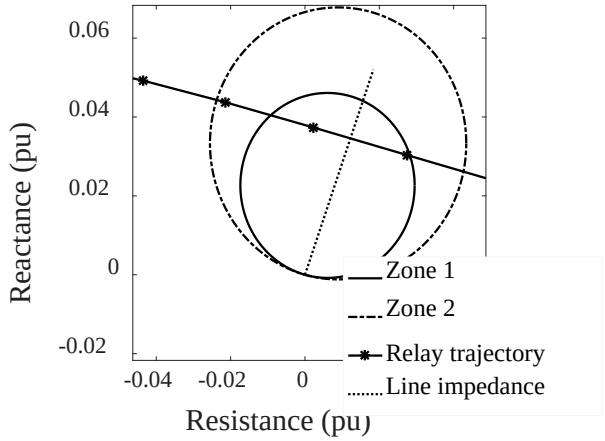

Figure 4.15 Relay Impedance Trajectory for a Mis-operating Relay on a 115 kV Transmission Line

Figure 4.16 shows the impedance trajectory of the same relay without considering the effects of other relay mis-operations. As seen in Figure 4.16, the relay impedance trajectory does not intersect the line impedance, which is why the projected relay trajectory method [32] is not able to predict the mis-operation of this line. Therefore, the projected relay trajectory method [32] is sensitive to the network topology and is inaccurate without modeling protection systems when conducting the initial transient stability study. To this date, due to the complexity of integrating,

maintaining, and updating protection system data with the transient stability data, these two different sets of data are usually handled separately. Therefore, a method with a high level of sensitivity to the protection system operation is less desirable. In addition, based on these results, it can be concluded that failing to detect relay mis-operation may cause additional relays to mis-operate.

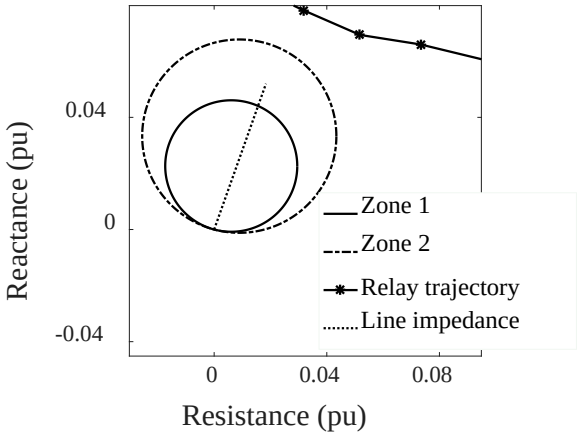

Figure 4.16 Relay Impedance Trajectory for a Mis-operating Relay on a 115 kV Transmission Line without Modeling any Distance Relay

As mentioned earlier in this section, seven additional distance relays mis-operate if the OOS blocking scheme is designed based on the projected relay trajectory method [32]. While modeling TOT2A RAS and as a result of mis-operation of these seven relays, four additional uncontrolled islands are formed: a 38-bus island, an 11-bus island, a 9-bus island, and one individually isolated bus. The 38-bus uncontrolled island is formed due to the mis-operation of 4 distance relays along with tripping of 3 other transmission lines due to the NE/SE separation. The bus voltage magnitudes and frequencies of these 38 buses are shown in Figure 4.17 and Figure 4.18 respectively. Similarly, the bus voltage magnitudes and frequencies of the 11-bus island are shown in Figure 4.19 and Figure 4.20.

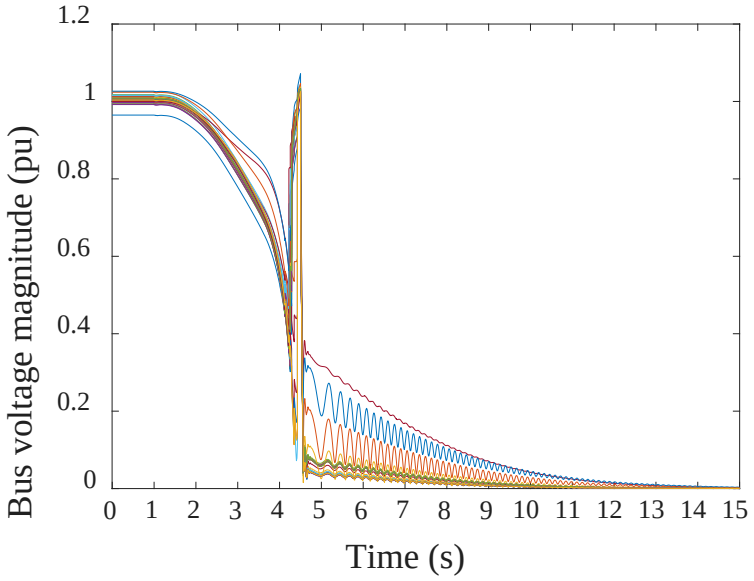

Figure 4.17 Voltage Magnitudes at 38 Buses of an Uncontrolled Island

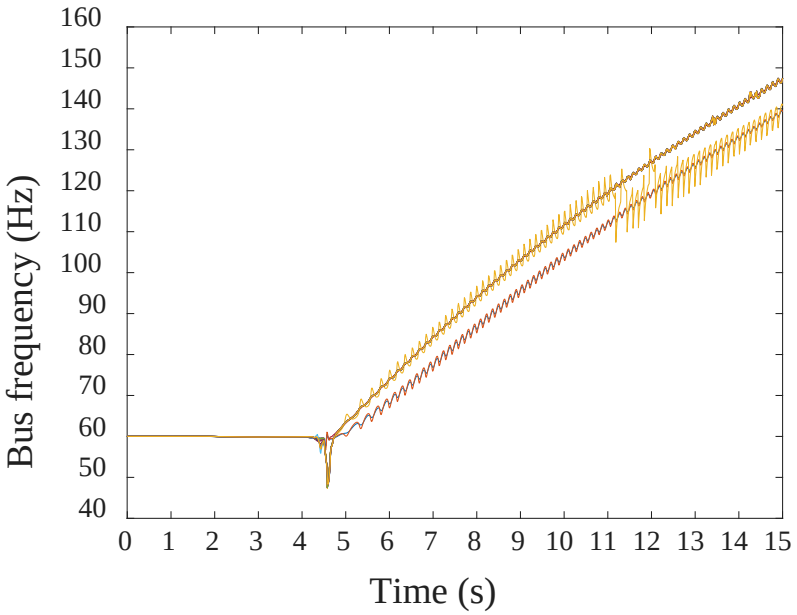

Figure 4.18 Frequency at 38 Buses of an Uncontrolled Island

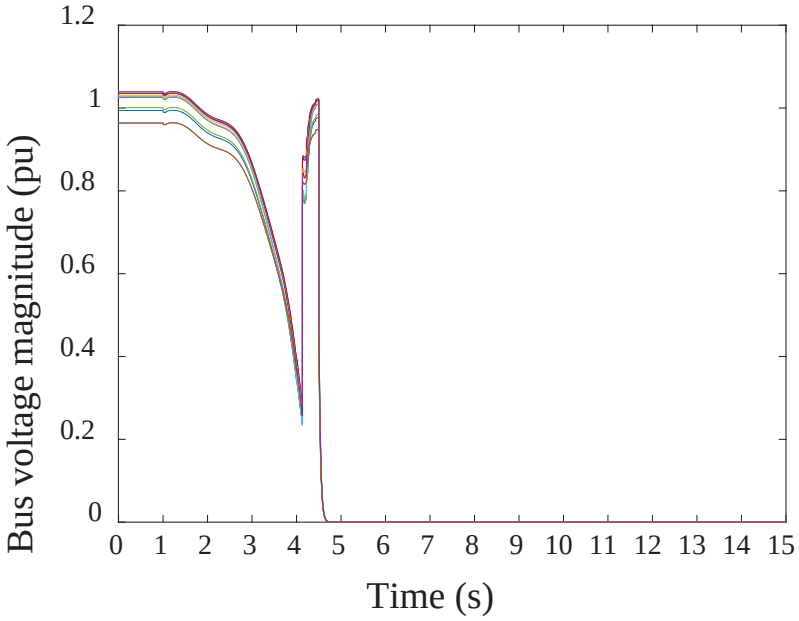

Figure 4.19 Voltage Magnitudes at 11 Buses of an Uncontrolled Island

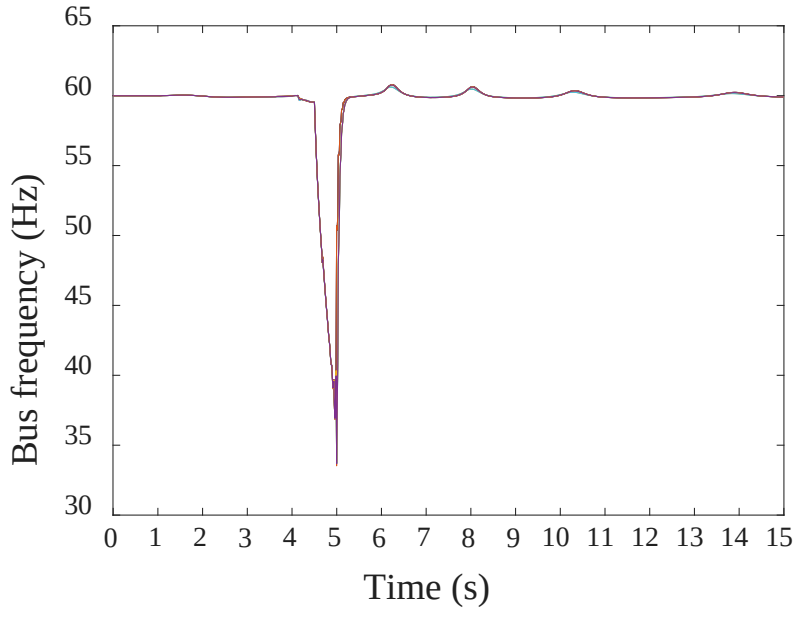

Figure 4.20 Frequency at 11 Buses of an Uncontrolled Island

The frequency at these 11 buses does not show disruptive behavior. However, Figure 4.15-Figure 4.17 show the collapse of voltage and frequency in these uncontrolled islands. It can be concluded that improper design of OOS blocking functions may lead to uncontrolled islanding, which in turn may result in voltage and frequency collapse in parts of the system. Finally, note that if the TOT2A RAS is not modelled, the results are similar to the results already presented above. Instead of the

formation of 4 uncontrolled islands, 3 uncontrolled islands are formed at roughly the same locations.

4.5.4 Controlled islanding

The simulated contingency, implemented distance relays, OOS tripping, and time sequence of the events are similar to section 4.5.3. However, the OOS blocking function is implemented based on the minimum voltage evaluation method. Using this proposed method, all of the potential mis-operating relays, including the seven relays that mis-operated using the projected relay trajectory method [32] in section 4.5.3, are successfully detected. By implementing the OOS blocking functions for these transmission lines along with the OOS tripping functions, the system is divided into two controlled islands (north and south islands). None of the distance relays will mis-operate; each of the two islands stay connected and synchronized. The voltage magnitudes and frequencies of the 38 buses and 11 buses, which constitute uncontrolled islands in Section 4.5.3, are shown in Figure 4.21- Figure 4.24. These buses stay connected to the rest of the system and their voltage magnitudes and frequencies show non-oscillatory and stable behavior at the end of the time horizon of the study.

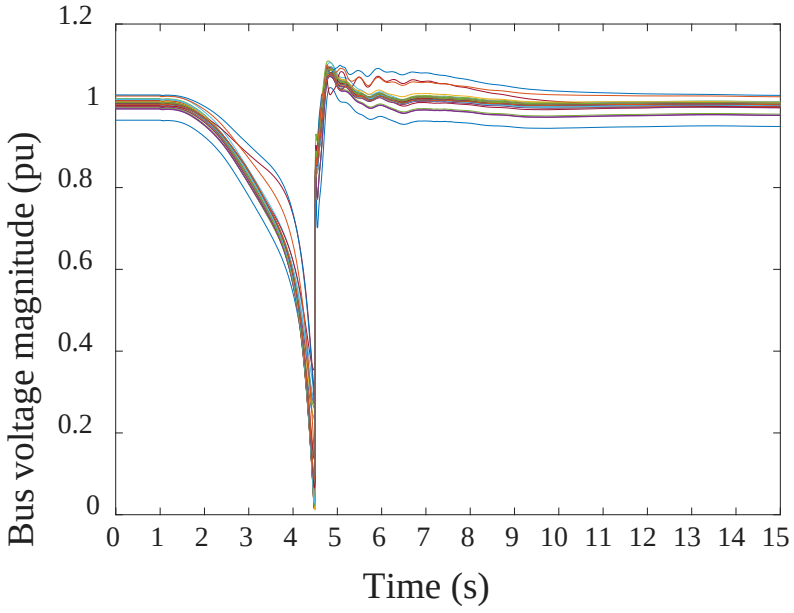

Figure 4.21 Voltage Magnitudes at 38 Buses for Controlled Islanding Case

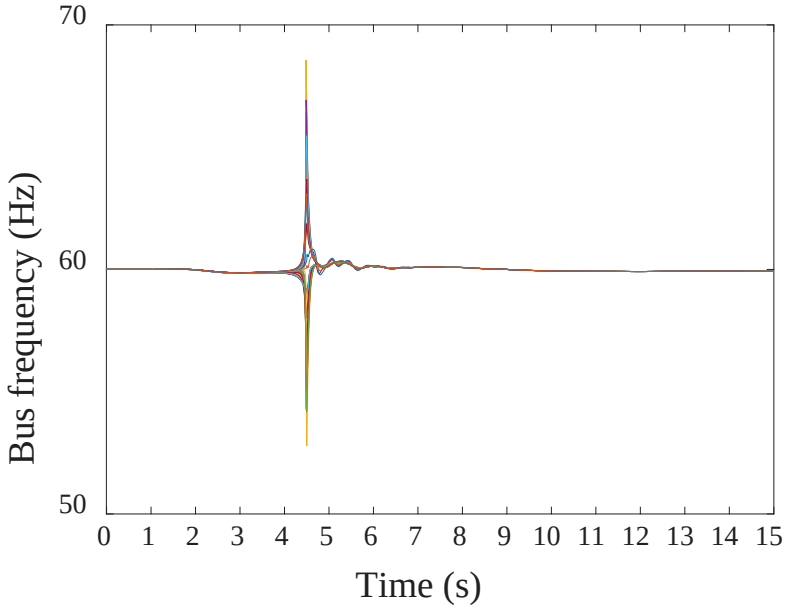

Figure 4.22 Frequency at 38 Buses for Controlled Islanding Case

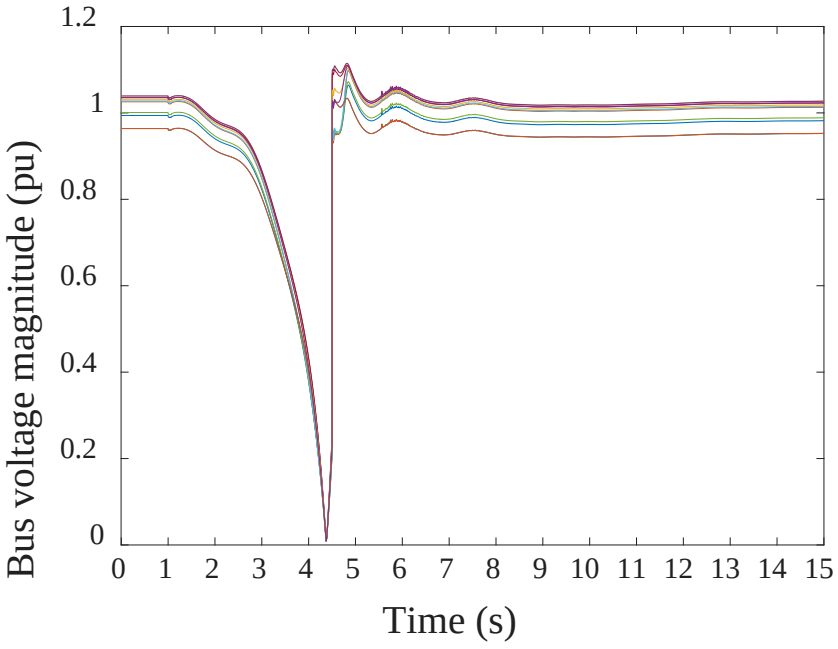

Figure 4.23 Voltage Magnitudes at 11 Buses for Controlled Islanding Case

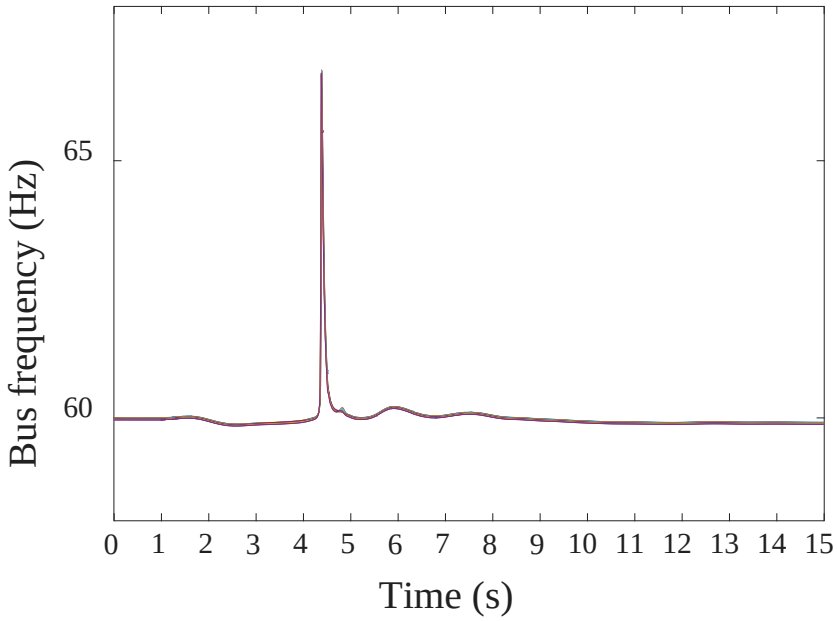

Figure 4.24 Frequency at 11 Buses for Controlled Islanding Case

Reference [8] indicates that a voltage dip in the range of 0.5 to 0.6 pu can be used to identify a power swing. Reference [8] explains that the buses that are close to the electrical center experience a voltage dip below 0.6 pu. The voltage magnitude profile for terminal buses of some of the transmission lines, which were recognized only by this proposed method (and not by the method [32]), are shown in Figure 4.25. As shown in these figures, the voltage magnitudes at these buses are compatible to the explanation of [8]. Similarly, other transmission lines, which were detected to be along the electrical center by the proposed method, satisfy this criterion. Note that there are cases where one bus voltage magnitude does not fall below 0.6 pu but still the line is along the electrical center. This confirms that the voltage dip screening method [8] requires more testing to be generalized.

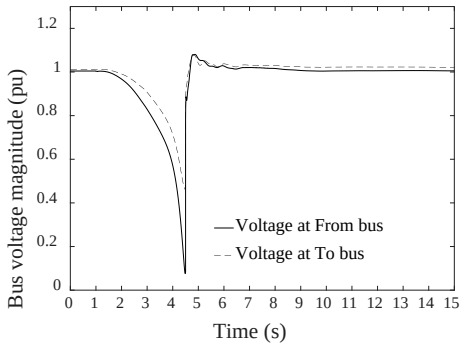

(a)

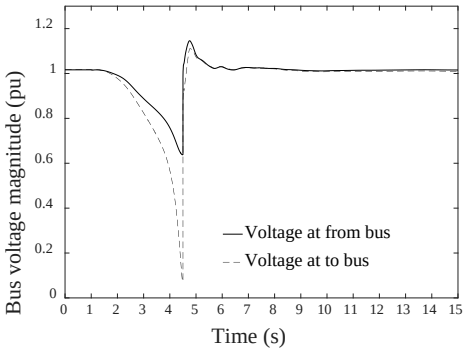

(b)

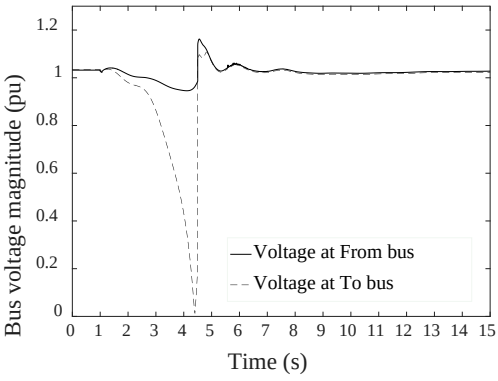

(c)

Figure 4.25 Bus Voltage Magnitudes for Buses Connected to the Potentially Mis-operating Relays with Voltage Level: (a) 115 kV; (b) 230 kV; (c) 345 kV

4.6 Summary

The impedance, which would be observed by the relay at the relay location, is studied in section 4.1. A review of the literature for electrical center detection is presented in this chapter. Most of the presented methods in the literature are based on finding a two-machine equivalent network. Each machine represents a coherent group of generators, which swing together with respect to the other generators. Such equivalent network methods require knowledge of the electrical center and the lines along that electrical center in advance, i.e., it requires knowing the two groups of generators that will form separate groups. Otherwise, the two groups of generators that are not in phase cannot be modeled as a single equivalent generator. Electrical center locations vary and need to be studied for various operational conditions, fault types, and fault locations. The challenge to complete multiple complex studies and the inaccuracy of the equivalent models are the primary causes of relay mis-operation. While this problem is well understood, the issue persists.

Section 4.3 describes a new method, which is proposed within this report. This method is based on finding and evaluating the minimum voltage through each transmission line at each time step of transient stability study. The proposed method of this report and the method of [32], which is explained in section 4.2.3, are tested on the WECC system.

In general, the exact location of the electrical center is a function of the operational condition, network configuration, and last but not least, the contingency. Several transient stability studies should be performed in order to find proper locations for OOS protection functions for each critical contingency.

5. Identification of Critical Protection Functions for Time-Domain Simulations

Lack of situational awareness is considered as one of the major causes of recent blackouts [44]-[47]. Improving situational awareness and observability is one of the key concerns of utilities and reliability coordinators. Inaccurate representation of power system assets in operation and planning software, lack of measurement data from unobservable parts of the system, and insufficient communication and coordination between associated operating entities are common factors of insufficient situational awareness in power systems [48].

After a major event, the power system behavior is highly dependent on protection scheme behavior and system dynamics, which is governed by generators, loads, and control devices [49]. Improving situational awareness requires proper and simultaneous assessment of both of these aspects: protection scheme behavior and dynamic characteristics. Power system analysis that is conducted without adequate modeling of these two aspects may result in inaccurate assessment of system behavior during a contingency. One critical simulation tool where appropriate protection system modeling is essential, is positive sequence time domain transient stability analysis. Sectionr 3 of this report shows the impact of modeling protection schemes in transient stability study. The proper representation of protection functions in stability software has been a long term goal for utilities. The records from previous blackouts confirm the necessity of representing protective devices within transient stability studies.

Modeling all of the protective relays within transient stability studies may result in a better estimation of system behavior. However, representing, updating, and maintaining the protection system data within dynamic study data is an intractable task. Misrepresentation of the protective relays in transient stability software may result in incorrect assessment of the system behavior. Therefore, developing a method that can properly determine *essential relays* to be modeled within transient stability studies would be extremely useful and it would address a long-lasting unsolved problem.

Previous research has developed strategies to identify the most vulnerable protective relays during a specific contingency. Reference [50] suggests that the transmission assets surrounding the faulted lines are the most vulnerable to hidden failures. Similarly, [51] proposes a strategy to identify the most vulnerable protection scheme by suggesting that the size of the vulnerable region depends on the size of the initiating event and the design of the protection schemes in the area surrounding this event. Reference [52] estimates the risk associated with the contingency in the vulnerable region of the initiating event. The vulnerable region and the vulnerable protection schemes in this prior work are identified based on the location and size of the initiating event.

The initiating event may lead to several hidden failures, which exacerbate the system state and may result in more outages. This chain of events may threaten system operations far away from the initiating event and may lead to a system wide blackout. Therefore, only modeling vulnerable protective relays of the initiating event may result in inaccurate estimation of the system behavior in an emergency state. In order to obtain a more accurate assessment of the system behavior and to design better control mechanisms, all of the vulnerable protective schemes, which may mis-

operate during emergency states, need to be identified so that they can be adequately modeled and represented in dynamic simulation tools.

The preferred methodology to identify vulnerable protective relays should specify relays that are critical for various operating conditions and contingencies. However, determining the critical relays for various operational transient conditions is a complex problem. Such a problem could be formulated as a stochastic mixed-integer non-linear program that would incorporate transient stability constraints. Given the complexity of this mathematical program, an exact algorithm is unlikely to be functional for large-scale systems. However, a heuristic strategy for this complex problem can be developed.

Many prior research efforts propose clustering systems into groups for various applications such as controlled islanding or regional requirements for ancillary services. One potential strategy for identifying critical protective relays is to partition the system such that the critical distance relays are located at or near the boundaries of these groups. Groups may be identified based on generators that exhibit similar responses to disturbances. The relays along the defined cutsets of these groups are, thus, assumed to have a higher likelihood to mis-operate.

Strategies to partition the power system include methods based on system characteristics, such as slow-coherency and eigenvalue analysis of the system dynamics [53]-[55], or based on measurements [56], [57]-[59]. Most of the previous partitioning approaches that are based on system characteristics mainly focus on the generator coherency and do not incorporate load buses. Slow coherency is a physical indication of a weak connection [60] and is a viable solution for the problem of identifying critical relays.

Reference [61] proposes a slow coherency method, which includes load buses. Reference [39] proposes software for controlled islanding based on slow coherency. Reference [40] tests the proposed slow coherency method in [39] on the Western Electricity Coordinating Council (WECC) system. The proposed method of [39]-[40] is aimed at identifying a proper separation scheme. A similar strategy can be implemented in order to identify the critical protective relays. However, the slow coherency and cutset determination depend on the operating condition, i.e., [39] and [40] do not address this challenge regarding the determination of slowly coherent generator groups over a wide range of operational states.

Moreover, [59] explains the application of fuzzy clustering for power system coherency partitioning. It is explained that fuzzy clustering employs a soft partitioning strategy, meant to provide more flexible clusters relative to the inherent data structure. Reference [59] proposes to use fuzzy c-means (FCM) clustering analysis, which uses the coherency measure as a basis for classification. A flexible partitioning strategy may be more appropriate for the problem of identifying critical relays as the desired method should identify all critical relays for various operational conditions and contingencies.

There are two main drawbacks with the prior research, which make them less suitable for the problem of identifying critical distance relays: 1) the majority of the previous research efforts aim at categorizing the system for a specific operating condition and/or contingency. Such approaches are not even guaranteed to identify the critical relays for that particular condition or contingency

due to the inability to precisely predict load, generator dispatch, voltage control, planned outages, or even other remedial action schemes. 2) Most of the previous approaches group only generators (generators buses). Therefore, other buses will not be allocated to any specific group, which does not adequately address the problem of determining the cutset across critical transmission lines in order to identify the critical and vulnerable protective relays.

Several previous research efforts aim at identifying various partitions (also referred to as zones) based on the network structure. References [62] and [63] specify various zones in the power system based on power transfer distribution factor (*PTDF*) values. Buses that have similar impacts on transmission lines are considered to be in the same zone. The specified zones are used for determining reserve sharing policies and dynamic reserve requirements. If such a strategy were to be implemented in order to find critical protective relays, the distance relays located on the transmission lines, which connect the buses of various zones, are the critical distance relays.

Similarly, a strategy may leverage line outage distribution factors (LODF). Lines that have high LODFs with regards to critical contingencies, e.g., the California-Oregon Intertie (COI) in the WECC, can be considered to have critical relays.

This report proposes a network partitioning strategy for the problem of identifying vulnerable protective relays for various operating states [64]. The proposed method uses a collection of features related to the previously discussed strategies. Due to the complexity in the nature of the problem of interest, a heuristic strategy is implemented to identify the critical relays. Many other heuristic strategies, other than what is proposed here, can be used in order to address this problem. The proposed strategy is a mixed-integer linear program (MILP) based on prior generator grouping information of critical contingencies and network structure. This proposed strategy can be implemented during offline planning studies to identify critical protective relays to be modeled in transient stability analysis.

5.1 Network partitioning to identify critical protective relays

After the initiating event, a power swing may result in relay mis-operations. These relays need to be identified and equipped with out-of-step (OOS) blocking schemes [65]. However, any additional forced outage may expose a different situation on the system and result in a vulnerability of a different set of protective relays. These vulnerabilities and mis-operating cases cannot be identified without analyzing transient stability results while modeling critical protective relays.

This report proposes a method to identify the critical distance relays, which are prone to mis-operate during various operating conditions and contingencies. In order to improve situational awareness, it is crucial to identify and model these protective relays during transient stability studies. The desired strategy should identify any distance relays, which may be affected by any power swing in a given system. Such a strategy can be implemented in offline long-term planning studies in order to identify the protective relays, which need to be modeled in transient stability studies during short-term operational study purposes, e.g., real-time security assessment tools.

A network partitioning strategy based on a MILP model is proposed here for the problem of identifying vulnerable protective relays. Two main characteristics of power systems are used in

this proposed strategy: 1) the generators' grouping pattern and 2) the transmission network (structure and impedance). The generators' grouping pattern can be obtained from historical data of critical contingencies, if such information is available, or from results of initial transient stability studies for critical contingencies. The transmission network characteristic is captured through shift factors, i.e., *PTDF*. These two characteristics are captured through the objective function of this network partitioning model.

The objective of this model is to group generators that show similar system responses to a disturbance. With the generator groupings defined, the protective relays connecting these groups are identified as the critical relays to monitor in transient stability studies. To accomplish this goal, the proposed approach uses the generator grouping information from one or several critical contingencies and a given operating condition as an input. This grouping information is considered in the form of penalizing the allocation of the generator buses, which were grouped together, in different partitions of the network.

In addition, a different metric needs to be used to allocate non-generator buses to different groups. This proposed strategy uses a *PTDF* based criterion similar to [62]-[63] to allocate the buses, which have similar impacts on the transmission network, to the same partition. This criterion, which is shown in (5.1), is based on comparing the average impact of injections at any two buses on all transmission lines. Note that, $PTDF_{k,n}^{R} - PTDF_{k,m}^{R}$ is the same as $PTDF_{k,n}^{m}$; equation (5.1) is based on the calculation of the *PTDF* for a given reference bus *R*.

$$\frac{\sum_{\forall k} \left| PTDF_{k,n}^{R} - PTDF_{k,m}^{R} \right|}{K} \tag{5.1}$$

The proposed network partitioning strategy, depicted by (5.2)-(5.12), identifies the critical protective relays. Generator grouping information from one or several critical contingencies and (5.1) is incorporated through the objective function, (5.2). This model is a MILP model with two functions in the objective, which are weighted by the coefficients, α and β. The binary variable $X_n^i = 1$ specifies that bus n belongs to group i. $X_n^i = 0$ identifies that bus n does not belong to group i. r_i is the predefined reference bus for group i, which imposes that $X_{r_i}^i$ must equal 1. This is equivalent to giving each group at least one member bus as a start. The choice of which bus to put within a group must be driven by engineering insight; however, it is often not too difficult, based on prior knowledge or simulations, to identify a few buses that should be included in different groups.

$$\begin{aligned} \textit{Minimize} \quad & \alpha \Big(\sum_{\forall c,n,m} C_{n,m}^{c} \lambda_{n,m} \Big) \\ & + \beta \sum_{\forall n,m} \Big[\frac{\sum_{\forall k} \left| PTDF_{k,n}^{R} - PTDF_{k,m}^{R} \right|}{K} \Big] \delta_{n,m} \end{aligned} \tag{5.2}$$

Subject to:

$$\lambda_{n,m} \geq 0 \qquad \forall n,m \quad (5.3)$$

$$\lambda_{n,m} \geq X_n^i - X_m^i \qquad \forall n \in N_g, m \in N_g, i \quad (5.4)$$

$$0 \leq \delta_{n,m} \leq 1 \qquad \forall n,m \quad (5.5)$$

$$\delta_{n,m} \geq X_n^i + X_m^i - 1 \qquad \forall n,m,i \quad (5.6)$$

$$\sum_{\forall i} X_n^i = 1 \qquad \forall n \quad (5.7)$$

$$X_{r_i}^i = 1 \qquad \forall i \quad (5.8)$$

$$\sum_{\forall k:\, k_{to}=r_i} l_k^i - \sum_{\forall k:\, k_{from}=r_i} l_k^i + \sum_{\forall n} X_n^i = X_{r_i}^i \qquad \forall i \quad (5.9)$$

$$\sum_{\forall k:\, k_{to}=n} l_k^i - \sum_{\forall k:\, k_{from}=n} l_k^i = X_n^i \qquad \forall n : n \neq r_i, i \quad (5.10)$$

$$-M\, X_n^i \leq l_k^i \leq M\, X_n^i \qquad \forall k : n = k_{from} \text{ or } n = k_{to}, i \quad (5.11)$$

$$X_n^i : \{0,1\} \qquad \forall n,i \quad (5.12)$$

The first element in the objective applies a penalty if two generator buses, which were grouped together in offline analysis (historical data of outages, hypothetical simulation results, or expert opinion), were forced to be in separate groups by the MILP model. With a positive coefficient in the objective for a minimization problem and with only lower bounds for $\lambda_{n,m}$, the MILP problem will push $\lambda_{n,m}$ to its greatest lower bound. Constraint (5.4) imposes a lower bound of 1 whenever the two generators are in different groups; (5.4) will impose a lower bound of 0 when the generators are in the same group. Thus, $\lambda_{n,m} = 1$ only when the two generator buses are placed in different groups. Note that (5.4) is only defined for generator buses.

The value of α and β are general scaling factors. However, $C_{n,m}^c$ can be used based on various strategies. For instance, if historical data places buses n and m in the same group frequently, the model user may wish to make the value of $C_{n,m}^c$ high. On the other hand, if buses n and m rarely

show up together in the offline analysis, a much lower value for $C^c_{n,m}$ may be chosen, even a value of zero. For this report, $C^c_{n,m}$ is chosen to be zero or one; a value of zero is given unless two buses were in the same group based on the offline analysis.

Equations (5.5)-(5.6), along with the second term in the objective, encourage buses to be assigned in the same group if they have a similar impact on the transmission network. Linear shift factors (*PTDF*) are used to estimate the impact of an injection at bus n relative to the impact on the network for an injection at bus m. These shift factors are the well-known dc-based *PTDFs*, not ac-based *PTDFs*, which still adequately capture the general impact of an injection at a bus without getting into more precise analysis regarding the actual operating case.

Equation (5.7) identifies and forces each bus to belong to just one of the groups. Equation (5.8) allocates a predetermined bus (r_i is the initial bus, the reference bus, for group i) to each group. The role of (5.8) is important to the success of the proposed approach. For instance, for a known outage at a critical transmission interface, historical data or simulation would show that the separation of the system will start around the interface. Even though those buses are generally close to each other and have very similar impacts on the transmission network (for injections at their locations), after the outage of the interface, they belong to different islands. Therefore, (5.8) guides the MILP model to a solution based on engineering judgement, leveraging insight based upon forcing a bus to be assigned to a particular group. Of course, additional constraints can be added to force other buses to be assigned to a particular group. This may be beneficial for large-scale systems that are hard to solve and when there is a high confidence that certain buses will be grouped together. For this report, there is only one bus initially assigned to each group and all other buses are free to be assigned to any group, based on the MILP solution.

Equations (5.9)-(5.10) are node-balance constraints and (5.11), combined with (5.9)-(5.10), ensure a connectivity requirement for each group. The difference between (5.9) and (5.10) is that the node-balance constraint for each group's reference bus includes an additional term on the left hand side, as can be seen from (5.9); the summation over X^i_n for all n calculates the number of buses assigned to group i. This summation term represents an injection equal to the number of buses in group i while the right hand side of (5.9) and (5.10) include a demand based on X^i_n if bus n is assigned to group i. Both (5.9) and (5.10) include summation terms for the net injections and withdrawals associated to line transfers to complete the node-balance constraints. The reference bus applies an injection equal to the number of buses assigned to the group; the lines transmit the reference bus injection to the buses assigned to the group. Essentially, (5.9) and (5.10) combine to create node-balance constraints for all buses in the network, for each group. Constraint (5.11) shows that each branch can be assigned to a group if and only if both the *to bus* and the *from bus* of the branch are in the same group; (5.11) imposes that l^i_k equals zero if either the *to bus* or the *from bus* is not a part of group i. Constraint (5.11) allows l^i_k to take on a large positive or negative value if both the *to bus* and the *from bus* are a part of group i. The M value is set to a large number so that (5.11) is non-binding if $X^i_{k_{from}} = X^i_{k_{to}} = 1$. This is known as a big *M* reformulation where a large multiplier is selected to allow the constraints to be inactive whenever it is not supposed to

be binding [66]. Equation (5.12) states that the variable must be binary. Together, (5.7)-(5.12) ensure that each bus is assigned to one group and that each group has no islanded buses, i.e., a connectivity requirement for each grouping.

The transmission lines, which are the links between different groups, form the solution cutset of the network partitioning model. It is proposed that the distance relays along the cutset as well as all of the neighboring lines should be modeled during transient stability studies. It is crucial to model the neighboring lines of the specified cutset in transient stability studies as distance relays of any of these transmission lines may mis-operate during slightly different operational conditions.

5.2 Numerical results and analysis

The proposed method is tested on the IEEE 145-bus and the WECC 179-bus test cases. Each test case is an equivalent WECC model. Power System Simulator for Engineering (PSS/E) [67] was used for the transient stability analysis. The proposed MILP strategy is implemented in JAVA. CPLEX 12.5 is used as the solver.

For both test cases, a transient stability study is performed for the original operating condition along with a contingency that results in an unstable power swing. The generator groups are identified using the result of this study. The proposed strategy is applied for each of the test cases using the generator grouping information from the initial transient stability study.

In order to test the results of the proposed strategy, distance relays are defined on all lines using a model from PSS/E, i.e., DISTR1 [67]. Out-of-sample testing is performed for various operating conditions and contingencies for each of the test cases. The results of transient stability studies, while modeling distance relays on all transmission lines, are compared with the case of modeling only the distance relays identified by the proposed approach. The details of these two test cases, and the corresponding results and analysis of results, are presented in Section 5.2.1 and Section 5.2.2.

5.2.1 WECC 179-bus test case

The system includes 179 buses, 29 generators, 203 transmission lines, and 60 transformers. The load is about 54 GW. Figure 5.1 shows this test system.

The initial transient stability study is performed for the described operating condition. A fault is modeled at bus 83, which represents bus MALIN in the WECC system. It is assumed that the fault causes outages on three transmission lines: 83-89, 83-94, and 83-98. These outages, which represent the outage of the COI in the WECC, result in an unstable power swing. A transient stability study is performed for 10 seconds. During this unstable power swing, the generators divide into 5 groups.

Note that the coefficients α, β are to be set by the operator in order to achieve efficiency of the proposed method. The proposed method is tested for various values of α, β in order to evaluate the sensitivity of the results to these values. The protective relays on transmission assets along the cutsets identified by the proposed method, and their neighboring lines, are considered as the critical

protective relays to be modeled in the transient stability study. Moreover, two methods of identifying neighboring lines are tested.

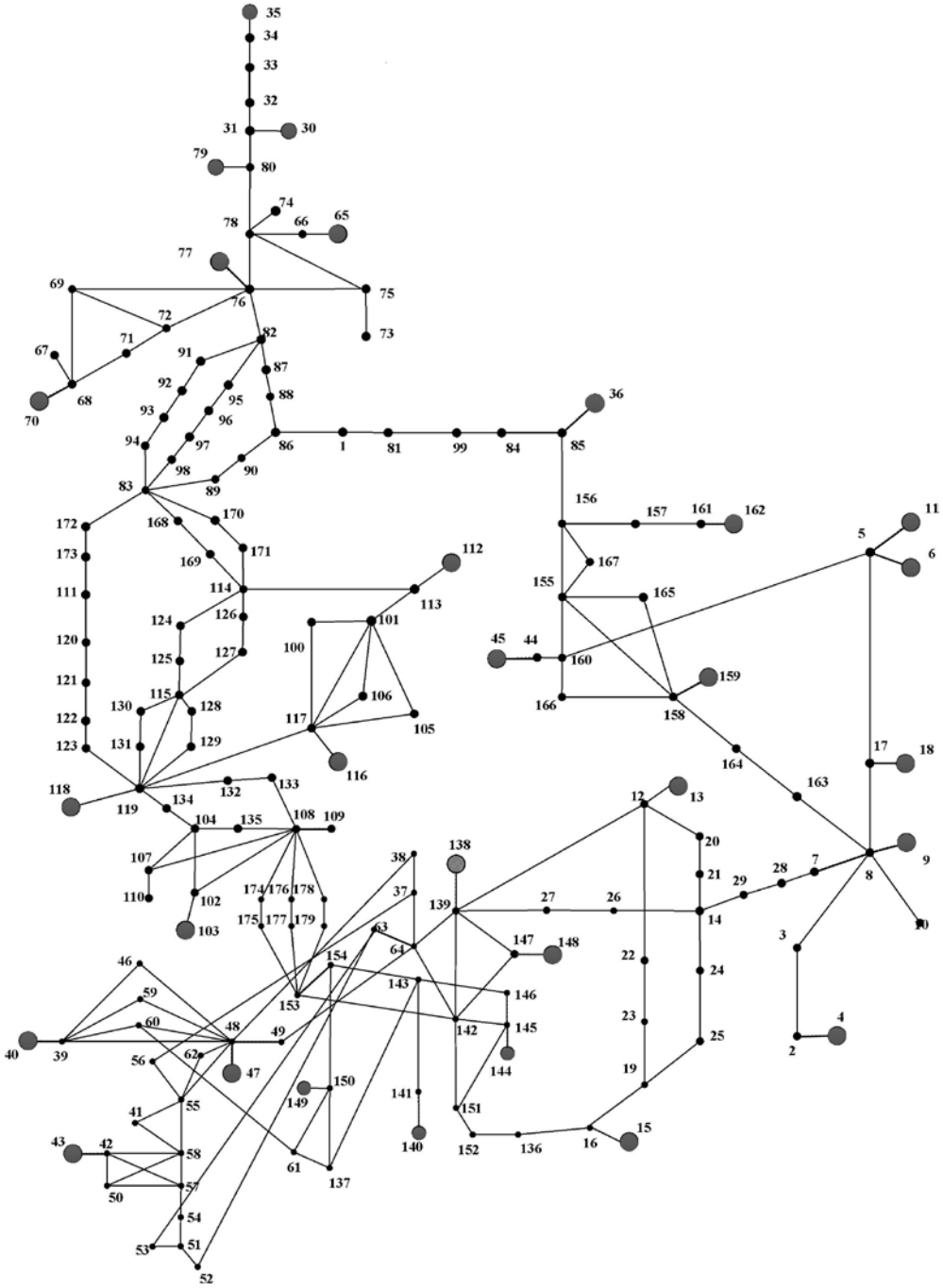

Figure 5.1 WECC 179-bus Test Case

Various values of (α, β) are tested: (1000,1), (10,1), (5,1), (1,1), (0.5,10), (1,10), and (1,100). The results show that whenever the first part of the objective (related to α) is scaled higher, a consistent set of transmission assets are identified as critical. On the other hand, if the second part

of objective (related to β) is scaled higher, a different set of transmission lines is consistently identified as the cutset. Conservatively, all transmission lines for these two sets, along with their neighboring transmission lines, are identified as critical lines. The protective relays, which protect these transmission lines, are critical and need to be modeled within transient stability.

Next, various neighboring strategies are tested:

Strategy 1: All of the transmission lines of the identified cutset, along with their neighbors, were considered as critical transmission lines. Moreover, all of the transmission lines, which are in a series connection with any of the critical transmission lines, are considered to be critical. In total, 53 transmission lines were identified as critical transmission lines.

Strategy 2: All of the lines along the identified cutset as well as the transmission lines that are within 2 buses of the cutset are considered as critical transmission lines. This strategy represents consideration of the neighboring lines and the zone 3 reach point of their distance relays. In total, 62 transmission lines were identified as critical transmission lines.

Using *Strategy 1* and *Strategy 2*, only 33% and 39% of the distance relays are identified as critical relays to be modeled in transient stability study respectively. Note that these percentage values are calculated using the total number of distance relays. Distance relays are not modeled for the equivalent transmission lines, i.e., lines with negative resistance. Representation, updating, and maintaining the protection system data of such a low percentage of distance relays (33% or 39% of total distance relays) increases the efficiency, reduces the chance of misrepresentation of the protective systems, and helps avoid the inaccurate estimation of system behavior.

In order to validate the proposed method, a transient stability study is conducted while modeling distance relays on all transmission lines (except the equivalent lines), 158 transmission lines. The results are compared with the results of a transient stability study while modeling the 33% of relays identified by *Strategy 1*.

A total of 316 distance relays are defined, which protect both sides of 158 transmission lines. The zone 1, zone 2, and zone 3 of the distance relays are considered to be 0.85, 1.25, and 1.5 times the transmission line impedance respectively. Operating time of zone 1 is set to 1 cycle [68]. Zone 2 and zone 3 of the distance relays operate with delay of 0.3 and 2 seconds respectively. The breaker operation time is modeled to be 0.03 seconds. Although the protective relay settings vary for different transmission lines, these relay settings are assumed to be similar for all transmission lines due to the lack of data for protection systems. Please note that OOS protection is not defined for these distance relays in order to study the effects of mis-operation of these relays. Although OOS blocking schemes provide another layer of protection for mis-operation of the related distance relays, it is important to monitor these distance relays carefully through transient stability studies as those relays are likely to be exposed to power swings.

In order to validate whether the proposed strategy is able to successfully identify critical relays for transient stability studies, transient stability studies are performed for two operating conditions and various contingencies. Table 5.1 shows the various in-sample and out-of-sample cases, which are

tested in order to validate the proposed strategy. The two tested operating conditions are Case 1 and Case 2. The load level in Case 2 is 20% more than the load in Case 1.

Table 5.1 Tested Scenarios and Operating Conditions for WECC 179-bus Test Case

	Tested Contingencies
Case 1	Outage of transmission line 28-29
	Outage of transmission line 86-1
	Outage of transmission line 86-88
	Outage of transmission line 16-136
	Outage of transmission line 12-139
	Outage of transmission line 81-99
	Outages of transmission lines 83-89, 83-94, 83-98
Case 2	Outages of transmission lines 83-89, 83-94, 83-98
	Outage of transmission line 82-91
	Outage of transmission line 28-29
	Outage of two transmission lines 64-139
	Outage of transmission line 142-147
	Fault at bus 83
	Fault at bus 86
	Fault at bus 139

The results of transient stability study, while modeling all protective relays, show that a total of 25 transmission lines were tripped during these cases. All of these 25 transmission lines were identified by *Strategy 1* and *Strategy 2*. Therefore, if transient stability is performed while modeling only the relays identified by *Strategy 1* and *Strategy 2*, the transient stability results are similar to modeling all relays.

In addition, the results of a transient stability study, while modeling all of the 316 distance relays, are compared with the results of a transient stability study while modeling 106 distance relays of *Strategy 1*. For this study, a bus fault is modeled at bus 86 for four cycles. It is presumed that this fault results in an outage of line from bus 86 to bus 88. In addition, other distance relays operate while this fault is present in the system. Mis-operation of these relays reduces the transfer capability from the eastern side of the network, which is shown in Figure 5.1. At 1.5 seconds, the generator at bus 36 loses synchronism. The distance relays on the line 85-156, which is exposed to this loss of synchronism (OOS condition), mis-operate. The loss of synchronism and the relay mis-operations exacerbate the system condition resulting in additional generators slipping poles. At around 4.5 seconds, the generator at bus 35 loses synchronism, which results in mis-operation of distance relays on transmission line 31-32. Finally, the generators on the northwestern part of the network (generators at buses 30, 65, 70, 77, and 79) lose synchronism with the rest of the system. The loss of synchronism of these generators results in mis-operation of the distance relays on the transmission lines at around 6.8 seconds. This process is exactly the same for both cases: a) modeling all 316 distance relays; b) modeling 106 identified distance relays. In both of these cases, the same distance relays trigger at the same time step of the transient stability study. Figure 5.2 and Figure 5.3 show the generators' relative rotor angles for the two cases.

Similarly, transient stability studies are performed for a fault at bus 83, which is followed by outages of transmission lines 83-89, 83-94, and 83-98. Figure 5.4 and Figure 5.5 show the generators relative rotor angles while modeling all distance relays and 33% distance relays respectively.

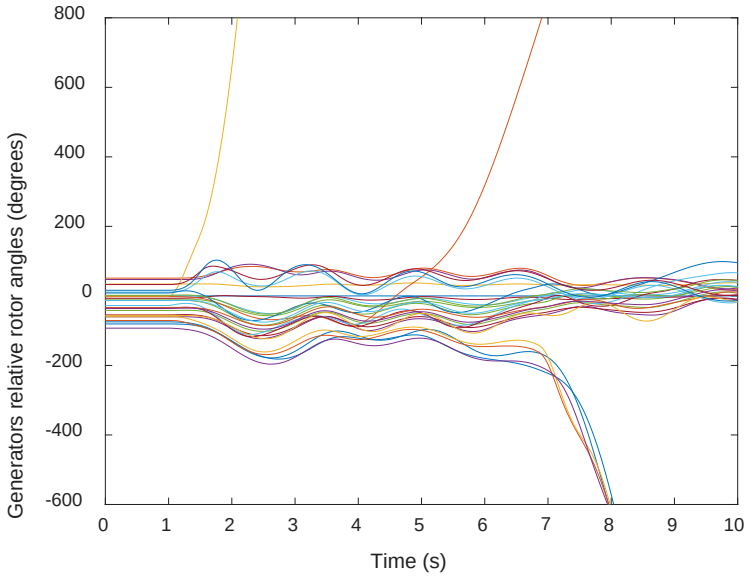

Figure 5.2 Generators Relative Rotor Angles: (i) WECC 179-bus Case; (ii) Outage of Line 86-88; (iii) All Distance Relays Modeled

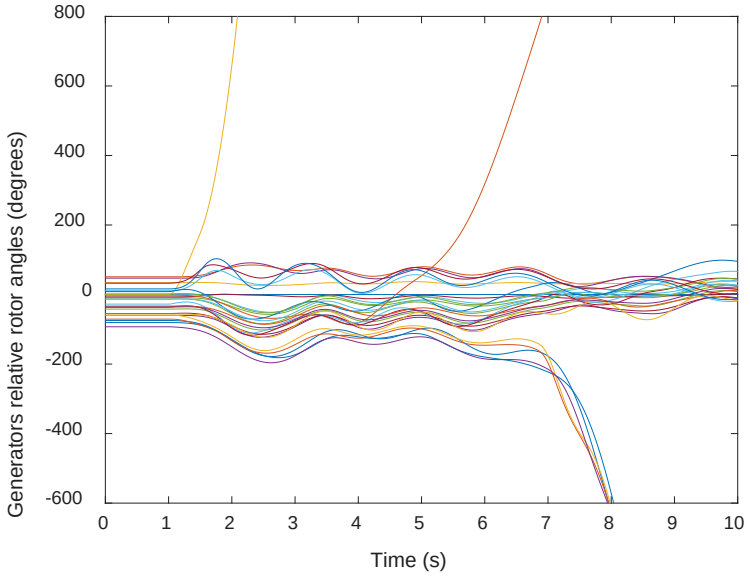

Figure 5.3 Generators Relative Rotor Angles: (i) WECC 179-bus Case; (ii) Outage of Line 86-88; (iii) Only Identified Distance Relays Modeled

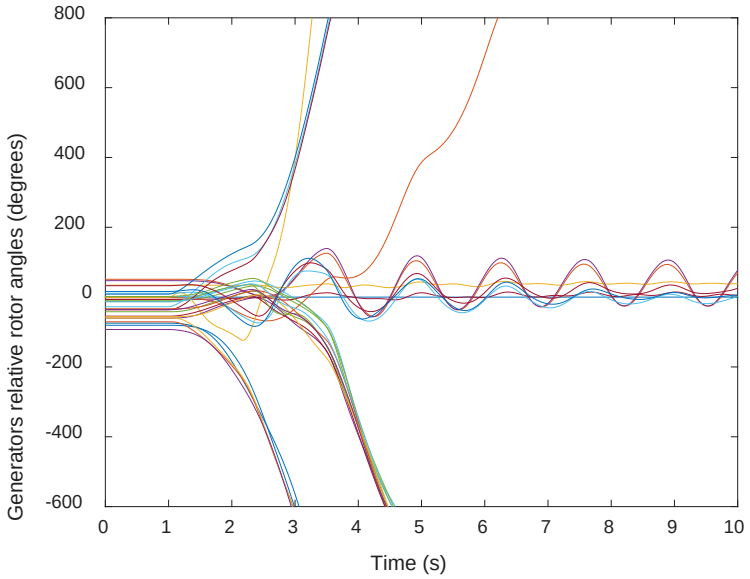

Figure 5.4 Generators Relative Rotor Angles: (i) WECC 179-bus Case; (ii) Outage of Lines 83-89, 83-94, and 83-98; (iii) All Distance Relays Modeled

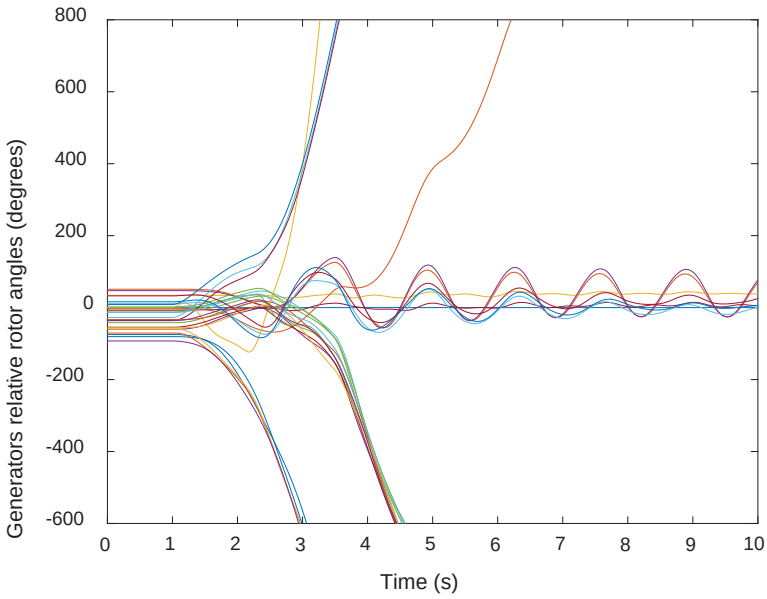

Figure 5.5 Generators Relative Rotor Angles: (i) WECC 179-bus Case; (ii) Outage of Lines 83-89, 83-94, and 83-98; (iii) Only Identified Distance Relays Modeled

These figures confirm that modeling only identified distance relays of the proposed method (33% of total relays) produce similar results in comparison to modeling all distance relays. As a result of the initiating event (fault and outages of lines 83-89, 83-94, and 83-98), the generators in the northern area (generators at buses 36, 30, 65, 79, 77, and 70) lose synchronism and slip poles. In addition, the generators, which are located south of these lines (generators at buses 112, 116, and 118) lose their power transfer path to load and slip poles. At around 2.2 seconds, the generator at

bus 36 loses synchronism with its group (northern group) and slip poles. This loss of synchronism results in the tripping of lines 81-99 and 85-156. Moreover, the generator at bus 35 loses synchronism in both cases, which results in the loss of line 31-32. At around 3.4 seconds, the eastern and western sides of the network lose synchronism followed by the outage of line 28-29. This process is exactly the same in both studies conducted, i.e., modeling all distance relays and modeling 33% of distance relays.

5.2.2 IEEE 145-bus test case

This test case is shown in [69] and consists of 145 buses, 50 generators, 402 transmission lines, and 53 transformers. The demand in this system is 283 GW. An initial transient stability study is performed for the original operating condition. A fault is modeled at bus 7, which results in the outage of transmission line 6-7. As a result of this fault and outage, the generators divide to three synchronous groups. For this test case, (α, β) are set at (100, 1). The identified transmission lines along with their neighboring relays are considered as the critical protective relays to be modeled in the transient stability study. Using this strategy, 65% of total distance relays are identified as the critical relays; note that the calculation of the 65% does not involve equivalence lines (and their corresponding relays) in the network (lines with negative resistance).

In order to validate the proposed strategy, the transient stability study is performed while modeling all protective relays; the results of this test are compared with the results of a transient stability study while modeling just 65% identified distance relays. In order to test the proposed strategy, the distance relays with settings similar to Section 5.2.1 are modeled on all of the transmission lines of this test case.

Transient stability studies are performed for three operating conditions and various contingencies. Table 5.2 summarizes the tests. The operating conditions in Case 1, Case 2, and Case 3 consist of the original load condition, 75% of the original load level, and 125% of the original load level respectively.

The results confirm that the proposed strategy is able to successfully identify all mis-operating relays for the tested operating conditions and contingencies. Figure 5.6 and Figure 5.7 show the generators relative rotor angles for Case 3 and a fault at bus 1, which is cleared by opening lines 1-2 and 1-6. After the initial event, the generators located at buses 93 and 99, lose synchronism with the rest of the system, which causes relay mis-operation for lines: 49-51, 50-51, and 58-87. As a result of this mis-operation, the northwestern part separates from the rest of the system. As shown in Figure 5.6 and Figure 5.7, the results are the same while modeling only the identified distance relays (65% of relays) or all relays. Therefore, based on the presented empirical results, the proposed strategy is able to successfully identify the critical protective relays. The proposed strategy can be implemented offline during a power system planning phase in order to identify the set of protective relays, which are critical to model during transient stability studies.

Table 5.2 Tested Scenarios and Operating Condition for IEEE 145-bus Test Case

	Tested Contingencies
Case 1	Outage of transmission line 6-7
	Outages of transmission lines 1-2 and 1-6
	Outages of two transmission lines 25-27
	Outages of two transmission lines 6-12
	Outage of transmission line 102-117
Case 2	Outage of transmission line 6-7
	Outages of transmission lines 1-2 and 1-6
	Outages of two transmission lines 25-27
	Outages of two transmission lines 6-12
	Outage of transmission line 102-117
Case 3	Outage of transmission line 6-7
	Outages of transmission lines 1-2 and 1-6
	Outages of two transmission lines 25-27
	Outages of two transmission lines 6-12
	Outage of transmission line 102-117

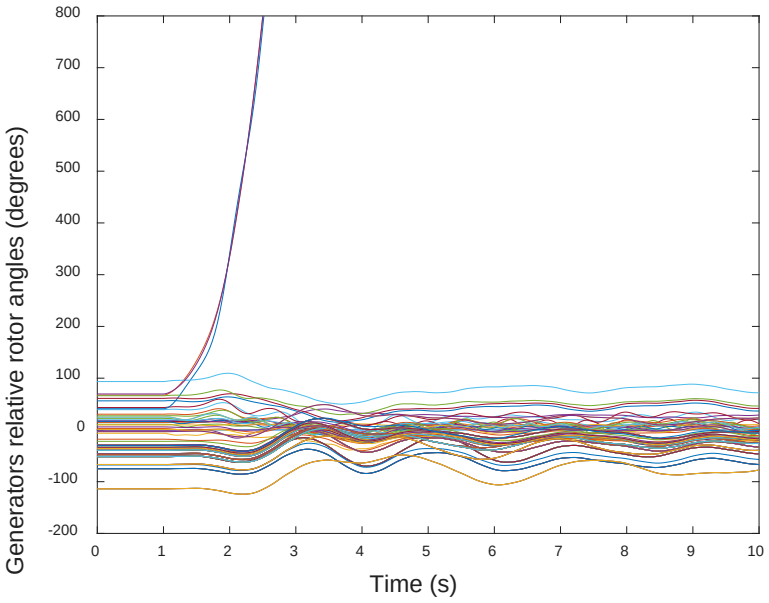

Figure 5.6 Generators Relative Rotor Angles: (i) IEEE 145-bus Case; (ii) Outages of Lines 1-2 and 1-6; (iii) All Distance Relays Modeled

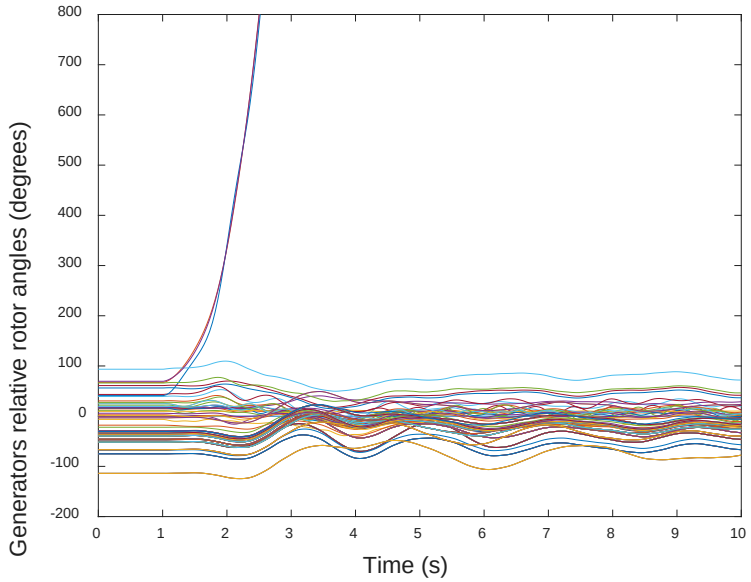

Figure 5.7 Generators Relative Rotor Angles: (i) IEEE 145-bus Case; (ii) Outages of Lines 1-2 and 1-6; (iii) Only Identified Distance Relays Modeled

5.3 Summary

This section emphasizes the importance of modeling protection function within transient stability study tools. It is explained that mis-representation of protective relays in power systems analysis tool may result in inaccurate estimation of system behavior. Therefore, a strategy that can selectively identify critical protective relays to be modeled in transient stability studies is very useful. This section proposes a strategy that, based on empirical evidence, has successfully identified the critical protective relays, which may be exposed to power swings for various operating conditions and contingencies. These protective relays are the critical protective schemes that need to be modeled within transient stability study tools. The proposed strategy is a network partition model, which is framed as an MILP. The generators' grouping information and transmission network are considered as inputs for the proposed strategy. The proposed strategy is validated through out-of-sample testing for various operating conditions and contingencies on the WECC 179-bus and the IEEE 145-bus test cases. The transient stability results show that modeling only the identified protective relays of the proposed strategy produces the same results as modeling all of the protective relays.

6. Conclusions and Future Work

6.1 Conclusions

Accurate stability studies are essential to obtain a proper assessment of system behavior. Only when the system behavior is properly modeled in stability simulation tools is it possible to identify the critical control actions necessary to maintain reliable and secure operations of the electric power grid. While this fact is well-established and widely recognized for decades, there are still rudimentary limitations with existing power systems modeling procedures for stability analysis. One essential limitation that still exists is the lack of representation of automated protection schemes even though they have existed for decades.

This report addresses the following critical research and practical challenges associated with the identification and representation of protection systems in stability studies. First, this report starts with the investigation and verification of the importance of modeling protection systems during transient stability studies, including out-of-step conditions. The results have clearly confirmed the critical nature of accurate protection system modeling within stability studies. Second, this report proposes a method to identify the proper locations of out-of-step blocking schemes in order to prevent relay mis-operations during unstable power swings. Third, the proposed method then enables the avoidance of unintentional islanding during unstable power swings. Finally, this report also proposes a methodology to identify which protection systems are critical to model within stability studies. Due to the cumbersome task of trying to maintain accurate data for all protection systems along with maintaining accurate models of those protection systems within stability studies, it is critical to identify the key subset of protection systems that should be accurately modeled within stability studies.

The occurrence of power swings during critical events is one key reason why the modeling of protection systems in stability studies is important. Severe and sudden changes in the state of the system may result in stable or unstable power swings. During unstable power swings, mis-operation of relays may cause a system wide blackout. Prior historical data recorded during cascading events further confirm the substantial influence of relay mis-operation. Large blackouts often include multiple relay mis-operations which cause further stress on the system and are a main cause of the blackout. Therefore, it is critical to study power system behavior during power swings while also having a proper representation of the various protection systems. Such representation is important not just for operations but also for planning studies.

Out-of-step protection schemes, both for transmission and generators, are designed to perform appropriate control actions during unstable power swings. Out-of-step protection systems should be designed accurately in order to help prevent a system collapse. Both out-of-step tripping and out-of-step blocking functions should be placed and designed properly during the planning stage and adjusted, as needed, for actual operations. While the need for proper out-of-step protection schemes is well-known, there are two fundamental challenges: a) to identify the critical locations and functionality of the out-of-step protection schemes and b) to maintain a proper up-to-date dataset and characteristic models of all protection schemes for stability studies. The presented work addresses both of these critical challenges.

This report has proposed a methodology to determine the proper locations of out-of-step blocking relays. During power swings, a generator or group of generators may slip poles. This condition causes angular separation between different areas of the system. When the two individually synchronized systems become separated by 180 degrees, the voltage magnitude may drop to zero on some transmission lines connecting the separated area; the identified location is known as the electrical center. In order to avoid mis-operation of the related relays, these relays should be temporarily blocked from tripping. These potentially mis-operating relays during a power swing should be recognized during planning studies and appropriate out-of-step blocking relays should be located along these lines.

Most of the methods presented in literature are based on approximating the system with a two-source equivalent network. These methods are neither accurate nor appropriate for large power systems; such approaches are also not appropriate for studies involving the modeling of protection systems. More recent research proposes a fast and innovative electrical center detection method [32], which is not based on a two-source equivalent network approximation. This method utilizes results of a transient stability study in order to evaluate whether the swing impedance characteristic intersects the line impedance. However, this method is not able to detect all of the mis-operating relays properly. The deficiency of the proposed method of [32] is shown in this report.

This research proposes a method that is able to detect stable and unstable power swings within transient stability studies. Moreover, this method can be easily used in power system planning studies to identify the necessary locations for the OOS blocking functions. The proposed method is based on evaluating the minimum voltage through each transmission line for each time interval of the transient stability study. The minimum voltage evaluation method is tested on peak summer data from the WECC. The proposed method is also compared to the projected relay trajectory method [32]. The results show that the proposed method is able to detect the potential mis-operating relays correctly.

The proposed method also augments and enhances the remedial action scheme associated with the COI outage. The OOS blocking scheme based on the proposed method, along with the NE/SE separation scheme, provides a proper controlled islanding scheme.

In addition, the results show that the proposed method is less sensitive to the network topology in comparison to prior approaches, e.g., [32]. It can be concluded that assessing the voltage drop is a reliable method to detect the electrical center. The results further confirm that if the blocking only occurs for the relays where their relay impedance trajectories intersect the line impedance, uncontrolled islanding may still occur.

Moreover, the voltage dip screening strategy, which is explained by NERC [8], confirms the accuracy of the proposed method. The conducted studies indicate that OOS relays have to be designed with great care. Failure to detect all mis-operating relays may result in failure of the islanding scheme and may lead to a system wide collapse.

This research identifies a solution for distance relay mis-operation during unstable power swings. Overall, a range of operating conditions and disturbances must be analyzed to design protection

systems. Such cases require extensive testing via simulations to verify that the designed settings work effectively and protect the system following disturbances.

This report also addresses the second main challenge, identifying which relays are critical to model within transient stability studies. The historical analysis of blackouts confirms the importance of modeling protective relays within power system transient stability analysis. However, representing, maintaining, and updating data for all protective relays is an intractable task. Misrepresentation or outdated representation of protective relays may result in inaccurate estimation of system behavior in critical emergency states.

Empirical results confirm that the proposed method successfully identifies the critical protective relays, which may be exposed to power swings for various operating conditions and contingencies. These protective relays are the critical protective schemes that need to be modeled within transient stability study tools. The proposed strategy is a network partition model, which is framed as an MILP. The generators' grouping information and transmission network are considered as inputs for the proposed strategy. The generator grouping information can either be obtained from historical data related to the previous critical contingency or from the result of a transient stability study for an initial critical contingency. The protective relays, which are located along the identified cutsets and their neighboring relays, are considered as critical protective relays to be modeled in transient stability study tools. Various strategies for identifying neighboring relays have been implemented and tested.

The proposed strategy is validated through out-of-sample testing for various operating conditions and contingencies on the WECC 179-bus and the IEEE 145-bus test cases. The results confirm that the proposed strategy is able to identify all of the mis-operating relays of various operating conditions and contingencies.

Furthermore, transient stability results are compared for the cases when all protective relays are modeled and when only the critical relays identified by the proposed strategy are modeled. This comparison shows that modeling only the identified protective relays of the proposed strategy produces the same results as modeling all of the protective relays. This confirms the accuracy and efficiency of the proposed strategy.

The proposed method can be implemented in the offline planning process. Therefore, solution time is not a restrictive metric and the proposed strategy can be scaled for large-scale systems. Additional modifications, such as clustering generators with similar responses, and/or implementing a weighting factor for the high voltage transmission lines to be selected in the cutset, can be added to the proposed method.

6.2 Future work

This report proposes two strategies for the problems of: a) identification of mis-operating relays for unstable power swings; b) identification of critical protection functions for time-domain simulations. Both of these two strategies mainly focus on distance relays. Similar strategies should be developed for any other transmission protective schemes, which observe power swings. Moreover, additional studies should be conducted to identify potential generators and transmission

lines protective relays mis-operations during stable power swings. Such mis-operations may exacerbate the system condition and lead to unstable power swings and cascading outages.

Moreover, both of these strategies focus on inter-area power swings. Therefore, these methods are aimed at relays that protect transmission assets. During a local power swing, the protective relays, which protect the generators and their step-up transformers, may observe the power swing. Similarly, a strategy can be developed in order to identify which specific protective relays would observe local power swings and may operate or mis-operate. The desired strategy should identify critical protective relays, which their operation would impact the results of transient stability studies.

References

[1] NERC, *System Performance Under Normal (No Contingency) Conditions (Category A)*, NERC Standard TPL-001-0.1, May 2009. Available: http://www.nerc.com/files/TPL-001-0_1.pdf.

[2] NERC Criteria for Reliability Coordinator Actions to Operate Within IROLs, NERC Standard IRO-009-1, Feb. 2014.

[3] NERC Criteria for Reliability Coordinator Actions to Operate Within IROLs, NERC Standard IRO-008-1, Feb. 2014.

[4] P. Pourbeik, P. S. Kundur, and C. W. Taylor, "The Anatomy of a Power Grid Blackout," *IEEE PES Magazine*, September 2006.

[5] M. J. Mackey, "Summary Report on Survey to Establish Protection Performance during Major Disturbances," *CIGRE Working Group 34.09, Electra*, no. 196, June 2001, pp. 19-29.

[6] D. C. Elizondo, J. D. L. Ree, A. G. Phadke, and S. Horowitz, "Hidden Failures in Protection Systems and their Impact on Wide-area Disturbances," *Proceedings of the IEEE PES Winter Meeting*, vol. 2, pp. 710-714, 2001.

[7] M. Li, , A. Pal, A. G. Phadke, J. S. Thorp, "Transient Stability Prediction based on Apparent Impedance Trajectory Recorded by PMUs," *International Journal of Electrical Power & Energy Systems*, vol. 54, pp. 498-504, January 2014.

[8] NERC, *Protection System Response to Power Swings*, System Protection and Control Subcommittee, NERC, August 2013. Available: http://www.nerc.com.

[9] P. M. Anderson and A. A. Fouad, *Power System Control and Stability*, Wiley-IEEE Press, 2002.

[10] J. Berdy, "Application of Out-Of-Step Blocking and Tripping Relays," General Electric Power Management, Ontario, Canada. Available: http://store.gedigitalenergy.com/faq/Documents/Alps/GER-3180.pdf.

[11] IEEE, *Power Swing and Out-Of-Step Considerations of Transmission Line*, A report to the Power System Relaying Committee of the IEEE Power Engineering Society, IEEE PSRC WG D6, July 2005.

[12] R. Van and C. Warrington, *Protective Relays Their Theory and Practice*, vol. 1, 2nd Ed, Chapman and Hall, 1968.

[13] NERC, *Protection System Misoperation Identification and Correction*, NERC Standard PRC-004-3. Available: http://www.nerc.com.

[14] W. A. Elmore, "System Stability and Out-Of-Step Relaying," *Applied Protection Relaying*, Westinghouse Electric Corporation, 1982.

[15] C. Russell Mason, *The Art and Science of Protective Relaying*, John Wiley & Sons, 1956.

[16] P. M. Anderson, *Power System Protection*, Wiley-IEEE Press, 1998.

[17] C. J. Mozina, "Advanced Applications of Multifunction Digital Generator Protection," Beckwith Electric Company. Available: https://www.beckwithelectric.com/docs/tech-papers/genprot01.pdf.

[18] J. Berdy, "Out-of-Step Protection for Generators," General Electric Power Management, Ontario, Canada. Available: http://store.gedigitalenergy.com/faq/Documents/CEB/GER-3179.pdf.

[19] N. Fischer, G. Benmouyal, Da. Hou, D. Tziouvaras, J. Byrne-Finley, and B. Smyth, "Tutorial on Power Swing Blocking and Out-Of-Step Tripping," *Proceedings of the 39th Annual Western Protective Relay Conference*, Spokane, WA, October 2012.

[20] J. Holbach, "New Blocking Algorithm for Detecting Fast Power Swing Frequencies," *Proceedings of the 30th Annual Western Protective Relay Conference*, Spokane, WA, October 2003.

[21] Q. Verzosa, "Realistic Testing of Power Swing Blocking and Out-of-Step Tripping Functions," *Proceedings of the 38th Annual Western Protective Relay Conference*, Spokane, WA, October 2011.

[22] C. W. Taylor, J. M. Haner, L. A. Hill, W. A. Mittelstadt, and R. L. Cresap, "A New Out-Of-Step Relay with Rate of Change of Apparent Resistance Augmentation," *IEEE Transactions on Power Apparatus and Systems*, vol. PAS-102, no. 3, pp. 631-639, March 1983.

[23] J. M. Haner, T. D. Laughlin, and C. W. Taylor, "Experience with the R-Rdot Out-Of-Step Relay," *IEEE Transactions on Power Delivery*, vol. 1, no. 2, pp. 35-39, April 1986.

[24] G. Benmouyal, D. Hou, and D. Tziouvaras, "Zero-Setting Power Swing Blocking Protection," *Proceedings of the 31st Annual Western Protective Relay Conference*, Spokane, WA, October 2004.

[25] Guzmán, V. Mynam, and G. Zweigle, "Backup Transmission Line Protection for Ground Faults and Power Swing Detection using Synchrophasors," *Proceedings of the 34th Annual Western Protective Relay Conference*, Spokane, WA, October 2007.

[26] Shrestha, R. Gokaraju, and M. Sachdev, "Out-of-Step Protection using State-Plane Trajectories Analysis," *IEEE Transactions on Power Delivery*, vol. 28, no. 2, pp. 1083-1093, April 2013.

[27] S. M. Rovnyak, C. W. Taylor, and Y. Sheng, "Decision Trees using Apparent Resistance to Detect Impending Loss of Synchronism," *IEEE Transactions on Power Delivery*, vol. 15, no. 4, pp. 1083-1093, October 2000.

[28] T. Amraee and S. Ranjbar, "Transient Instability Prediction using Decision Tree Technique," *IEEE Transactions on Power Systems*, vol. 28, no. 3, pp. 3028-3037, August 2013.

[29] K. H. So, J. Y. Heo, C. H. Kim, R. K. Aggarwal, and K.B. Song, "Out-Of-Step Detection Algorithm using Frequency Deviation of Voltage," *IET Generation, Transmission, and Distribution*, vol. 1, no. 1, pp. 119-126, January 2007.

[30] R. Jafari, N. Moaddabi, M. Eskandari-Nasab, G. B. Gharehpetian, and M. S. Naderi, "A Novel Power Swing Detection Scheme Independent of the Rate of Change of Power System Parameters," *IEEE Transactions on Power Delivery*, vol. 29, no. 3, pp. 1192-1202, June 2014.

[31] *PSLF User's Manual*, PSLF Version 18.1_01, General Electric.

[32] S. A. Soman, Tony B. Nguyen, M. A. Pai, and Rajani Vaidyanathan, "Analysis of Angle Stability Problems: a Transmission Protection Systems Perspective," *IEEE Transactions on Power Systems*, vol. 19, no. 3, pp. 1024-1033, July 2004.

[33] E. W. Kimbark, *Power System Stability, vol. II, Power Circuit Breakers and Protective Relays*, John Wiley and Sons, 1950.

[34] W. A. Elmore, "The Fundamentals of Out-of-Step Relaying," *Proceedings of the 34th Annual Conference for Protective Relay Engineers*, College Station, TX, April 1981.

[35] M. H. Haque, "ldentification of Coherent Generators for Power System Dynamic Equivalents Using Unstable Equilibrium Point," *IEE Generation, Transmission, and Distribution*, vol. 138, no. 6, pp. 546-552, November 1991.
[36] P. Kundur, *Power System Stability and Control*, McGraw Hill, 1994.
[37] A. Debs, "Voltage Dip at Maximum Angular Swing in the Context of Direct Stability Analysis," *IEEE Transactions on Power Systems*, vol. 5, no. 4, pp. 1497-1502, November 1990.
[38] *System Performance Following Extreme BES Events*, NERC Standard TPL-004-0, April 2005. Available: http://www.nerc.com/files/tpl-004-0.pdf.
[39] G. Xu and V. Vittal, "Slow Coherency based Cutset Determination Algorithm for Large Power Systems," *IEEE Transactions on Power Systems*, vol. 25, no. 2, pp. 877-884, May 2010.
[40] G. Xu, V. Vittal, A. Meklin, and J. E. Thalman, "Controlled Islanding Demonstrations on the WECC System," *IEEE Transactions on Power Systems*, vol. 26, no. 1, pp. 334-343, February 2011.
[41] CAISO, 2010-2011 Transmission Planning, California ISO, Available: http://www.caiso.com/Documents/110518Decision_TransmissionPlan-RevisedDraftPlan.pdf.
[42] L. Paine and J. Crook, "WECC-1 Remedial Action Scheme," Available: http://www.slideserve.com/velma/wecc-1-remedial-action-scheme.
[43] Major WECC Remedial Action Schemes (RAS), WECC, Available: https://www.wecc.biz/Reliability/TableMajorRAS4-28-08.pdf.
[44] Final Report on the August 14, 2003 Blackout in the United States and Canada: Causes and Recommendations, U.S.–Canada Power System Outage Task Force, 2004.
[45] Interim Report of the Investigation Committee on the 28 September 2003 Blackout in Italy, UCTE, 2003.
[46] Final Report System Disturbance on 4 November 2006, UCTE, 2007.
[47] Arizona-Southern California Outages on September 8, 2011: Causes and Recommendations, FERC and NERC, 2012.
[48] M. Panteli, P. A. Crossley, D. S. Kirschen, and D. J. Sobajic, "Assessing the Impact of Insufficient Situation Awareness on Power System Operation," *IEEE Transactions on Power Systems*, vol. 28, no. 3, August 2013.
[49] L. G. Perez, A. J. Flechsig, and V. Venkatasubramanian, "Modeling the Protective System for Power System Dynamic Analysis," *IEEE Transactions on Power Systems*, vol. 9, no. 4, November 1994.
[50] S. Tamronglak, "Analysis of Power System Disturbances due to Relay Hidden Failures," A thesis submitted to the Faculty of the Virginia Polytechnic Institute and State for the degree of Doctorate of Philosophy.
[51] D. P. Nedic, "Simulation of Large System Disturbances," A thesis submitted to the University of Manchester Institute for Science and Technology for the degree of Doctorate of Philosophy.
[52] D. S. Kirschen and D. P. Nedic, "Consideration of Hidden Failures in Security Analysis," *Proceedings of the 14th Power Systems Computation Conference*, Sevilla, pp. 24-28, June 2002.

[53] B. Yang, V. Vittal, and G. T. Heydt, "Slow Coherency based Controlled Islanding: A Demonstration of the Approach on the August 14, 2003 Blackout Scenario," *IEEE Transactions on Power Systems*, vol. 21, no. 4, pp. 1840–1847, November 2006.

[54] W. W. Price, A. W. Hargrave, and B. J. Hurysz, "Large-Scale System Testing of a Power System Dynamic Equivalencing Program," *IEEE Transactions on Power Systems*, vol. 13, no. 3, pp. 768–774, August 1998.

[55] H. You, V. Vittal, and X. Wang, "Slow Coherency Based Islanding," *IEEE Transactions on Power Systems*, vol. 19, no. 1, pp. 483–491, February 2004.

[56] Kamwa, A. K. Pradhan, and G. Joos, "Automatic Segmentation of Large Power Systems into Fuzzy Coherent Areas for Dynamic Vulnerability Assessment," *IEEE Transactions on Power Systems*, vol. 22, no. 4, pp. 1974–1985, November 2007.

[57] Kamwa, A. K. Pradhan, S. R. Samantaray, and G. Joos, "Fuzzy Partitioning of a Real Power System for Dynamic Vulnerability Assessment," *IEEE Transactions on Power Systems*, vol. 24, no. 3, August 2009.

[58] M. Jonsson, M. Begovic, and J. Daalder, "A New Method Suitable for Real-Time Generator Coherency Determination," *IEEE Transactions on Power Systems*, vol. 19, no. 3, pp. 1473–1482, August 2004.

[59] S. C. Wang and P. H. Huang, "Fuzzy C-Means Clustering for Power System Coherency," *Proceedings of IEEE International Conference. on Systems, Man, and Cybernetics*, vol. 3, pp. 2850–2855, October 2005.

[60] X. Wang and V. Vittal, "System Islanding using Minimal Cutsets with Minimum Net Flow," *Proceedings of the IEEE PES Power System Conference Exposition*, New York, October 2004.

[61] S. Yusof, G. Rogers, and R. Alden, "Slow Coherency based Network Partitioning Including Load Buses," *IEEE Transactions on Power Systems*, vol. 8, pp.1375–1381, August 1993.

[62] F. Wang and K. W. Hedman, "Dynamic Reserve Zones for Day-Ahead Unit Commitment with Renewable Resources," *IEEE Transactions on Power Systems*, vol. 30, no. 2, pp. 612-620, March 2015.

[63] F. Wang and K. W. Hedman, "Reserve Zone Determination based on Statistical Clustering Methods," North American Power Symposium *(NAPS) Conference*, pp. 1-6, September 2012.

[64] M. Abdi-Khorsand and V. Vittal, "Identification of Critical Protection Functions for Time-Domain Simulations," *IEEE Transactions on Power Systems*, under review, submitted April 2017.

[65] M. Abdi-Khorsand and V. Vittal, "Modeling Protection Systems in Time-Domain Simulations: A New Method to Detect Mis-operating Relays for Unstable Power Swings," *IEEE Transactions on Power Systems*, vol. 32, no. 4, pp. 2790-2798, July 2017.

[66] S. Binato, M. V. F. Pereira, and S. Granville, "A New Benders Decomposition Approach to Solve Power Transmission Network Design Problems," *IEEE Transactions on Power Systems*, vol. 16, no. 2, pp. 235-240, May 2001.

[67] Power System Simulator for Engineering (*PSSE) Manual, version 34, Siemens Power Technologies International*, March 2015.

[68] Arun G. Phadke, "Electric Power Engineering," in *Handbook of Electrical Engineering Calculation*, 1st ed., New York, Marcel Dekker, 1999, ch. 1, sec. 1.5.3, pp. 38.

[69] Md. Rakibuzzaman Shah, “Test System Report,” Power and Energy Research Group, School of Information Technology and Electrical Engineering, The University of Queensland, Australia, April 2011.

Part II

Evaluation of Relay Dynamic Response by Utilizing Co-simulation Platform (PSS/E- CAPE)

and

Loss of Excitation Detection Algorithm to Prevent LOE Relay Mis-operation during Power Swing

Iman Kiaei
Saeed Lotfifard
Anjan Bose

Washington State University

For information about this project, contact

Saeed Lotfifard, Project Leader
School of Electrical Engineering and Computer Science
Washington State University
Pullman, WA 99164-2752
Phone: 509-335-0903
Email: s.lotfifard@wsu.edu

Power Systems Engineering Research Center

The Power Systems Engineering Research Center (PSERC) is a multi-university Center conducting research on challenges facing the electric power industry and educating the next generation of power engineers. More information about PSERC can be found at the Center's website: http://www.pserc.org.

For additional information, contact:

Power Systems Engineering Research Center
Arizona State University
527 Engineering Research Center
Tempe, Arizona 85287-5706
Phone: 480-965-1643
Fax: 480-727-2052

Notice Concerning Copyright Material

Table of Contents

List of Figures

List of Tables

1. Introduction

1.1 Background

The investigations on the major disturbances and outages during the last decades have shown that significant blackouts had triggered due to the variety of factors such as human mistakes, extreme weather events, imbalance of generation and demand, congestion and overloading on the transmission paths, inaccurate calibration of the protective devices and etc.[1]. The North American Electric Reliability Corporation (NERC) concluded that the August 14, 2003 blackout was triggered by a simple natural cause and exacerbated by mis-operations of protective relays that ultimately led to a cascading failure phenomenon [1]. Inaccurate relay settings and coordination may lead to widespread outages with millions of people losing power. The protective devices may not operate correctly based on the steady state settings during the transient conditions. Protective relay mis-operation can be in the following forms [2]:

1. The protective relay fails to operate within a specified time interval when a fault occurs inside the protection zone (i.e. dependability issue)
2. The protective relay operates in the case of faults that are not in the protection zone (i.e. selectivity issue)
3. The protective relay operates when there is no fault in the system (i.e. security issue).

After large disturbances in power systems, the system tries to adjust and settle to the new stable condition. Therefore the system frequency starts to oscillate in different part of the system which results in the amplitude and phase angle of voltages and currents swing. In consequence the impedance measurements based on the varying voltages and currents will also oscillate. During the power swing, the impedance-based protection relays may mis-operate in the non-faulty condition. In swing condition, the impedance trajectory seen by a relay may traverse inside the mho characteristic of the distance element in impedance relays or loss of excitation (LOE) relays and leads to mis-trip [3]. This mis-operation is expressed as one of the fundamental factor of initiating and widening the blackouts [4]. According to literature more than %70 of immense power outages triggered by relay mis-operations which most of these unwanted operations are caused by the distance element in various types of relays such as distance/impedance relay and LOE relay [**Error! Bookmark not defined.**, 5- 6]. Thus, different strategies have been proposed to prevent the impedance element mis-operations which will be explained in the following section.

Furthermore, the catastrophic outages demonstrate the importance of testing relays during transients conditions [7]. Protective relays performance indices such as dependability, security, selectivity, and operating time can be verified more accurately during transients [8].

An overview of the methodology for the transient relay testing is described in this part. The dynamic performance of LOE and impedance relays during power swings is investigated. Response of protective relays is demonstrated using CAPE-Transient Stability (CAPE-TS) module that links CAPE software with PSS/E software. In addition, this paper provides a more realistic dynamic simulation of the relay performance characteristics in the large Western Electricity Coordinating Council (WECC) system during the critical outages. The results demonstrate a

system with a large disturbance and a subsequent protective and remedial action schemes (RAS) may not be successful in preventing cascading outages because of relay mis-operation, and the system eventually breaks up into several parts as a results of unintentional islanding. Also, an adaptive technique is proposed which can distinguish LOE and swing conditions and prevent mis-operation.

1.2 Distance/Impedance Relay Mis-operation

Transmission lines are equipped with distance relays. During the swing cycle, the load impedance, which is outside the relay's protection zones under the steady state, may traverse into the distance relay mho characteristic and causes relay mis-operations.

According to Figure 1.1, the apparent impedance seen by distance element of the relay at point A is as follows [3]:

$$Z_A = \frac{(Z_S + Z_L + Z_R)}{2} \times \left(\frac{k\left[(k - \cos\delta) - j\sin\delta\right]}{(k - \cos\delta)^2 + (\sin\delta)^2} \right) - Z_S \qquad (1.1)$$

Where k is the ratio of the source voltage magnitudes $|E_S|/|E_R|$ and it is assumed E_S (sending source) leads E_R (receiving source) by δ phase.

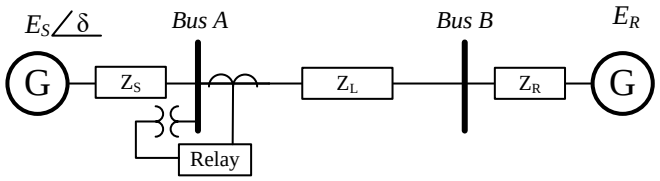

Figure 1.1 Thevenin equivalent circuit of power system

In the power swing cycle, the phase-angle difference of two sources (δ) varies, thus the measured impedance traverses on the R-X plane with respect to the k ratio and where the system electrical center is located. In the equivalent two area power system, when two generators fall out of synchronism (δ =180°), a voltage zero point is created on the tie line between areas which is known as the electrical center [9]. Location of electrical center is affected by the fault location, fault type, network configuration and operating point of the system. The protective relays adjacent to the electrical center are sensitive to the power swings, so if the electrical center of the swing is along the protected line, the apparent impedance trajectory may pass through the protective relay's characteristic.

When E_S is smaller than E_R the trajectory is a circle below the electrical center. When the frequency f_S is larger that f_R the direction of the swing is from right to left, whereas, it will move from left to right if f_S is smaller than f_R. Figure 1.2 illustrates the distance relay mho characteristic and swing impedance loci.

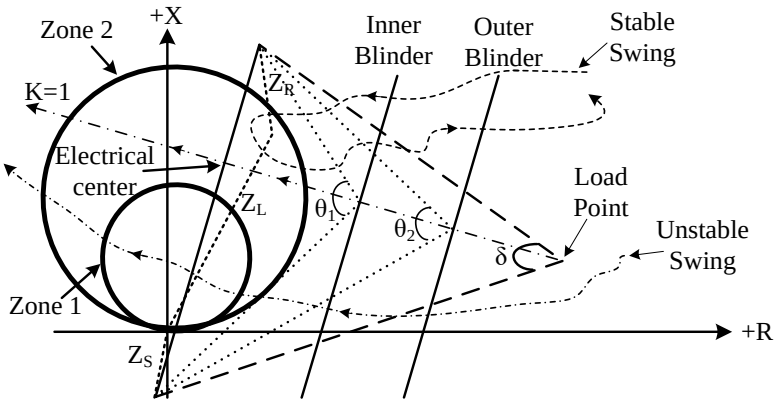

Figure 1.2 Distance relay characteristic and Impedance locus during stable & unstable swing

As shown in Figure 1.2 the distance zones can see some of the power swings (stable or unstable) and can potentially operate and trip the circuit breaker. Some operations may be desired but many will be undesired tripping particularly when the swings are stable. Thus, power swing blocking (PSB) function is utilized in distance relays to prevent unintentional operations during power swings. If the apparent impedance remains between inner and outer blinder elements for a predefined time delay, the PSB recognizes faults from power swing and blocks distance relay elements from operating.

Different methods have been proposed to detect the power swing conditions and prevent the relay mis-operations. These methods include the approaches that are based on rate of change of impedance, rate of change of resistance *dR/dt*, rate of change of swing center voltage (SCV), and rate of change of current [5], [10]. A widely used algorithm operates based on the impedance displacement speed in the R-X plane. The rate of change of impedance seen by the relay depends on the sources, transmission line impedances and the slip frequency ($\omega=d\delta/dt$) which the system is oscillating and expressed as follows [11]:

$$\left|\frac{dZ_A}{dt}\right| = \frac{\left|Z_S + Z_L + Z_R\right|}{(2\sin\frac{\delta}{2})^2} \times \left|\omega\right| \tag{1.2}$$

The conventional method is based on measuring the rate of change of apparent impedance between two right and left impedance elements (blinders). If time interval for crossing between these two predefined blinders exceeds a predefined time period, the relay blocks the distance element during the swing cycle (PSB function) [12]. The inner blinder is determined such that it does not encroach into the most over- reaching mho element and the outer blinder is set to not encroach to the load region with some safety margin [13]. The PSB time delay is determined from the inner and outer blinders setting and the power swing slip rate as follows:

$$PSBD\ (\text{cycle}) = \frac{(\theta_1 - \theta_2) \times F_{nom}}{360^\circ\ f_{stable}} \tag{1.3}$$

Where θ_1, θ_2, F_{nom} and f_{stable} are the machine angles at the outer and inner blinder reaches (degree), system nominal frequency (Hz) and power swing rate (Hz) (which is assumed to be 1.2 Hz), respectively. The blinder schemes are shown in Figure 1.2. Since the inner and outer blinder elements placements depend on the line impedance and equivalent source impedance magnitudes, finding the appropriate setting is challenging [11].

This conventional protection scheme with OSB may also mis-operate if it is not calibrated precisely.

1.3 Loss of Excitation (LOE) Relay Mis-operation

In power systems, the synchronism between generators is maintained by their magnetic fields. The excitation system of a generator is responsible to provide the required energy for the magnetizing reactance. The excitation system also affects the amount of reactive power that the generator produces or absorbs. Changing the excitation current changes the reactive power output of generators that in extreme cases may result in loss of synchronism of the generator. Different types of faults such as field short circuit, field open circuit, accidental tripping of the field breaker, or voltage regulation system failure may lead to the loss of excitation which may consequently lead to loss of synchronism of power generators [14].

Generally the generator terminal impedance can be described based on its output active and reactive power as follows:

$$Z = R + jX = \frac{V^2}{S^*} = \frac{V^2}{P - jQ} = \frac{V^2 \times P}{P^2 + Q^2} + j\frac{V^2 \times Q}{P^2 + Q^2} \tag{1.4}$$

Where V, S, P and Q are positive sequence voltage, apparent, active and reactive powers of the generator. In the normal operating condition, the generator injects active and reactive powers to the system thus R and X are positive and the terminal impedance is located in the first quadrant in the R-X plane. During the loss of excitation, the generators starts to draw reactive power form the power grid and X in Eq. (34) becomes negative. Consequently, the terminal impedance enters into the fourth quadrant in the R-X plane and the endpoint of terminal impedance ranges between the direct axis transient and synchronous reactances. Thus, to protect generators from loss of excitation, conventionally an impedance type relay is utilized at the terminal of synchronous generators. Mason proposed the one negative-offset mho element in 1949 [15]. In order to increase the security of this relay against stable power swing, another negative-offset characteristic with two protective zones was developed by Berdy in 1975 [16]. In this method, negative offset-mho characteristics are defined based on the system condition. The impedance circles diameters are equal to 1.0 p.u. for Zone 1 and X_d (generator synchronous reactance) for zone 2. The downward offset of the zones is equal to half of the generator transient reactance ($X'_d/2$) [17].The typical time delay of LOE is 3 to 5 cycles (0.1 s) for zone 1, and 30- 45 cycles (0.5- 0.75 s) for zone 2.
The impedance trajectory in the power swing condition may enter and leave the mho impedance zone of LOE characteristic in short period of time in comparison to the time for the loss of field condition [18].The impedance seen by the LOE relay traverses into the third quadrant on the R-X plane. The relay in this condition may undesirably detect loss of excitation or loss of synchronism

and mis-trips [16], [19]. The LOE relay characteristic and impedance loci during swing condition are shown in Figure 1.3.

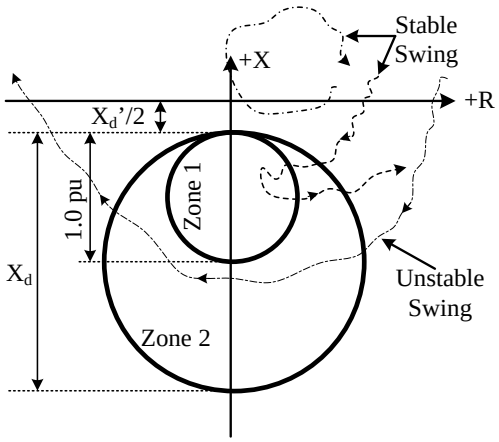

Figure 1.3 Loss of excitation characteristic and impedance loci during stable & unstable swing

In the next chapter the transient simulation (CAPE-PSS/E) platform is utilized to study the mis-operation conditions of the conventional distance and LOE relays.

2. Protection Dynamic Study Circumstance

2.1 Transient relay testing Interface

After recent blackouts in the United States like September 2011, and August 2003 disturbances, studying the protective relay responses on the dynamic behavior of the system becomes essential for the operators in the bulk power systems. In contrast to steady state methods, testing relays in transient conditions provides more realistic testing scenarios to study the response of protective relays during transient condition [10]. In this project, co-simulating platform, CAPE- Transient stability (TS) is used for this purpose. The relay models are implemented in CAPE (computer-aided protection engineering) software which is internally connected to the dynamic model in Siemens-PTI's PSS®E (power system simulator for engineering) software. The integration is carried out in a closed-loop and seamless scheme. The two-sided interface between PSS/E and CAPE is shown in Figure 2.1.

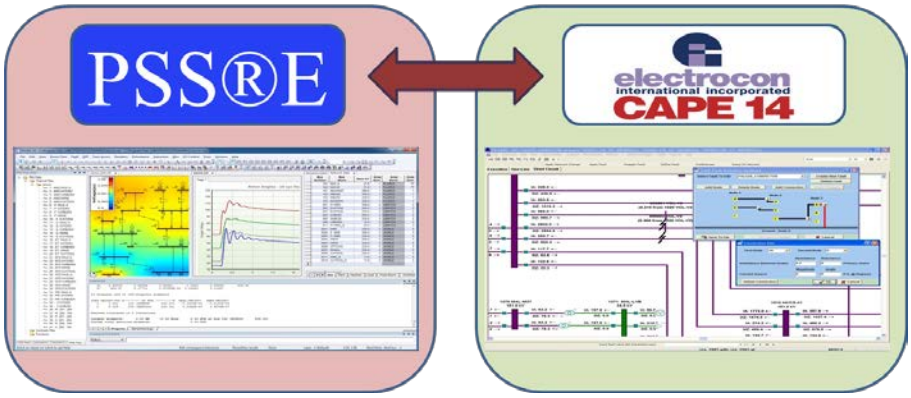

Figure 2.1 Integration between transient model and protection model

1. Description of PSS/E model

For performing the transient study in this project, professional software package PSS/E is internally utilized by the CAPE-TS module of the CAPE software. The basic functions of power system performance simulation work are handled by this computer program; some of the important ones are namely:

- Power flow: this module is basic toll and it is powerful ads easy to use for basic power flow network analysis. Besides analysis tool this module is also used for data handling, updating and manipulation. The Figure 2.3 show the network topology and Newton-Raphson power flow output result of the two-area power system test system. As it is written, the PF converged in 4 iterations.

- Optimal power flow: PSS/E optimal power flow (PSS/E OPF) is a strong toolbox that goes beyond traditional load flow analysis to fully optimize and refine a transmission system.

The final result is the globally optimal solution which simultaneously satisfies system limits and minimizes costs or maximizes the performance.

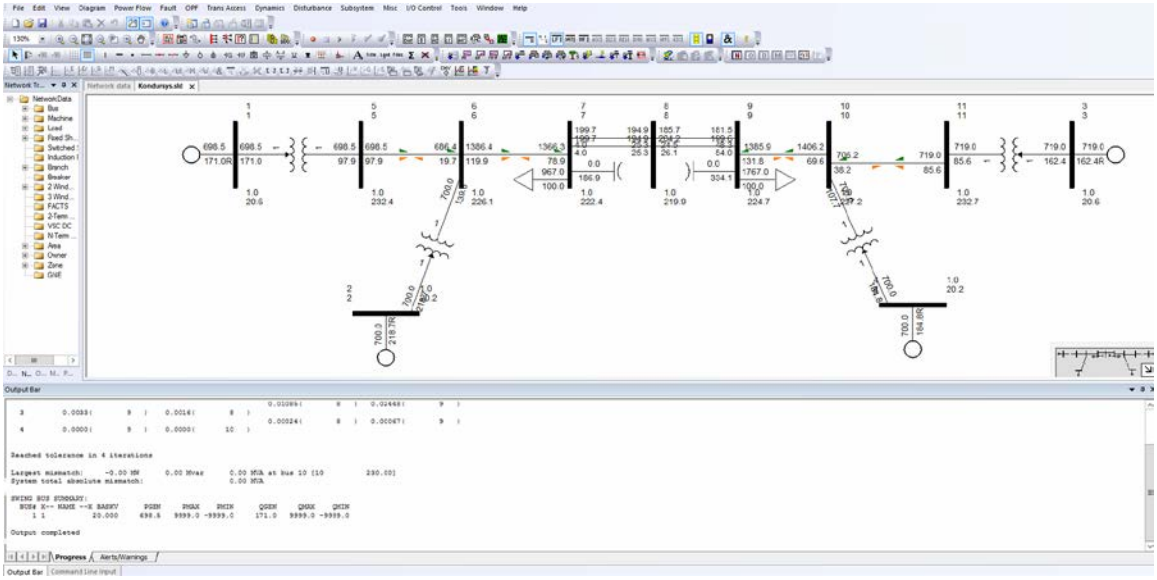

Figure 2.2 PSS/E model graphical interface

- Fault analysis: the PSS/E fault analysis program is fully integrated with the power flow tool. The balanced and unbalanced faults can be studied with this program.
- Dynamic simulations: PSS/E can model system disturbances such as faults, generator tripping, motor starting and loss of field. This program contains an extensive library of generator, exciter, governor and stabilizer models. It also has protection library including underfrequency, distance and overcurrent relays (Its protection library is limited in comparison to the CAPE relay library.).
- Equivalent construction: the large-scale networks can be modeled into internal and external areas to make the analysis easier. This module keeps the study area (internal area) in details and compress rest of the system into an equivalent model.

Since the 1976, the PSS/E program has become one of the most comprehensive, technically advanced and widely used commercial programs in the market. This program employs the updated techniques and numerical algorithms to efficiently solve large scale networks and data [20].

2. Description of CAPE-TS link

PSS/E has relay library but it is not completed, thus the protection system cannot be modeled in details and realistic, so CAPE as one of the well-known protection program is utilized to model the protective relays and devices and simulate their dynamic responses precisely. There is a CAPE-TS module utilizes the PSS/E for transient simulation. Its mean features are:

- Bulk power system can be modeled with thousands of the relays (distance, overcurrent, out-of-step, frequency, voltage, V/Hz, etc.) that have realistic settings.

- The planning and protection models are simulated together so that the interdependence between system dynamics and relay actions can be captured and cascading failures can be studied.
- The transient stability model is studied based on the relay operation in reality.
- Different contingencies and scenarios which may lead to cascading outages can be simulated and the appropriate calibrations can be defined in this platform to prevent those events.
- Different remedial action schemes (special protection schemes) and their associated wide-area control methods can be tested in this platform.

2.1.1 Building the co-simulation platform

Some preliminary data requirements must be prepared prior the transient relay testing, such as [21]:

- *CAPE database file (.gdb)*: This file contains the accurate network data including the sequence data, the protection model and the relays' settings and coordination schemes.
- *PSS/E load flow case (.sav)*: The power flow model of the network is stored in this file.
- *PSS/E dynamic snapshot file (.snp)*: Positive sequence steady-state condition of the system is stored in this file. The faults and disturbances are simulated by applying changes in this file. Based on the fault type, extra nodes are added to the dynamic model of system at pre-specified fault location.
- *Bus and Branch mapping files (.bme & .brm)*: The mappings between buses and branches of the dynamic model (PSS/E) and protection model (CAPE) are established in these files. Dynamic and protection paltforms internally connected to each other through these files during simulation. At each time step, the network topology and configuration are updated in these files after any status change in the protection system model.

In every simulation step, the positive-sequence voltage profile is updated in the transient stability program (PSS/E) and is passed to the protection model (CAPE). Depending on the type of fault (balanced or unbalanced), one or more sequence networks will be used in the fault analysis.

1. Balanced contingency

During the balanced contingency, currents seen by the protective relays are computed by dividing the obtained positive-sequence voltage differences between two ends of the relay line over the line impedance, as follows:

$$I_{\mathrm{Re}lay} = \frac{V_{i1} - V_{j1}}{Z_{Line}} \tag{2.1}$$

Where V_{i1}, V_{j1} and Z_{Line} are the positive sequence voltages at two ends of the line buses and line impedance, respectively.

2. Unbalanced contingency

In the unbalance fault scenario, the fault type and fault location are known. The positive sequence fault current (I_{F1}) can be calculated from the known positive sequence voltages of all neighboring buses of faulted line obtained from the dynamic simulation. Positive, negative and zero sequence circuits are connected together depending on the type of the fault. Then, the negative and zero sequence fault currents (I_{F2}, and I_{F0}) are calculated from the calculated positive sequence current (I_{F1}). For instance, for a single-line-ground fault, three sequence networks are connected in series, so the positive, negative and zero sequence fault currents are equals (I_{F1}=I_{F2}= I_{F0}). The phase currents (I_{af}, I_{bf}, and I_{cf}) at fault location are calculated from the sequence fault currents. Furthermore, the negative and zero sequence voltages at all buses in the protection model are calculated as follows:

$$Y_{BUS} \times \Delta V = I_F \tag{2.2}$$

Where I_F is the fault current at faulted node (zero at all non-faulted buses), Y_{BUS} is the nodal admittance matrix of the faulted network, ΔV is the vector of voltage variation from pre-fault to fault at all buses ($\Delta V = V_{fault} - V_{prefault}$). Since pre-fault negative and zero sequence voltages are assumed to be zero in this calculation, the negative and zero sequence of ΔV are equal to the post-fault negative and zero sequence voltages. The phase voltages (V_{ABC}) of the entire network are calculated from the sequence voltages. The relay currents are then calculated based on the computed voltages and the network impedances. Relays operate based on these calculated currents [21].

Once the phase currents are determined, the operation of protective relays and statuses of breakers are evaluated in the protection model (CAPE). If any of protective devices operates, the network topology in dynamic and protection models is updated simultaneously. In the next iteration, PSS/E calculates the new voltage profile in the new network configuration and passes to CAPE. The CAPE-TS co-simulation procedure is depicted in Figure 2.3.

2.2 Single Machine Infinite Bus System Simulation Results

A single machine infinite bus (SMIB) system is used to study the conventional transmission line distance and LOE relays' performance and mis-operation condition during the power swing phenomenon. The system shown in Figure 2.4, is simulated using CAPE-PSS/E platform. In PSS/E, the sending bus (bus 1) is modelled as a synchronous machine with dynamic model of GENROU type. This model is based on the swing equations for cylindrical rotor generators. The excitation system is modelled as IEEE ESST1A. The receiving end (slack bus) is modelled by the classical generator model, GENCLS. The test system data are given in the Appendix [22]. Prior to fault occurrence the phase angle difference is δ=20 degrees.

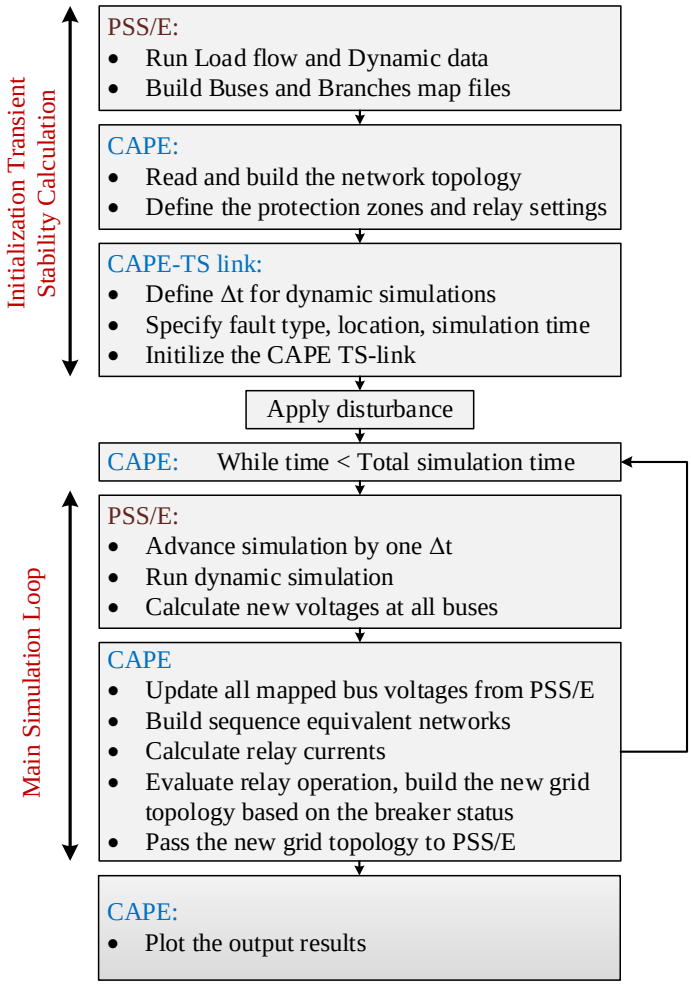

Figure 2.3 CAPE-TS co-simulation flowchart.

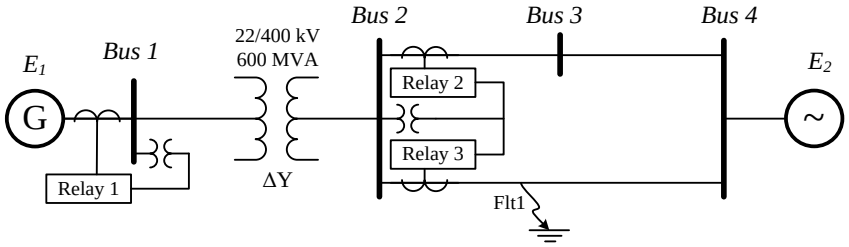

Figure 2.4 One line diagram for SMIB system.

Three protective relays are defined in the system. It is assumed two line protective relays (SEL-321 type) cover line 2-3 (Relay#2) and line 2-4 (Relay#3) and one relay (SEL-300G type) is protecting generator#1 (Relay#1) from LOE. The zone 1 and zone 2 of the transmission line distance relays are set %80 and %120 of the forward line impedance respectively. Typically, zone 1 trips without time delay while zone 2 has a time delay of 20- 30 cycles or (0.3–0.5 s) [23]. For

relay#2 which its response during power swing condition is studied, the quadrilateral inner and outer blinders are set according to section 1.2. The inner radius and outer radius are 65° and 45°, respectively. The blocking timer is set with the typical delay 2 cycles [11]. The LOE relay characteristic is set based on conventional two zone scheme. The designed mho characteristics of the installed relays are depicted in Figure 2.5.

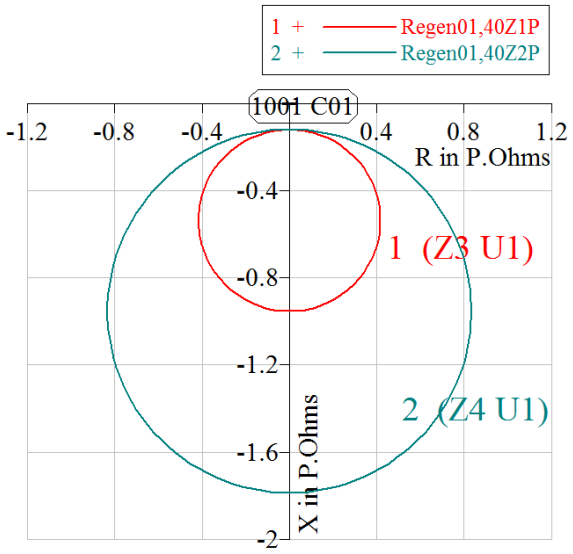

(a)

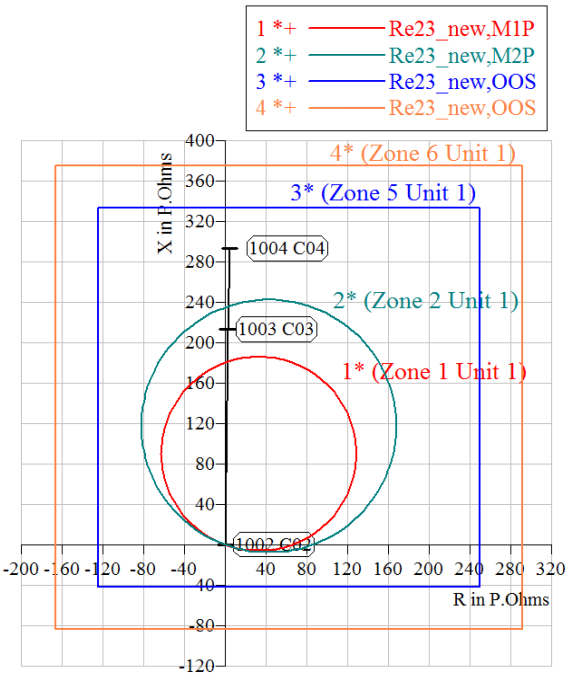

(b)

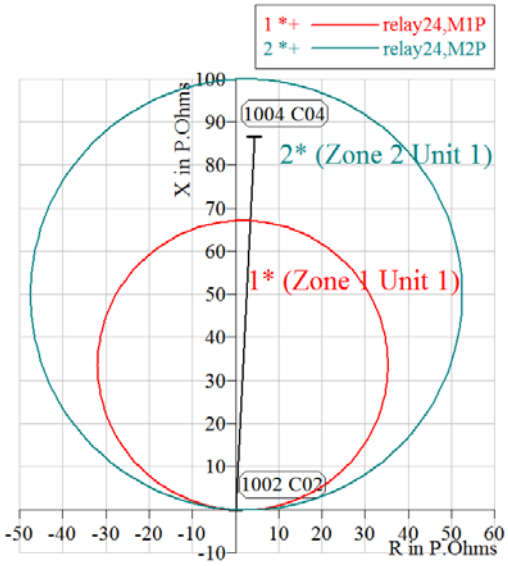

(c)

Figure 2.5 Designed mho characteristic of distance elements

(a) Relay#1 (SEL 300G- LOE relay), (b) Relay#2 (SEL321- Distance relay), and (c) Relay#3 (SEL321- Distance relay)

Once the protection scheme of the test system, which includes three relays as explained above, is defined, the responses of the relays to faults are studied. Then, some scenarios under which the relays mis-operate are discussed.

To study the response of the LOE relay to a fault in the excitation of the machine#1, a short circuit is applied to the excitation system of generator#1 at 0.3 s. The impedance trajectory in LOE condition is shown in Figure 2.6. The apparent impedance trajectory traverses toward the mho characteristic of the relay and enters zone 2 of the LOE relay at 1.37 s, afterwards, it enters smaller zone of the LOE relay. The pre-determined time delay for the zone 2 of the LOE relay expires after 0.65 s, then the breakers operate after 0.05 s delay, so the fault is cleared at 2.07 s by disconnecting the generator form the rest of the grid.

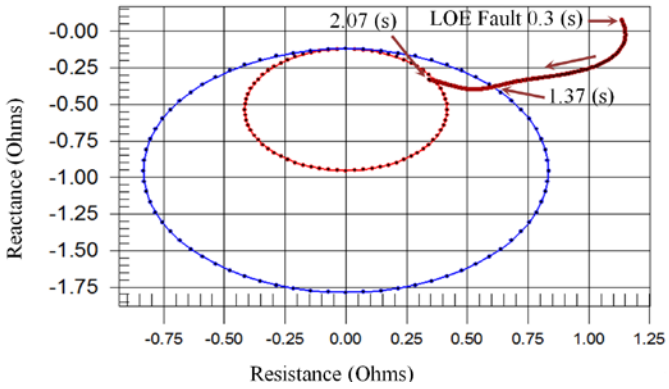

Figure 2.6 Apparent impedance loci and relay#1 operation during Loss of Excitation condition

In the next step, different fault scenarios are applied to the system and operation of the protective relays during stable swing cycles are studied. Some of the scenarios that lead to relay operations are summarized in Table 2.1.

Table 2.1 Operation scenarios of protective relays during stable power swing condition

Scenario No.	Mis-operated Relay	Operated element and condition	Fault clearing time (s)	PSB time delay (cycle)	Zone 2 Time delay (cycle)	Impedance trajectory inside relay zone2	
						Entrance Time (s)	Exit/ Trip Time (s)
1	Distance Relay 2	PSB Mis_operated	0.15	2	24	0.6	Trip (1.075 s)
2	Distance Relay 2	PSB Blocked	0.15	1.2	24	0.6	Exit (1.66 s)
3	LOE Relay	Zone 2 Mis_operated	0.49	—	<49	0.65	Trip (1.46 s)

2.2.1 Distance relay response

To study the response of distance relays during post fault conditions, a 3-phase fault is applied at 0.1 s in the zone 1 of protective relay#3 on the middle of the line between buses 2 and 4 (fault is shown as *Flt1* in Figure 2.4). The fault is detected instantaneously by the relay and cleared after breaker operation delay 3 cycles at 0.15 s. The post fault system experiences stable power swing condition.

Rotor angle of Machine#1 and impedance locus trajectory at distance relay#2 during the stable swing are depicted in Figure 2.7. The apparent impedance loci moves towards the relay (SEl-321) characteristics.

At first, it enters the blinders characteristic curves and then moves into the protection zones of the relays. The apparent impedance passes the distance between outer and inner characteristics in ΔT_B= 1.43 cycles (i.e. the period between 0.385 s to 0.409 s). In the first case study (scenario 1) the PSB

timer is set to 2 cycles, since it is larger than the time interval that impedance loci moves between the blinders (ΔT_B), the PSB element mis-operates and detects this condition as the fault, so the zones 1 and 2 are not blocked.

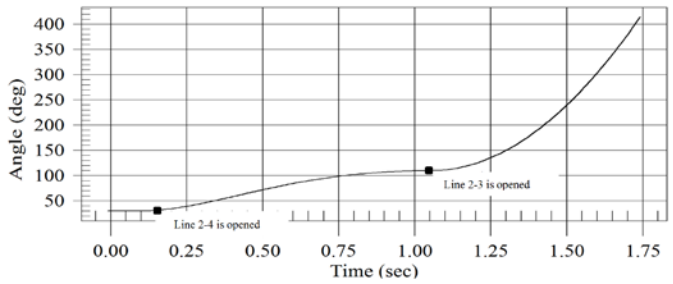

(a)

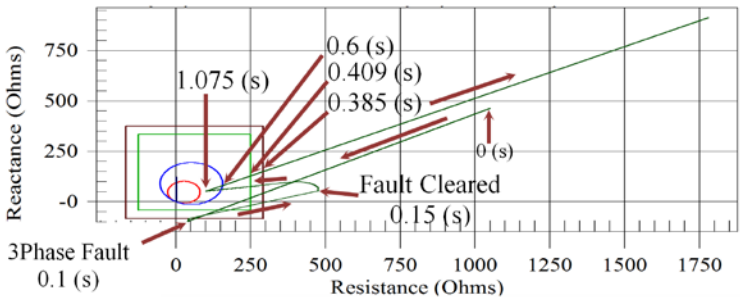

(b)

Figure 2.7 Relay#2 performance during stable swing- Scenario 1

(a) Angle swing of the system, and (b) Apparent impedance loci trajectory

During the stable post fault condition, the impedance trajectory enters the zone 2 at 0.6 s and after pre-defined zone 2 time delay (24 cycles), the unblocked relay# 2 mis-operates and detects the stable power swing condition as a fault. Then, the breaker operates after a time delay (3 cycles) and disconnects the protected line at 1.075 s (shown in Figure 2.7.b).

If the PSB delay of relay#2 is set to 1.2 cycles which is less than the ΔT_B, the blocking element operates correctly and blocks the mho characteristics. The rotor angle of Machine#1 and impedance locus trajectory at relay#2 during the stable swing are depicted in Figure 2.8. During the stable post fault condition, the impedance trajectory enters the zone 2 at 0.6 s and leaves the zone 2 at 1.66 s. the period which the apparent impedance traverses inside the zone 2 longer than the set zone 2 time delay (typically $t_{setting\_Z2}$= 24 cycles) but the PSB element blocks the relay correctly.

2.2.2 Loss of excitation relay response

To demonstrate scenarios that may lead to mis-operation of LOE relays, the electrical center should be located in generator's protection zone. Therefore, the line impedance values of the network shown in Figure 2.4 are reduced to the two third of the previous

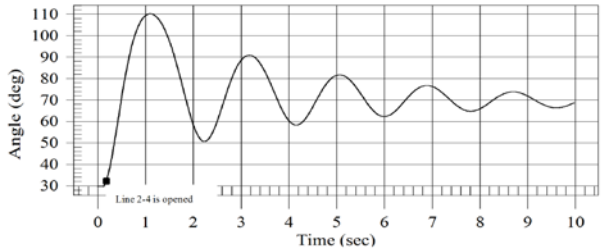

(a)

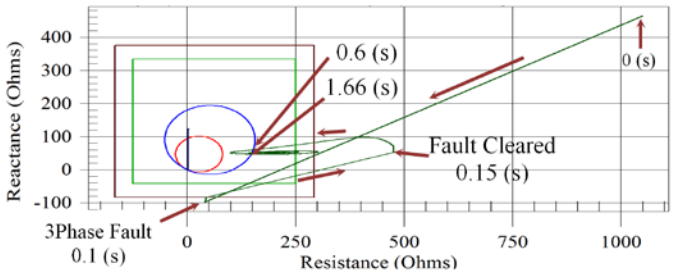

(b)

Figure 2.8 Relay 2 performance during stable swing- Scenario 2

(a) Angle swing of the system, and (b) Apparent impedance loci trajectory

cases. In this condition, the electrical center of the system moves toward the synchronous machine impedance value and the protective relay of generator may mis-operate during power swing. A 3-phase fault is applied on line 2-4 at 0.1 s and relay#3 clears the fault in zone 2 after the set time delay at 0.49 s. This condition causes stable power swing in the system. The rotor angle of machine# 1 and impedance locus trajectory at LOE relay location during the stable power swing are depicted in Figure 2.9.

During the first power swing, apparent impedance trajectory enters zone 2 of the LOE relay at 0.65 s, then moves slowly inside the protection zone, and exits zone 2 at 1.46 s. Since the typical time delay of LOE is 3 to 5 cycles (0.1 s) for zone 1, and 30- 45 cycles (0.5- 0.75 s) for zone 2 [17], relay#1 with these typical time delays that are smaller than the time interval that the impedance locus traverses into mho characteristics ($t_{setting\_Z2}$ < 0.81 s) mis-operates and detects the stable power swing as a fault and issues trip command.

2.3 WECC System Co-simulation

In this section, WECC data, representing the heavy load in summer (HS) 2016, is used to study

the dynamic performance of the protective relays. All the generators are equipped with a turbine governor, exciter, and PSS. The total active generation is 207358 MW in this case. WECC system has different areas, which are connected with strong tie lines. Moreover, the distance relays (SEL-321) are modeled in details in the protection platform based on the typical settings which were explained in pervious section. The inter ties over 100 kV between different areas of WECC system are shown in the Figure 2.10 [24].There are three intertie lines (500 kV) between Oregon and California. The California- Oregon Interties (COI) transfers more than 4800 MW from north to south in this peak load case.

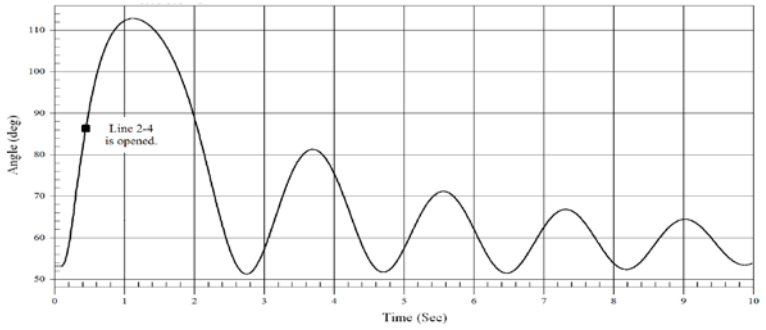

(a)

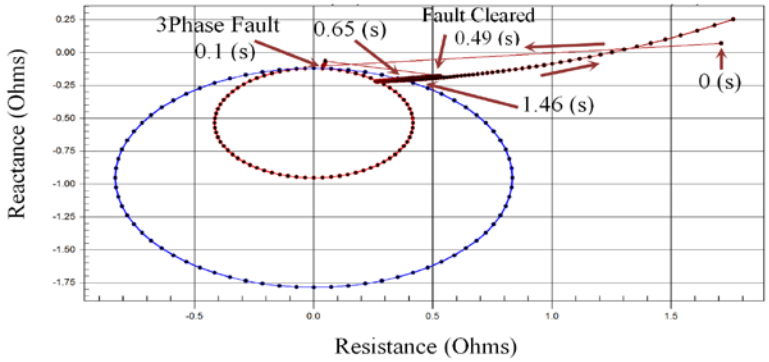

(b)

Figure 2.9 Generator 1 relay performance during stable swing- Scenario 3

(a) Angle swing of the system, and (b) Behavior of LOE relay during stable swing

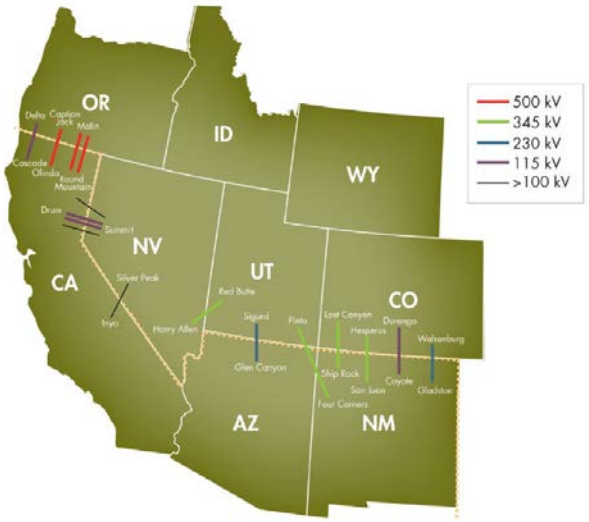

Figure 2.10 Interties between WECC areas (over 100 kV) [24]

The investigated reports on the WECC system described the extreme contingencies as combination of events which are followed by actions of protective relays and RAS devices [25]. Since the COI are the major transmission lines in the WECC system, any events on them causes sever swing condition for the system. The COI tie lines are shown in the Figure 2.11. Two 500 kV lines are paralleled between Malin and Round Mountain substations and the last one is between Captian Jack and Olinda substaions.

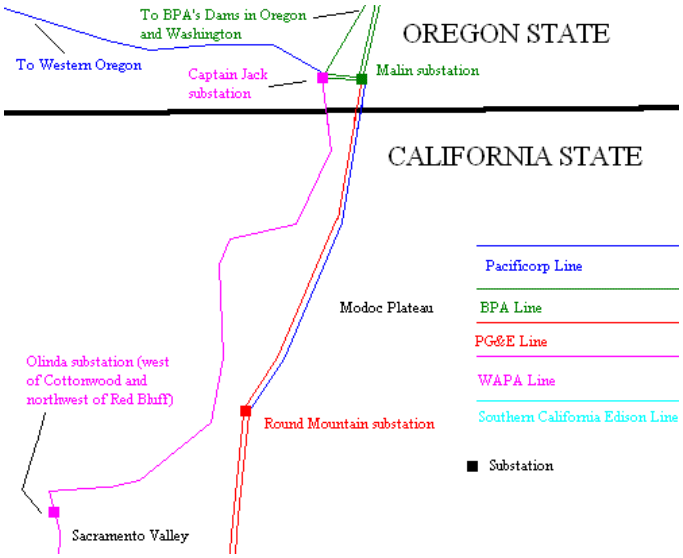

Figure 2.11 Marginal substations of COI interties [24]

In the next step, different fault scenarios are applied to the system and operation of the protective relays during swing cycles are studied. However, two types of outages which occur at the COI lead to critical contingencies in the WECC, such as follows [25]:

2.3.1 Stable Swing Condition

A 3-phase fault on the marginal bus# 40687 (Malin substaion), located in the Northwest area (area#40) is applied at 0.1 s. This contingency is cleared at 0.15 s (after 3 cycles, time delay of the breakers) by tripping all the connected lines to this bus included two parallel COI tie lines connected to the Malin substation. This sever double line outage (SDLO) initiates a stable power swing. The tielines configuration between PG&E and northwest areas and the marginal substaions are shown in Figure 2.12. The relative angles of the generators in area#30 (PG&E) and area#40 (Northwest area) are shown in the Figure 2.13. All the generators rotate as a coherent group. In the stable swing, none of the distance relays mis-operated.

2.3.2 Unstable Swing Condition

If a fault occurs on the bus#45035 Captain Jack in area#40 (Northwest area) at 0.1 s and cleared by disconnecting all the connected lines to this bus at 0.15 s. So all the three 500 kV tie-lines will be tripped because of overloading. Losing the strong transmission paths causes large mismatch between load and supply in the system. Therefore the generators start to oscillate and split in two separate groups. The generators in the northern part of the COI lose their synchronism and accelerate in comparison to the generators located in the southern part (California).

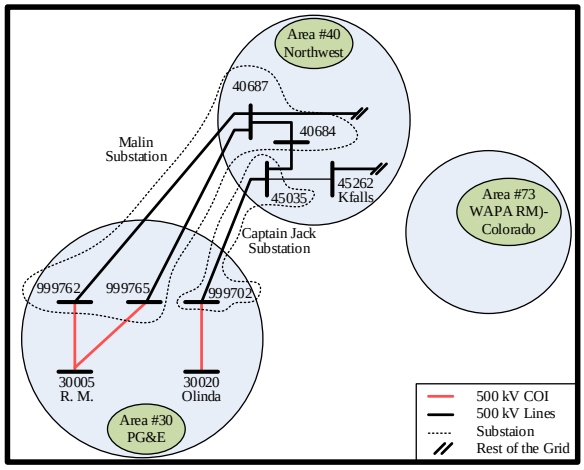

Figure 2.12 Marginal substations of COI interties

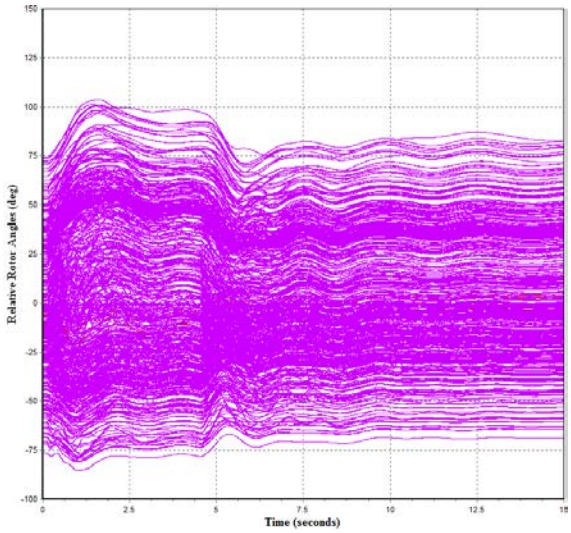

Figure 2.13 Generators relative rotor angles in the stable swing period

This triple line outage (TLO) leads to an unstable swing oscillation. The rotor angles of generators are shown in Figure 2.14. In such situation, there is a event-based operation of remedial action schemes (RAS) to protect the system from cascading events [26]. One of the significant actions for this outage is northeast/southeast separation (Ne/SE separation) strategy that provides controlled separation within the WECC system along the predetermined branch groups [24]. The severe outages are summarized in

Table 2.2.

Table 2.2 Extreme contingencies in wecc System

Scenarios	**Operating Conditions**	**Contingency Locations**	**Outage**	**Swing Condition**
Case#1	HS	COI	SDLO	Stable
Case#2	HS	COI	TLO	Unstable

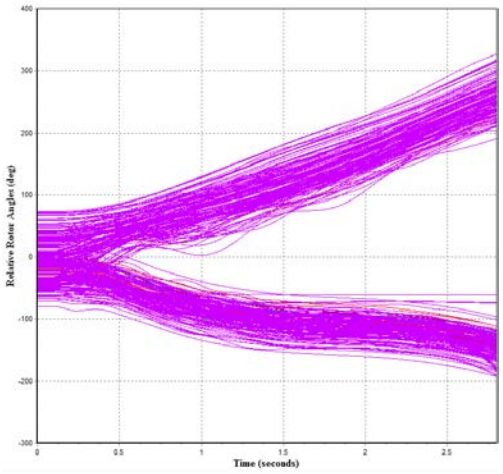

Figure 2.14 Generators relative rotor angles in the unstable swing cycle

During the unstable condition, some of the distance relays in the area#73 WAPA RM (Western Area Power Administration Rocky Mountain-Colorado shown in Figure 2.12) on the eastern part of WECC network mis-operate.

Distance relays are modeled to protect %80 and %120 of the line in zone 1 and zone 2. The zone 1 operates simultaneously, and the zone 2 has 24 cycles delay, and the blocking time delay is the typical value, 2 cylces (Typical time settings). For instance, two different apparent impedance trajectories are studied on the R-X plane of the distance relays in (WAPA RM).

1. The distance relay on 345 kV Line from bus 79049 (Montrosse) to bus 79072 (Hesperus)

If the OSB is disabled, the apparent impedance enters the zones 2 and 1 of the relay at 2.39 s and 2.58 s. After entering the zone 1, the relay detects the swing condition as a fault and mis-operates by passing 3 cycles (breaker delay), it trips the line at 2.63 s. The impedance trajectory is depicted in Figure 2.15.

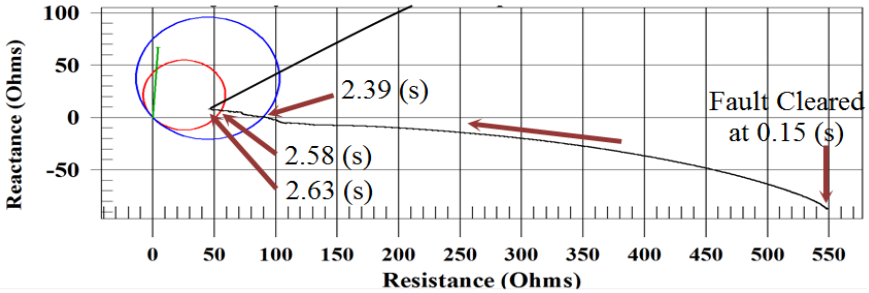

Figure 2.15 Relay mis-operation during unstable swing- Line 79049- 79072

If the OSB is enabled, the impedance enters the outer and inner blinders at 1.79 s and 2.14 s, respectively. Since the time interval between blinders are larger than 2 cycles (OSB typical delay), the relay is blocked. The impedance trajectory with the enabled blinders is shown in Figure 2.16.

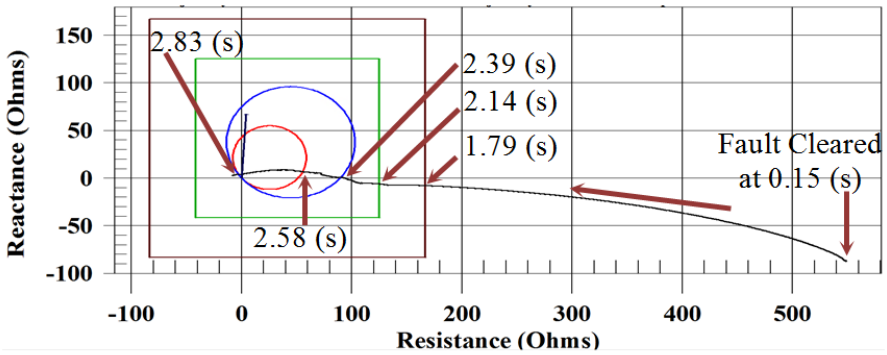

Figure 2.16 Relay blocked during unstable swing- Line 79049- 79072
The distance relay on 230 kV Line from bus 79021 (Curecant) to bus 79045 (Lostcany)

If the OSB is disabled, the apparent impedance enters zones 2 and 1 of the relay at 2.39 s and 2.60 s. After entering zone 1, the relay detects the swing condition as the fault and mis-operates after 4 cycles (breaker delay), it trips the line at 2.67 s. The impedance trajectory with the disabled blinders is shown in Figure 2.17.

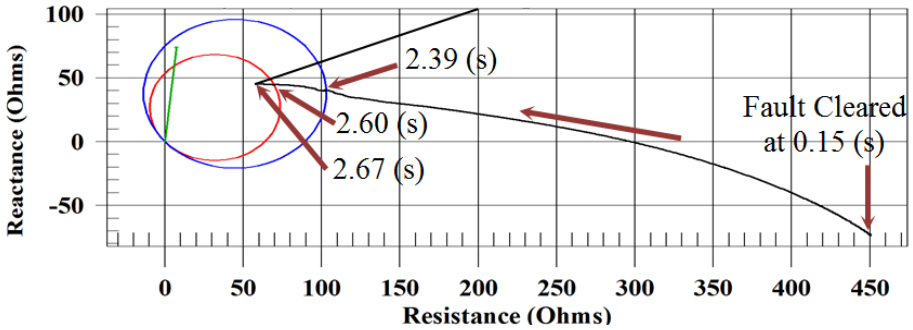

Figure 2.17 Relay mis-operation during unstable swing- Line 79021- 79045

If the OSB is enabled, the impedance enters the outer and inner blinders at 1.82 s and 2.19 s, respectively. Since the time interval between blinders are larger than 2 cycles (OSB typical delay), it is blocked the relay. The impedance trajectory with the enabled blinders is shown in Figure 2.18.

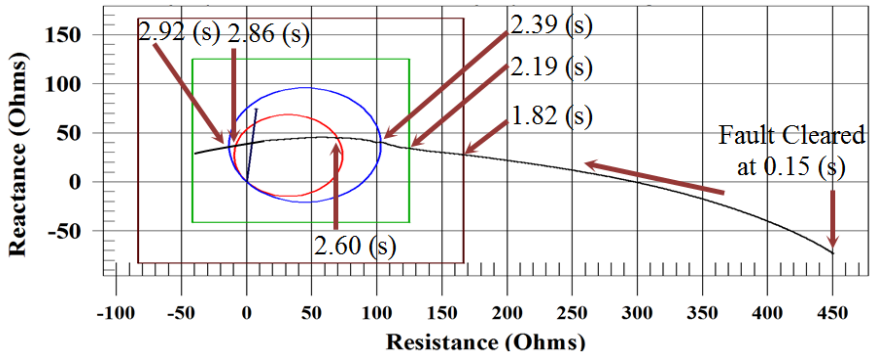

Figure 2.18 Relay blocked during unstable swing- Line 79021- 79045

Malfunction of these distance relays triggers a RAS action (TOT2A) (when the Nucla generators inject power above 60 MW to the grid, the Montrose- Nucla 115 kV line is automatically transfer tripped) [26], and by utilizing the appropriate blocking functions, the specific RAS (TOT2A) is not initiated which can minimize the cascading vulnerability impacts.

3. Power Swing and Fault Detection Methods

In this chapter, different methods that have been proposed for discriminating power swings and fault conditions for distance relay and LOE relay are introduced. Moreover, the new algorithm based on the rate of change of angle is proposed to prevent LOE relay mis-operation and detect the swing condition. Finally, the performance of the proposed technique is tested in the co-simulation platform.

3.1 Power Swing Detection Techniques for Distance Relays

As explained in the first chapter, the power swing blocking scheme is added to the conventional distance relay to detect power swing and prevent relay mis-operation. Traditional methods measure the positive-sequence impedance seen by the relay and the rate of change of impedance. During normal operating conditions the measured impedance is the load impedance and that point is far away from the distance protection zones. When a fault occurs the measured impedance jumps immediately from the load impedance to a point on the impedance plane that represents the fault. On the other hand, when a power swing occurs the measured impedance moves slowly at some trajectory in the impedance plane and at a rate depending on the slip frequency between the machines. This large difference in the speed of movement of impedance in used to differentiate between faults and power swings. Different combinations for impedance measuring elements were proposed for PSB function such as two-blinder scheme, and concentric characteristic scheme [10]. Moreover, a method based on the rates of change of swing center voltage (SCV) was explained in [27]. For instance in a two-source equivalent system when a power swing occurred, due to a slip frequency between the two machines the voltage at the electrical center becomes zero when the angel between two machines are 180 apart. The Figure 3.1 illustrates the voltage phasor diagram of a general two-machine system, with SVC shown as the pahsor from the origin to the O'.

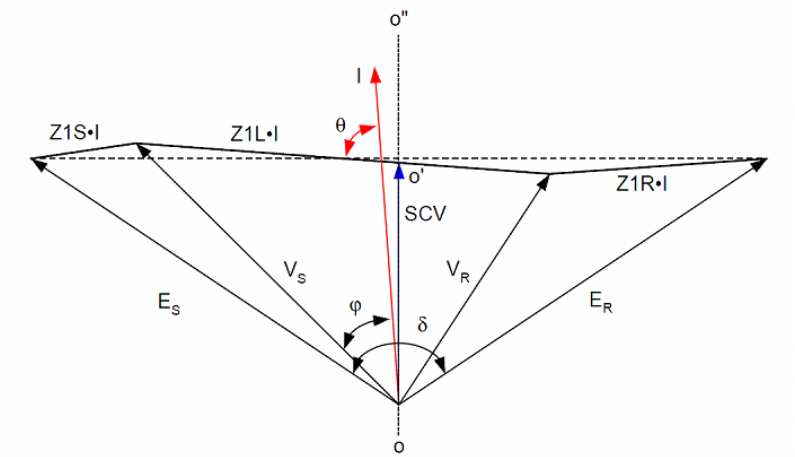

Figure 3.1 Voltage phasor diagram of a two-source system and the relative SVC

The power swing condition is detected when the rate of change of SVC is larger than a threshold. More details of this method is provided in [27]. In [10] the continuous changes of current (ΔI) is

used to detect power swing. If the difference of ΔI value in three consecutive cycles is greater than 5% of the nominal current, the power swing condition is detected.

These methods can easily detect very fast swings but may need to be complemented by conventional rate-of-change-of-impedance method for extremely slow power swings [10]. By utilizing newer technologies such as phasor measurements units and signal processing techniques various methods have been proposed to detect power swing. In the following section one of the non-traditional power swing detection method for distance relays based on the wavelet transform algorithm is explained and simulated results are presented.

3.1.1 Wavelet transform to detect fault condition in distance relay

In [22] a method based on the wavelet transform is introduced to reliably detect power swing as well as detecting symmetrical faults. Wavelet analysis can be used to find abrupt changes in any signals. A wavelet is a waveform of effectively limited duration that has an average value of zero. Wavelet analysis is the breaking up of a signal into shifted and scaled versions of the original (or mother) wavelet. Since the symmetrical fault and power swing signals have different frequency behavior, they can be detectable by extracting the high frequency components from the voltage and current waveforms. There are different mother wavelets, which are used to compare with the original signal. The most used ones are Haar, Daubechies (db), and Morlet.

- Discrete wavelet transform

In this method, the signal is filtered by a high band and low band filters as explained in Fig. 28. The detail coefficients of the each level are defined by the high pass filter (D stages) and the approximated coefficients are calculated by low pass filters (A stages). The wavelet tree is depicted in Figure 3.2.

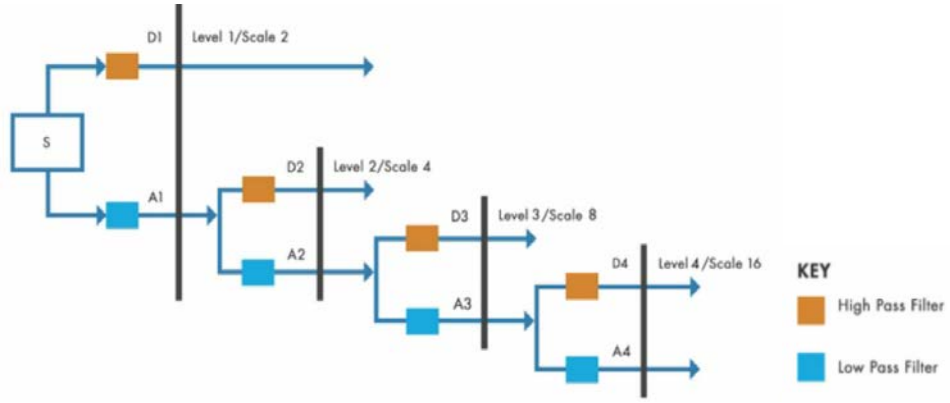

Figure 3.2 Decomposing the data into different coefficients

By this technique the abrupt changes of transient conditions in the voltage, current, and impedance signals can be captured at different levels.

In [22], the level 1 (D1) with mother wavelet Daubechies (db4) is chosen for fault detection from swing. If the changes in the detail coefficients of current and voltage signals are larger than a

threshold, transient condition is detected. By using the D1 coefficient criteria, the out of step blocking function in protective relay can distinguish power swing from fault.

- Simulation results

Single machine infinite bus system is modeled in Matlab Simulink (Figure 3.3). Two different symmetrical faults is studied for detecting the power swing and fault condition.

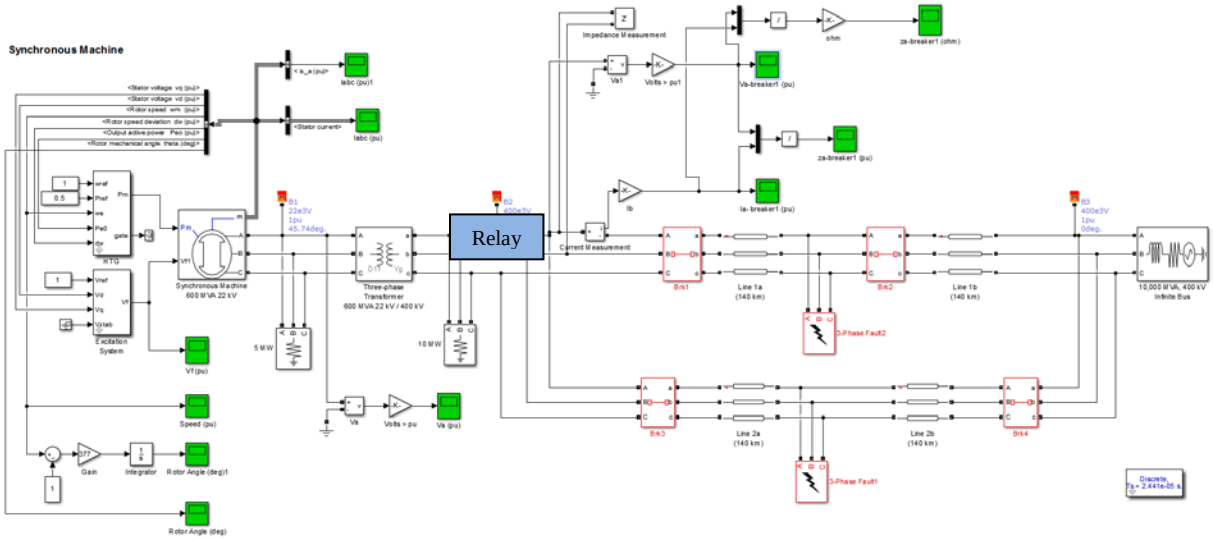

Figure 3.3 Single machine infinite bus system

1. 3-phase fault

A 3-phase to ground fault is applied on the lower line at t=1 s, then breaker#3 and breaker#4 operate and disconnect the line and clear the fault after 5 cycles at t_c=1.1 s. This contingency leads to a stable swing condition.

During the swing cycles, out of step blocking (OSB) function, blocks the distance element of the relay, then if a fault happened in this condition, the relay should detect it and operate. So, a fault on the upper line (fault#2) occurs at 6 s and it is cleared after 0.1 s. The sampling rate is 40.96 kHz in this simulation. Daubechies wavelet db4 is used as the mother wavelet. The wavelet transform is performed in a window length of two cycles (data point in each window N=1365=40.96kHz*2/60). This window moves along the signal as shown in Figure 3.4 and different levels detail coefficients (D) are calculated by decomposing the original signal.

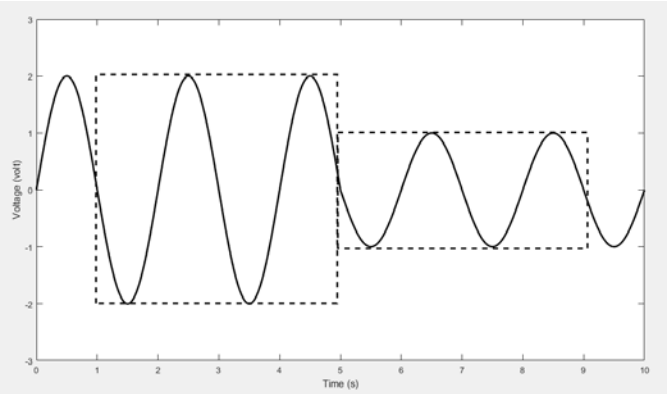

Figure 3.4 Two cycle sampling window

The relay terminal voltage signal and its 4-level detail coefficients are shown in Figure 3.5. As it is clear the detail coefficients are equaled to zero except for the changes inceptions caused by swing or fault conditions. For instance, during the swing, the D1 coefficient variations (in the red rectangle) are between -30 to 30 but in the fault condition (Blue rectangle) this coefficient changes between -90 to 90. The D1 abrupt changes in the rectangles during swing cycle and fault are magnified in Figure 3.6and Figure 3.7, respectively.

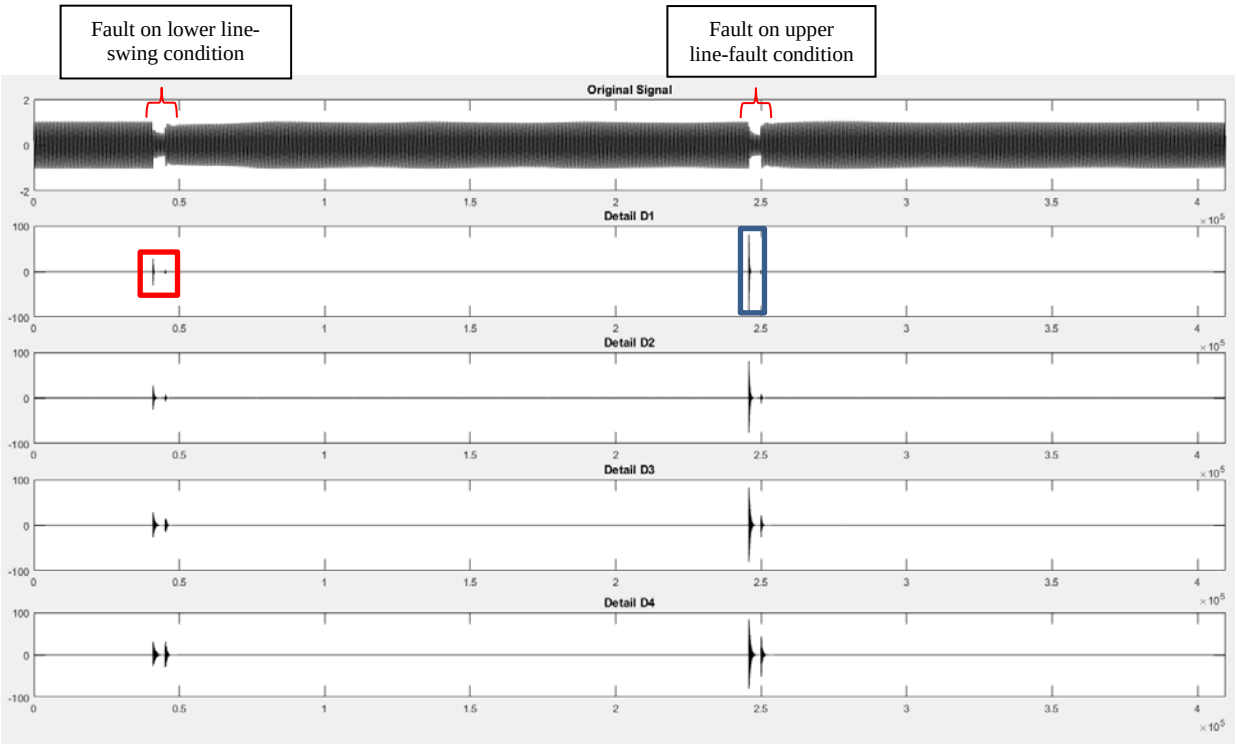

Figure 3.5 Terminal voltage signal and its 4-level detail coefficients

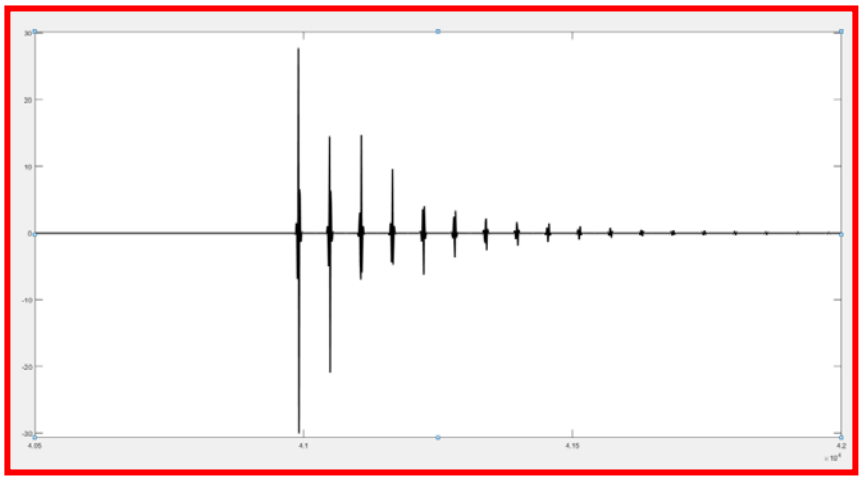

Figure 3.6 D1 variations (voltage signal) during the power swing

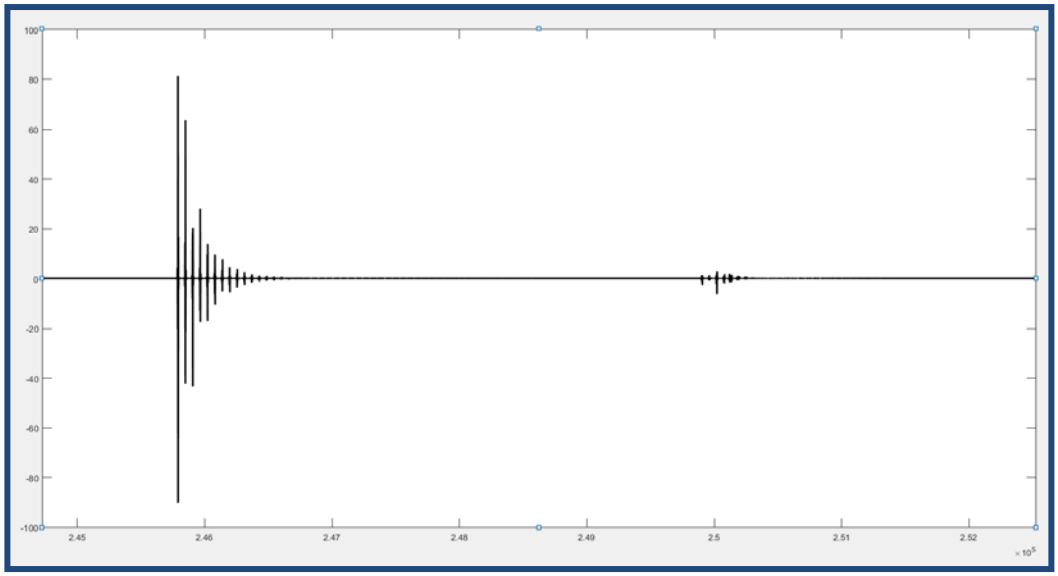

Figure 3.7 D1 variations (voltage signal) during the 3-phase fault

Furthermore, the current at the relay terminal and its 4-level detail coefficients is depicted in Figure 3.8 The detail coefficients are equaled to zero except for the changes inceptions caused by swing or fault conditions. D1 coefficient during the swing (in the red rectangle), is much greater than the one during the fault (Blue rectangle). During the swing they change between -12 to 12 while the changes in the fault are very small. The D1 abrupt changes in the red rectangle during swing cycle is magnified in Figure 3.9.

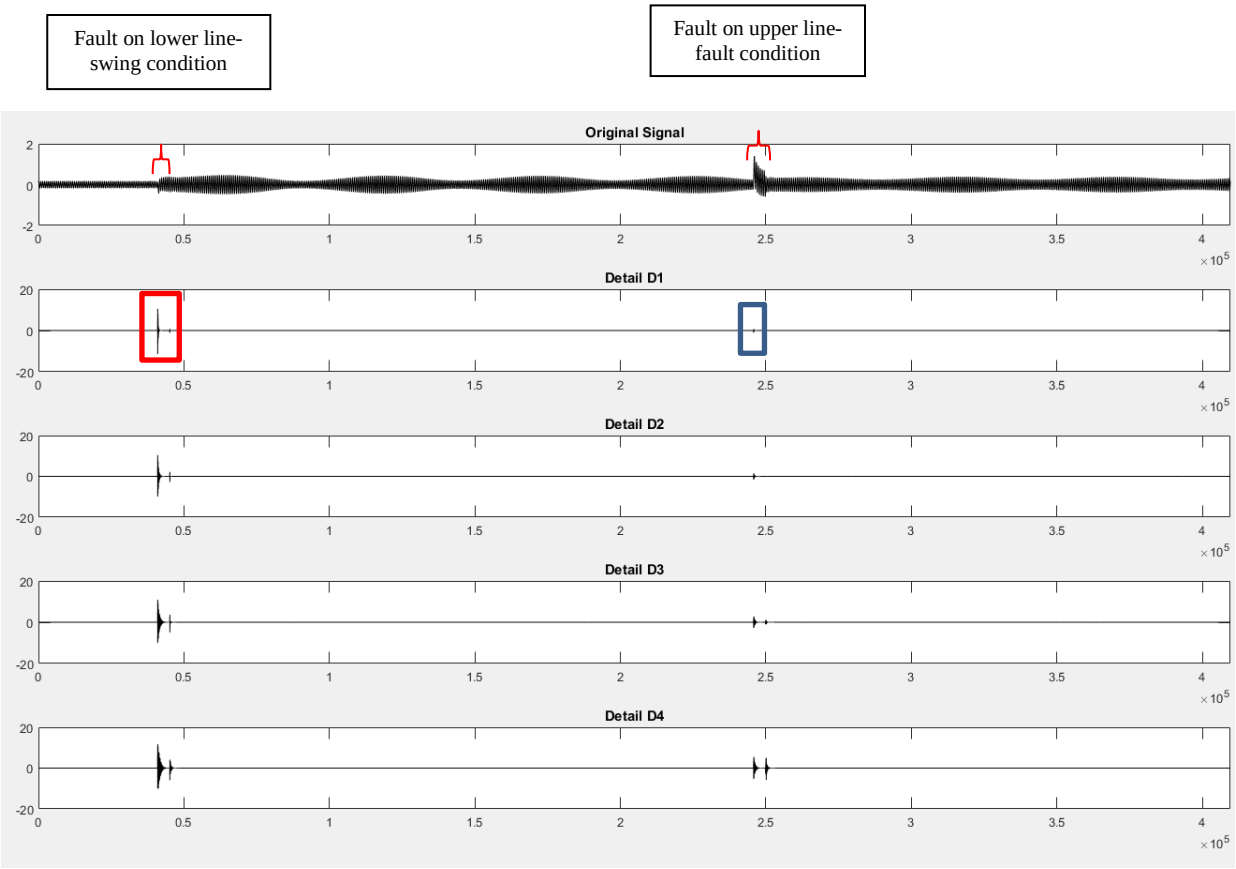

Figure 3.8 Relay terminal current signal and its 4-level detail coefficients

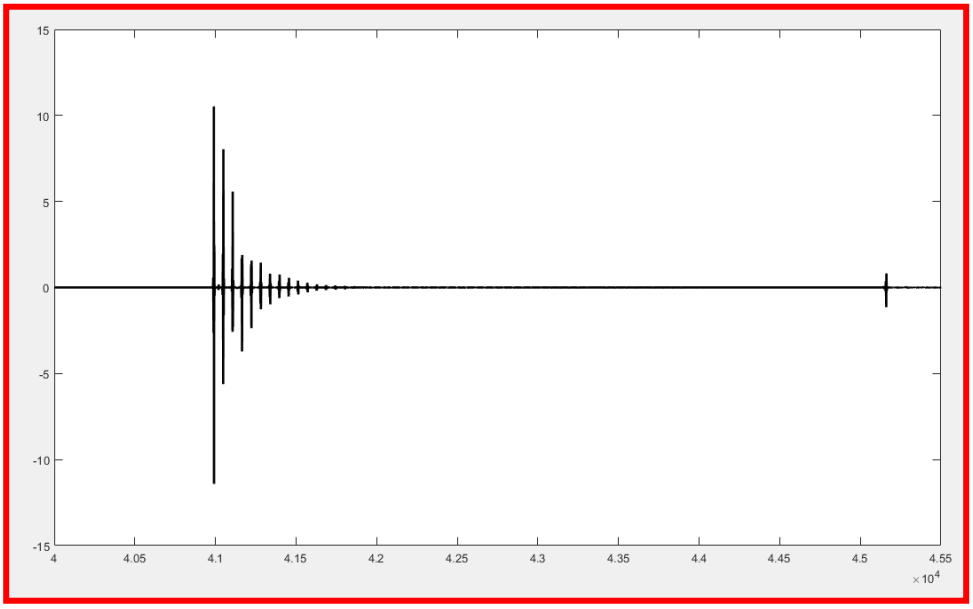

Figure 3.9 D1 variations (current signal) during the power swing

2. Phase to phase fault

Line to line fault is occurred between two phases. The fault between phases A and B is applied with similar location and timing as the pervious case (3-phase fault).

The detail coefficients for voltage and current at the relay location are depicted in Figure 3.10. The D1 abrupt changes in the rectangles during swing cycle and fault are magnified in Figure 3.11 and Figure 3.12, respectively.

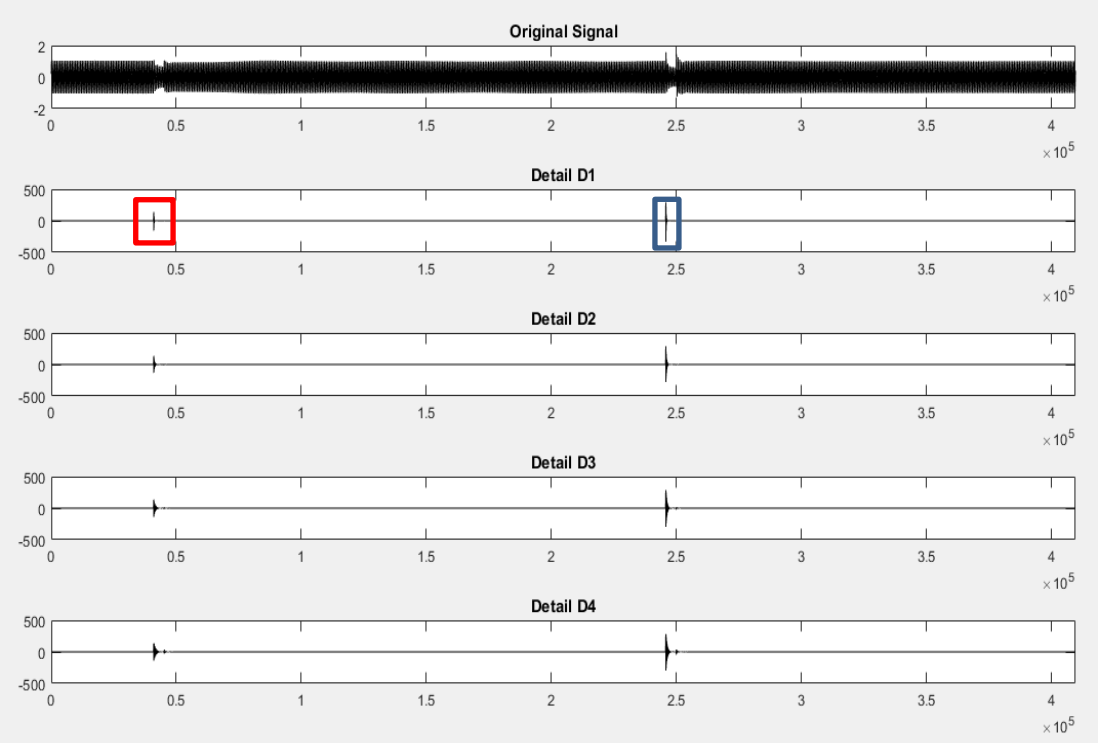

Figure 3.10 Terminal voltage signal of relay and its 4-level detail coefficients- line-line fault

It is obvious, the D1 coefficient in fault condition are larger in comparison to the swing cycle. By choosing an appropriate threshold for D1 coefficient of the voltage the relay can distinguish fault from swing. If the D1 coefficient of voltage is larger than the threshold, the relay should operate for the fault.

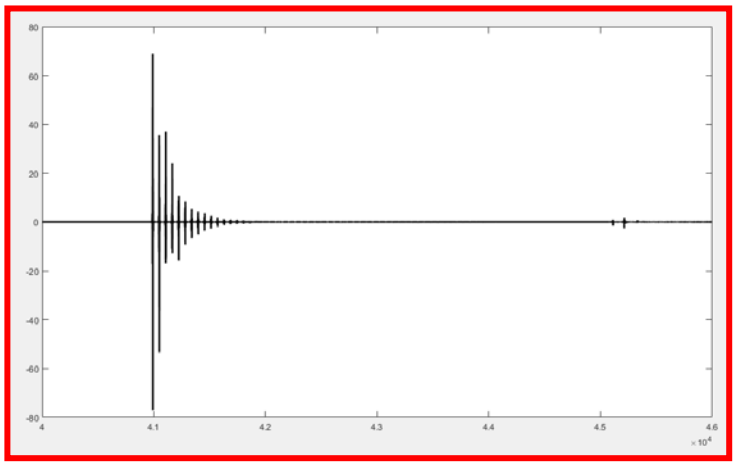

Figure 3.11 D1 variations (voltage signal) during the power swing

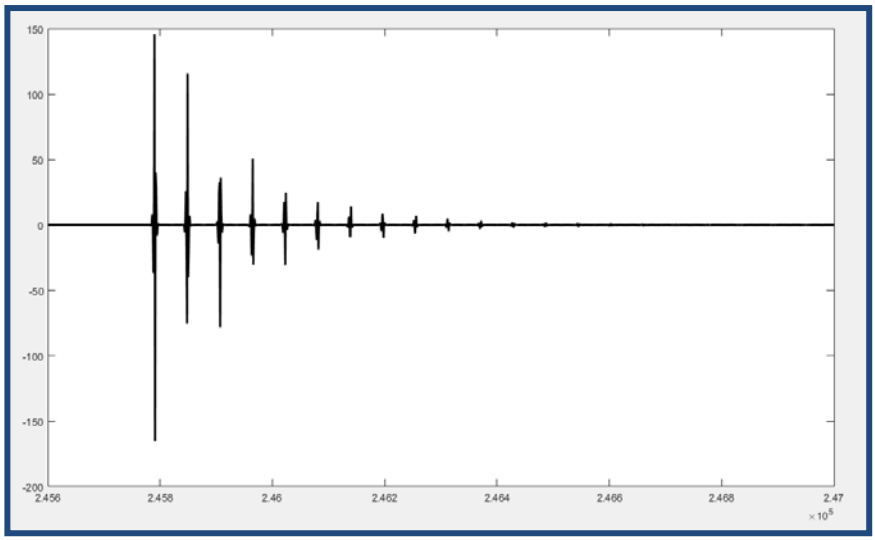

Figure 3.12 D1 variations (voltage signal) during the line-line fault

The current signal and its detail coefficients are shown Figure 3.13. The D1 coefficient of current in swing cycle is bigger than L-L fault condition. By choosing a threshold for this criterion the relay can detect the swing and be block by OSB function.

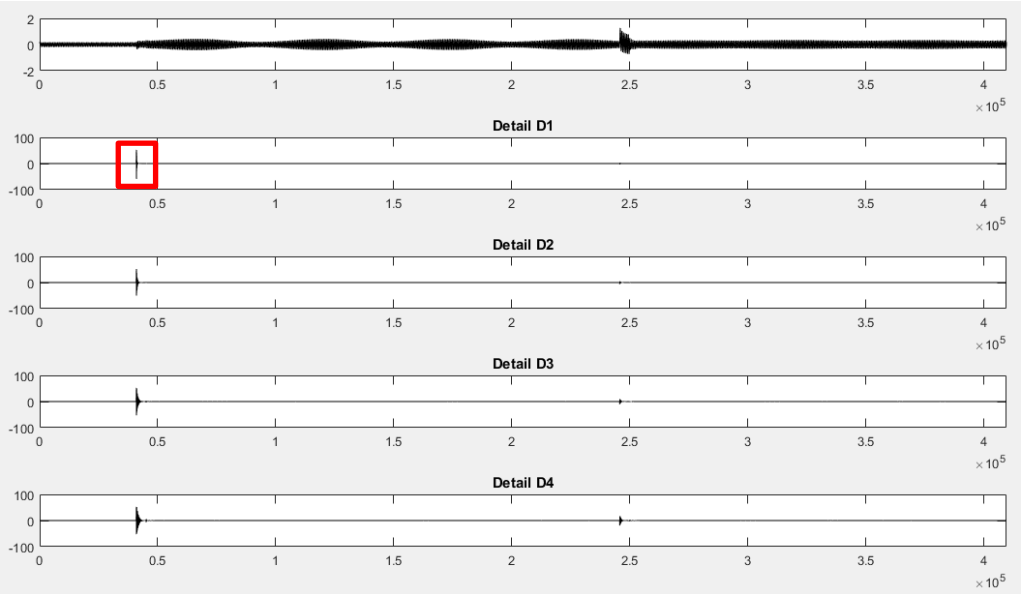

Figure 3.13 Relay terminal current signal and its 4-level detail coefficients

The D1 abrupt changes in the red rectangle during swing cycle is magnified in Figure 3.14.

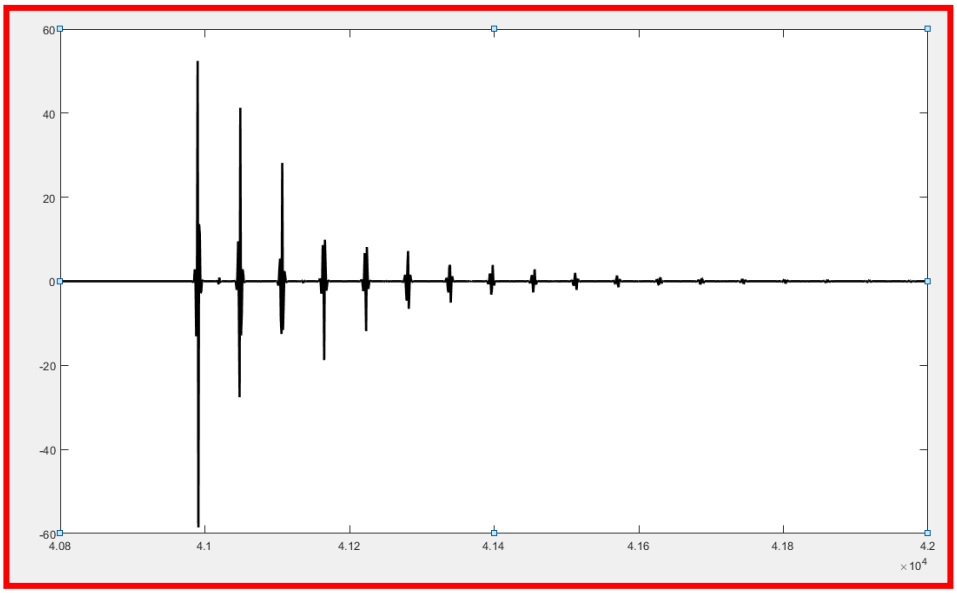

Figure 3.14 D1 variations (current signal) of relay current during the power swing

3.2 Power Swing Detection Techniques for Loss of Excitation Relays

As mentioned in the chapter 1, Bredy proposed the negative-offset mho characteristics for loss of excitation protection of the synchronous generators. Besides the impedance based LOE protection scheme which is the most popular one in industrial applications, there are also some other type LOE technique, such as impedance scheme enhanced with directional element, admittance scheme

(G-B plane), and active power- reactive power (P-Q) scheme or V-I one [17], and [28]. Based on the operation condition and fault location and types, the traditional LOE relay may detect the power swing as the fault and mis-operates. In [29] fuzzy logic-based technique which utilizes the impedance trajectory and generator terminal voltage to improve the conventional method is proposed which requires comprehensive simulation studies. In [30] the derivative of voltage and reactive power is utilized to detect generator LOE. This technique has a time delay and may misoperate with highly loaded generator during stable swing condition.

In addition a setting-free approach is presented in [31] that the rate of change of resistance variations at the generator terminal is introduced as the LOE detector. In the following section this technique is explained and its performance is studied on the test system.

3.2.1 Monitoring the Rate of Change of Apparent Resistance (*dR/dt*) to Detect LOE

In [31], a new algorithm for detecting LOE from power swing is proposed. The rate of change of generator terminal resistance is measured and if its value is negative and remains negative more than a specific time period, the generator suffers from loss of excitation. The apparent impedance at the generator terminal in the single machine infinite bus system (Figure 3.15) can be defined as Eq. (3.1) and (3.2) [31]:

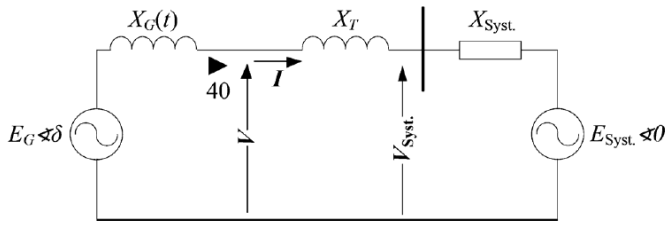

Figure 3.15 Thevenin equivalent circuit of power system

$$Z = \frac{k\sin\delta(t)}{1+k^2-2k\cos\delta} X_{Tot}(t) + j\left(\frac{1-k\cos\delta}{1+k^2-2k\cos\delta} X_{Tot}(t) - X_G(t)\right) \tag{3.1}$$

$$R(t) = \frac{k\sin\delta(t)}{1+k^2-2k\cos\delta} X_{Tot}(t)$$
$$X(t) = \frac{1-k\cos\delta}{1+k^2-2k\cos\delta} X_{Tot}(t) - X_G(t) \tag{3.2}$$

Where, $X_{Tot} = X_G(t) + X_T + X_{Sys}$, and $k(t) = E_{Sys} / E_G$. It is assumed the angle δ is constant when LOE occurs then *k* starts increasing. *dR/dt* is:

$$\frac{dR}{dt} = \frac{(1-k(t)^2)\sin\delta}{(1+k(t)^2-2k(t)\cos\delta)^2}\frac{dk}{dt}X_{Tot}(t) + \left(\frac{k(t)\sin\delta}{1+k(t)^2-2k(t)\cos\delta}\frac{dX_{Tot}(t)}{dt}\right) \quad (3.3)$$

Since *k* increases, *dk/dt* is positive. Therefore, as long as *k* is less than 1 (*k<1*), the first term will be positive. Since X_G changes during this period it is not possible to judge the sign of the second term. However, after a few seconds when X_G settles to its final value, the second term in (3.3) will become zero (*dX/dt=0*). At this time, *k* has increased far more than 1 (*k>1*) while *dk/dt* still remains positive. Therefore, after a period of time, the first term will become and remain negative and so will *dR/dt*. As a result, the relay will observe the rate of change of *R* and if *dR/dt* becomes and remains negative for a while, LOE can be detected.

During a power swing, similar condition can occur which means that *dR/dt* becomes and remains negative for a while. To distinguish the LOE from the power swing, it is then necessary to determine for how long *dR/dt* will remain negative during power swing at the worst case. The slip frequency is between 0.3 -7 Hz during swing period.

Thus, the longest period of *dδ/dt* that can be expected during a slowest power swing is 1/0.3=3.33 seconds, in half of this period, *dδ/dt* remains positive and *dR/dt* will not remain negative for more than 1.67 sec. To distinguish an LOE from the power swings, LOE relay should wait for 1.67 seconds and if still remains negative, an LOE can be detected.

- Simulation results

A SMIB system like Figure 3.3 is modeled in Matlab Simulink. The voltage and current phasors at the generator terminal are calculated, and then apparent *R*, *X*, *dR/dt* and *dx/dt* at relay are calculated in phasor domain.

1. LOE condition

LOE fault is modeled by changing the dc voltage input signal Vf of the generator. At t=4 s, Vf is changed to zero, so the generator lost its field. The dR/dt is depicted during fault period in Figure 3.16. As it is clear dR/dt in this condition became negative (before the fault dR/dt is zero) and remains in the negative section. After 1.7 s, LOE is detected and a trip signal will be sent to the generator circuit breaker at 5.7 s as shown in Figure 3.17.

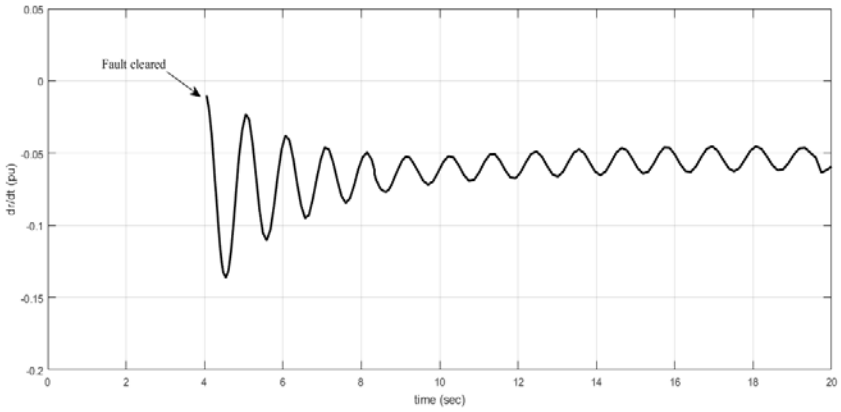

Figure 3.16 Variations of dR/dt measured by generator relay after LOE

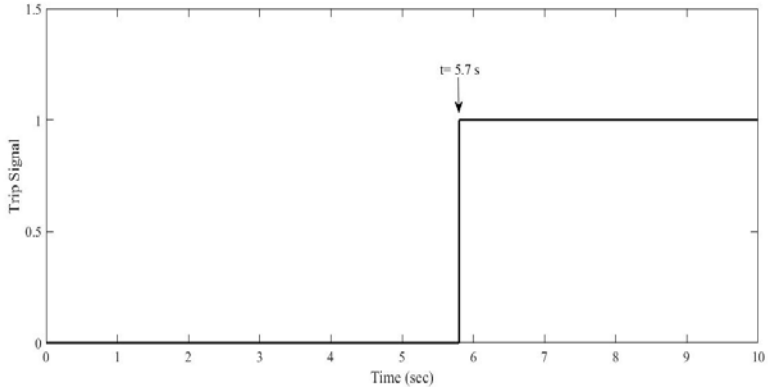

Figure 3.17 LOE Trip signal issued at 5.7 s

On the other hand, after LOE the impedance locus enters the conventional LOE characteristic of the relay. Impedance enters the zone#2 at 6.44 s and after 0.7 s (zone#2 delay+ breaker delay), the trip signal will issue at 7.14 s. the impedance locus and the trip signal instant are depicted in Figure 3.18 and Figure 3.19, respectively.

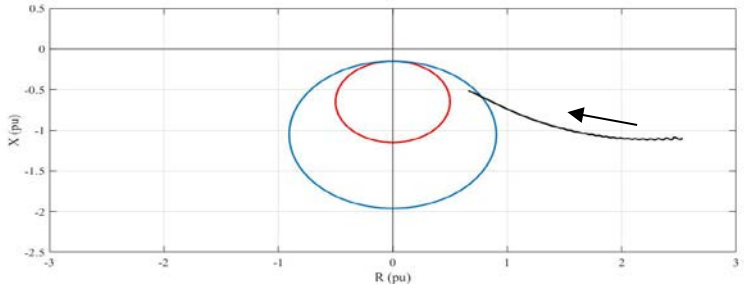

Figure 3.18 Impedance locus after LOE- conventional LOE characteristic

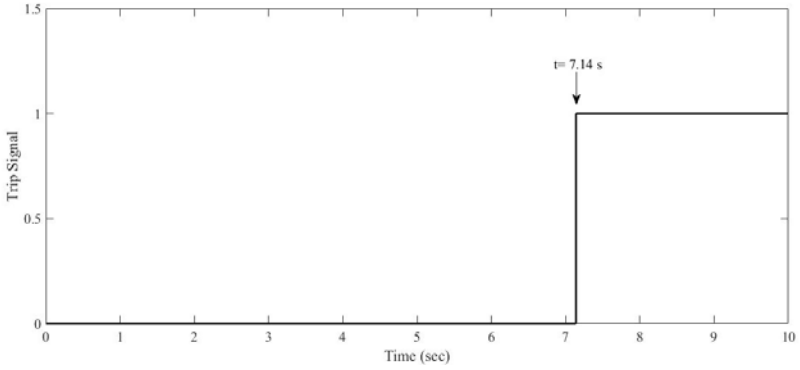

Figure 3.19 LOE Trip signal issued at 7.14 s- conventional LOE characteristic

2. Power swing condition

A fault is applied at the middle of the lower tie-line, and cleared after 5 cycle (fault occurs at 6 sec and cleared after 0.1 sec), the system experiences stable power swing. dR/dt variation is shown in Figure 3.20. *dR/dt* changes in the positive and negative planes. The slip frequency of this simulated swing condition is 0.7 Hz (1/1.3 s) which is one of the slowest power swings. It remains negative for half a cycle (0.65 sec) and then become positive. By this variation, the relay detects this condition as the stable swing and does not trip the generator.

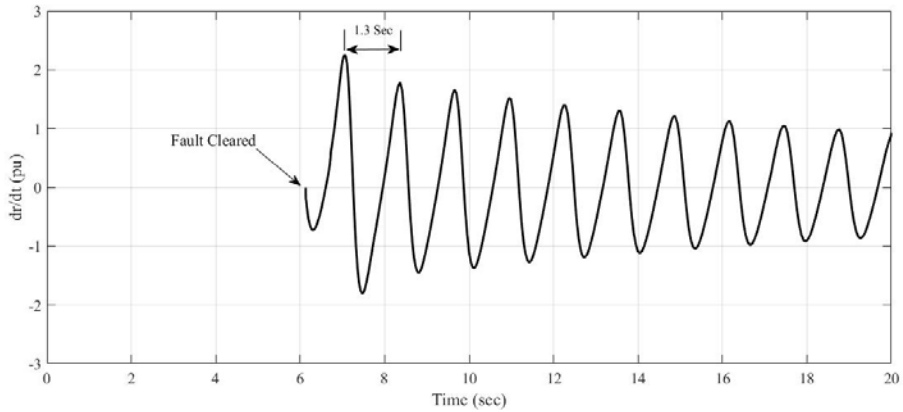

Figure 3.20 Variations of *dR/dt* measured by generator relay during power swing

3. LOE occurrence during swing condition

If during a stable swing a fault happened in the generator excitation system, the LOE relay should detect it and operate. A short circuit fault applied in the field circuit and V_f becomes zero at 10 sec, the *dR/dt* changes are shown in Figure 3.21. By LOE, *dR/dt* remains negative, after 1.7 s, trip signal will be sent at t= 11.7 s as shown in Figure 3.22.

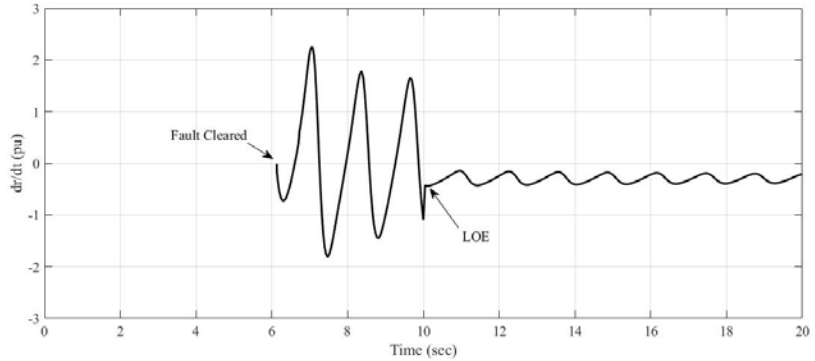

Figure 3.21 Variations of dR/dt measured- LOE during swing

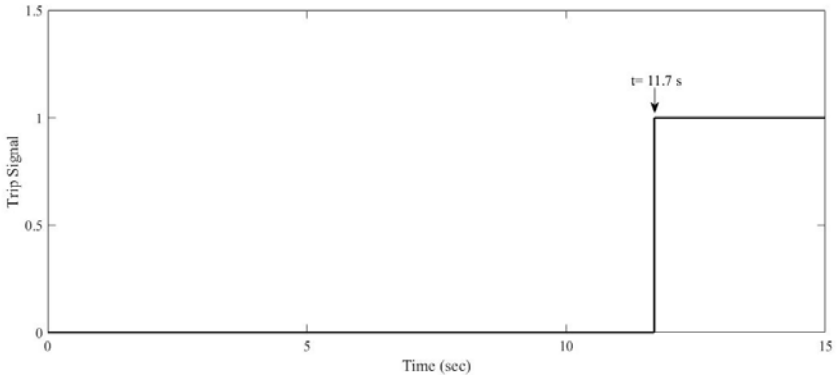

Figure 3.22 LOE Trip signal issued at 11.7 s

With respect to the conventional LOE characteristic, the impedance locus enters zone#2 at 12.83 s and after 0.7 s (zone#2 delay+ breaker delay), the trip signal will issue at 13.53 s. The impedance locus and the trip signal instant are depicted in Figure 3.23 and Figure 3.24, respectively.

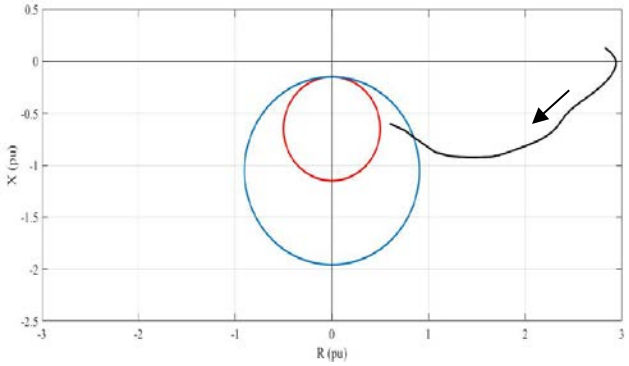

Figure 3.23 Impedance locus after LOE- conventional LOE characteristic

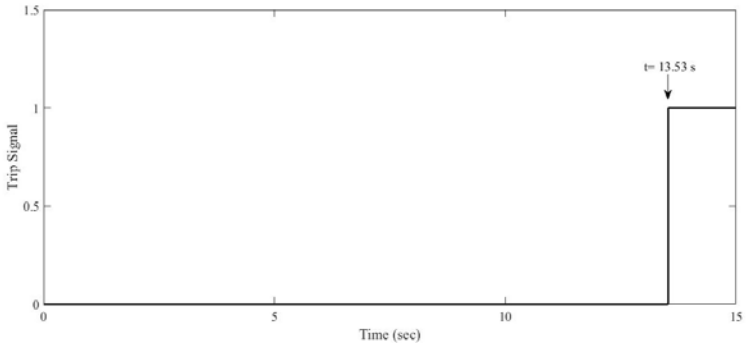

Figure 3.24 LOE Trip signal issued at 13.53 s- conventional LOE characteristic

The proposed method acts faster than the conventional 2 zone method and thus can isolate the generators suffering from LOE with less time delay. Since the measured resistance has an oscillatory nature due to the speed variation associated with slip frequency, this technique may not detect swing condition with the slow slip frequency [32].

3.3 Secure loss of excitation detection technique for synchronous generator

3.3.1 Principles of the proposed method

Synchronous generators as one of the significant equipment in the power system should be protected with highest rate of dependability, security and selectivity [33]. Thus, various types of protective relays such as differential relay (87G), ground fault protection (59GN and 27H), unbalanced current protection, loss of excitation protection (40),field ground protection (64F), out-of-step protection (78) and etc. are utilized to detect faulty conditions in the power supply rapidly, and prevent unwanted tripping of the generator [34].

The field circuit of synchronous generators keeps the generator synchronism with the power system by providing the required magnetizing energy. The excitation system establishes the rotor flux which generates the internal voltage of generators. Besides, the output reactive power of generator is dependent and changes by the internal voltage. The source tht excites the field winding may be interrupt due to incidents such as open or short circuit in the excitation system, equipment failure, inadvertent tripping of the field breaker, loss of field in the main exciter, a regulator control system failure, and slip ring flashover [31]. Following the occurrence of loss of excitation (LOE) the rotor current decays based on the field circuit time constant, as a result, the internal voltage of generator decreases with the same rate. Since the generator Var output is proportional to the internal voltage, it also decreases. The generator starts to absorb reactive power from the power system to replace the excitation previously provided by the field circuit. The reduction of the internal voltage causes voltage drops also weakens the coupling between rotor and stator. At some point during this period, active power cannot be transferred to the power system and the generator loses synchronism with the power system (loses synchronism torque). It can lead to high stator winding currents, severe pulsating torque, inducing AC voltage in field circuit, and stator end-core overheating. Moreover, the large amount of the Var absorbed by the generator from the system may jeopardize the voltage stability of the power system which can contribute to a wide area

system voltage collapse. Thus, the protective relays should detect the LOE quickly and accurately.

The effects of loss of synchronism resulted by a LOE event for the equivalent system shown in Figure 3.25, can be visualized based on the power angle equation. The active power injected to the system is defined based on the following equation:

$$P_e = \frac{E_I E_S}{X_d + X_{Sys}} \sin\delta + \frac{E_S^2 (X_d - X_q)}{2(X_d + X_{Sys})(X_q + X_{Sys})} \sin 2\delta \tag{3.4}$$

Where P_e, E_I, E_S, X_d, X_q, X_{Sys} and δ denote the electrical power, internal voltage, equivalent system voltage, d and q axis synchronous impedance, system impedance ($X_{Sys} = X_S + X_L$), and angle between E_I, and E_S, respectively. Ignoring the effect of the saliency is ignored by assuming $X_G = X_d = X_q$, then the power angle equation is expressed as:

$$P_e = \frac{E_I E_S}{X_G + X_{Sys}} \sin\delta \tag{3.5}$$

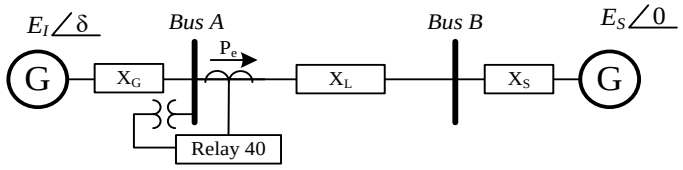

Figure 3.25 Thevenin equivalent circuit of power system

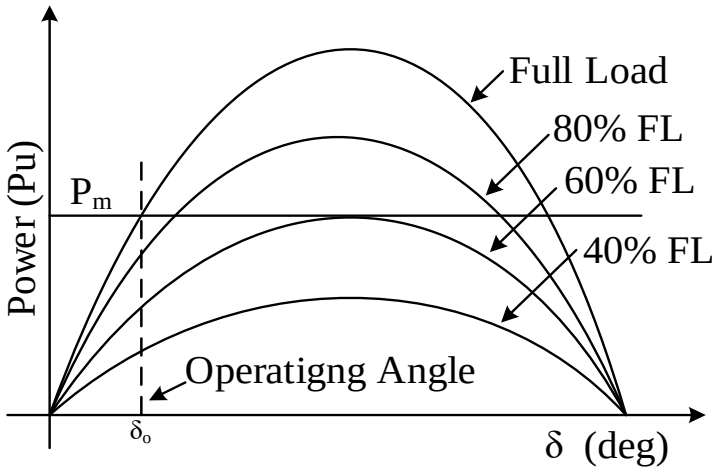

Figure 3.26 Power angle curve

As it is seen in the Figure 3.26 the intersection of the mechanical power of the turbine and the power angle curve define the operating angle of the generator with respect to the generator voltage. The delivered power to the system is proportional to the system and generator voltages and the sine of the angle difference between them. It is inversely proportional to the equivalent impedance of the network. During the LOE, the internal voltage decreases which leads to reduce the height of the power angle curve with time as shown by dotted curve. To maintain the equilibrium between the mechanical input (P_m) of the turbine and electrical output, the operating angle (δ) increases up to reaches the 90° which the electrical power is at maximum. Any decay in the field current after this point the generator loses its capability to transmit all the mechanical power to the power grid. The extra mechanical power increases the kinetic energy of the rotor and accelerating the shaft speed. As the angular speed rises over synchronous speed (60 Hz), the generator pull out of step and its synchronism is lost. The loss of synchronism is not a high-speed event, it is typically take a fully loaded generator several seconds to go out of step. So the out of step relay (78) can detect the loss of synchronism and trip the generator. During LOE period, the slip frequency for a machine at full load is typically at most in the range of 2-5% range. However, it is between 0.1-0.2% for light loaded generators [34].

During the LOE condition, the generator variables (E_I, X_G, and δ) changes with time while the system variables (E_S, and X_{Sys}) are almost constant, so the output power of generator can be expressed as follows:

$$P_e(t) = \frac{E_s^2 k(t)}{X_T(t)} \sin\delta(t) \tag{3.6}$$

Where

$$k(t) = \frac{E_I(t)}{E_S} \tag{3.7}$$

$$X_T = X_G(t) + X_{Sys} \tag{3.8}$$

Based on the aforementioned reasons, the generator maintains its active power equal to the mechanical input power during LOE before pulling out-of-step, so the rate of change of power (dP_e/dt) can be assumed equal zero in this period.

$$\frac{dP_e}{dt} = \frac{E_s^2}{X_T(t)} \frac{dk(t)}{dt} \sin\delta(t) + \frac{E_s^2 k(t)}{X_T(t)} \frac{d\delta}{dt} \cos\delta(t) - \frac{E_s^2 k(t)}{X_T(t)^2} \frac{dX_T(t)}{dt} \sin\delta(t) \tag{3.9}$$

From LOE occurrence, X_G moves toward the fourth quadrant with final value between the average of the d and q-axis subtransient reactances ($(X_d^{"} + X_q^{"})/2$) and the average of the d and q-axis synchronous reactances ($(X_d + X_q)/2$) [15]. Based on the initial loading of the generator, after some seconds, when the generator turns to a sink of reactive power, the X_G settles to the final value in the negative plane, then the derivative of machine reactance becomes zero ($dX_G/dt=0$), so the third term in the (3.9) will become zero. Since dP_e/dt equals to zero, so the rate of change of angle can be expressed as:

$$\frac{E_s^2}{X_T(t)}\frac{dk(t)}{dt}\sin\delta(t) + \frac{E_s^2 k(t)}{X_T(t)}\frac{d\delta}{dt}\cos\delta(t) = 0 \tag{3.10}$$

$$\frac{d\delta}{dt} = -\frac{dk(t)}{dt}\frac{1}{k(t)}\tan\delta(t) \tag{3.11}$$

In this interval, k decreases which is always positive, and dk/dt is negative. Besides, the operating angle (δ) is less than 90° , so the tan (δ) is positive, as a result, after LOE contingency, the generator operating angle always increases and its derivative (dδ/dt) becomes and remains positive and small before loss of synchronism.

During power swing, similar condition may happen which means the operating angle increases and dδ/dt becomes and remains positive for a few instants. According to the literature [22], and [35] the rate of change of angle dδ/dt oscillates with frequency between 1-7 Hz, also in [31] the slowest power swing is considered 0.3 Hz to guarantee the security issues. Thus during the swing condition dδ/dt sign will not remain positive and become negative after half a cycle as illustrated in Figure 3.27.

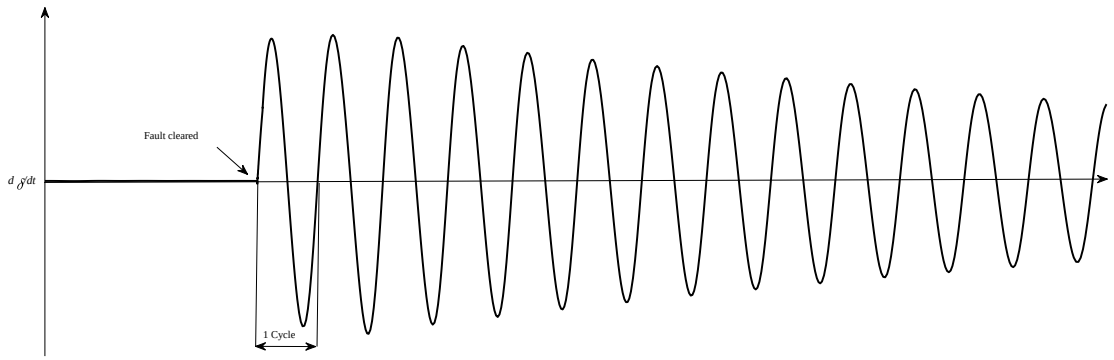

Figure 3.27 Oscillation of *dδ/dt* during the power swing condition

Moreover, as explained beforehand, during power swing condition, the slip frequency (*dδ/dt*) is in the range 0.3-7 Hz, which is different from the genuine LOE event. Therefore, the frequency of the measured signal can be utilized to discriminate between these two phenomena.

3.3.2 Defining the LOE detection delay (TD)

After the relay detects a disturbance at its terminal, if the dδ/dt remains positive for more than a half a cycle, the proposed method detects the LOE contingency. So a time delay (TD) is defined to guaranty the security of the detection algorithm. TD is defined based on the half cycle of the measured swing frequency (TSW) as follows (5% margin is also considered for security):

$$TD \geq 1.05 \times \frac{T_{SW}}{2} \tag{3.12}$$

or the sample rate (*S*) can be calculated as:

$$S \geq 1.05 \times \frac{f_S}{2 f_{SW}} \tag{3.13}$$

where f_{SW} and f_S denote the swing frequency and sampling frequency (which is typically 1kHz) [32]. The maximum time delay after disturbance detection is *TD*. For instance for the slowest power swing 0.3 Hz *TD* equals 1.75 s.

3.3.3 Logic of the proposed algorithm

Figure 3.28 shows the flowchart of the proposed method. Initially, the LOE relay (40) calculates the *P* and *dδ/dt* subsequently. The TD criterion is defined based on the half a cycle of the calculated slip frequency. Once the *dδ/dt* is non-zero a contingency is detected by the protection system, then if the slip frequency is out of swing frequency range and becomes and remains positive for more than predefined time delay (TD), the conventional relay (40) will operate and trip the generator. However, if the slip frequency is in the swing frequency range, it is distinguished as the swing event and the LOE relay will be blocked before the apparent impedance enters the mho characteristics of the LOE Relay.

If the relay estimates the slip frequency inaccurately and does not detects the swing frequency out of its typical range correctly, it will check the sign of rate of change of angle for TD period and correct its decision and block the mho zones. The proposed algorithm does not need any system parameters. The slip frequency is estimated based on the measured signal. While the other setting-free methods utilized the slowest swing (0.3 Hz) for the predefined time delay [31], [32].

3.3.4 Simulation results

Single machine infinite bus system is modeled in Matlab Simulink (Figure 3.29). The studied generator has the rated power of 600 MVA, and rated voltage 22 kV. The excitation model and system data are described in Appendix. To evaluate the performance of the proposed method, the generator in different initial loading conditions in lagging and leading power factor are investigated.

1. Generator heavy loading condition with lagging positive PF (L_1= 0.9+j0.3 p.u.)
    a. LOE condition

The excitation system of the generator is short circuit at t=2 s and the dc field voltage changes to zero. Since the generator lost its exciter, the output reactive power decays while the active power is still constant at its initial value. The output active and reactive powers of generator are depicted in Figure 3.30.

The polarity of the rate of change of power angle (δ) is always positive during loss of excitation. The trajectory of the power angle variations is always in the first quadrant of the $d\delta$-δ plane as illustrated in Figure 3.31.

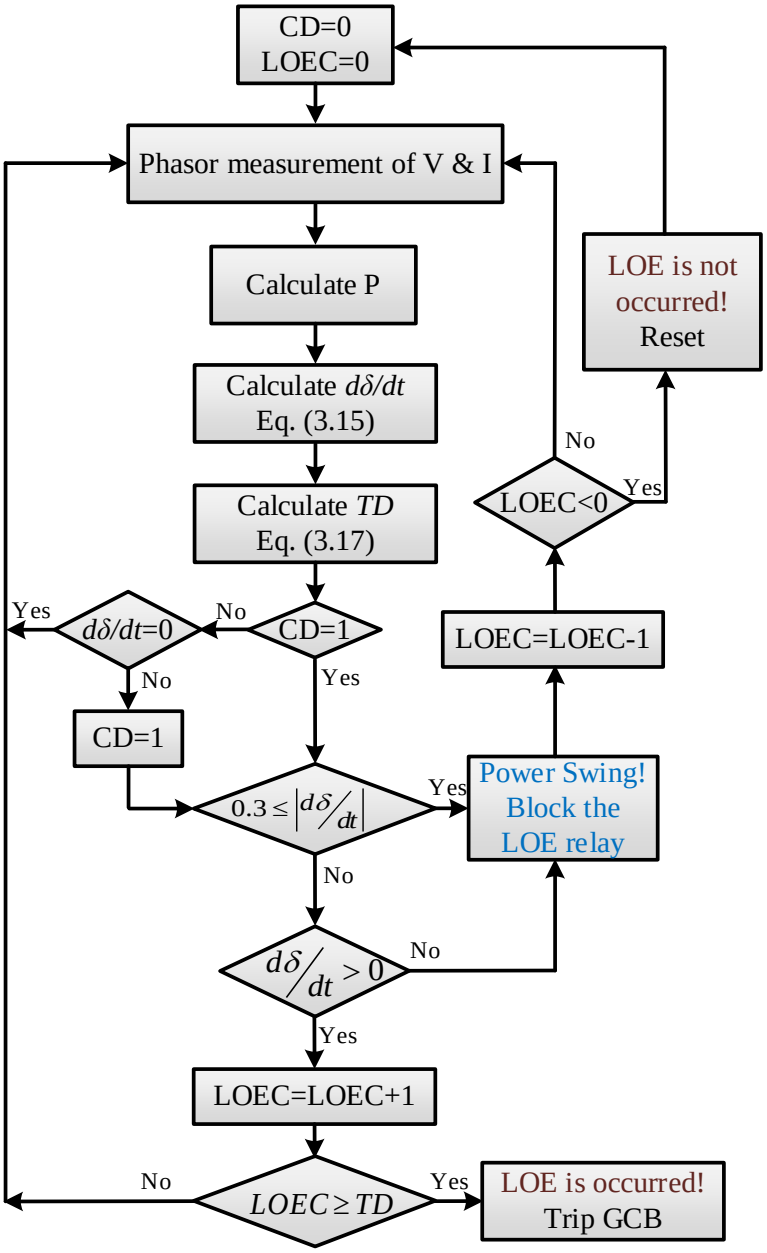

Figure 3.28 Flowchart of the proposed adaptive LOE detection technique

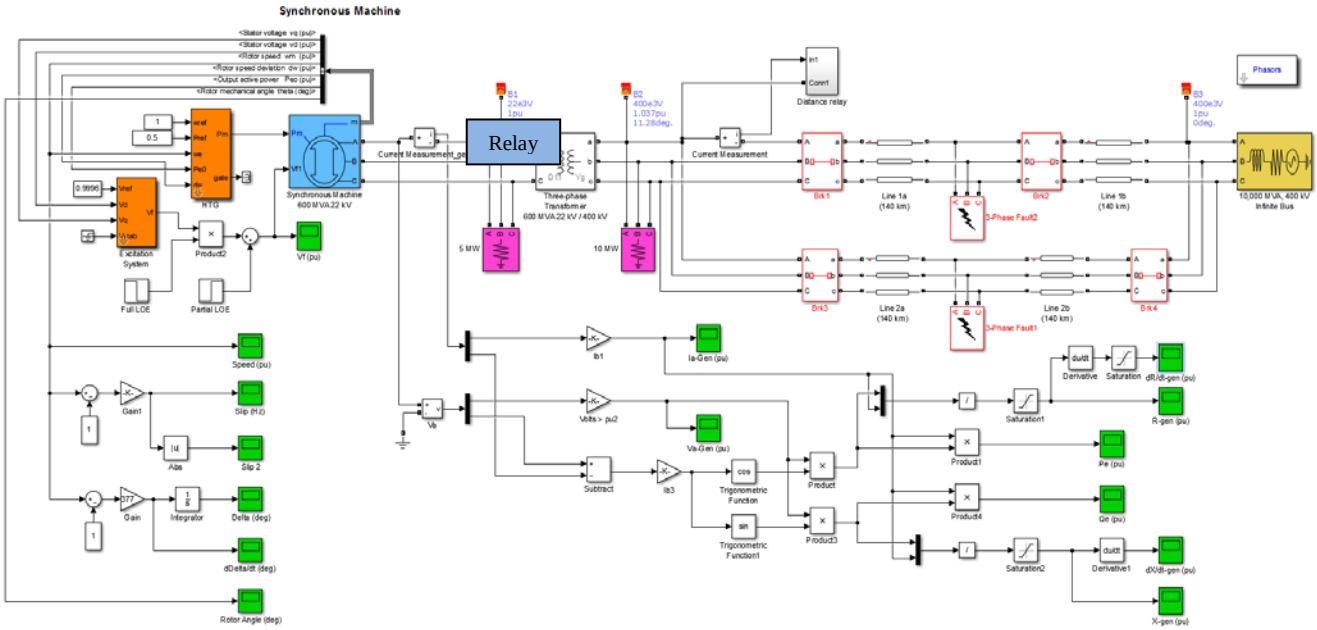

Figure 3.29 Single machine infinite bus system

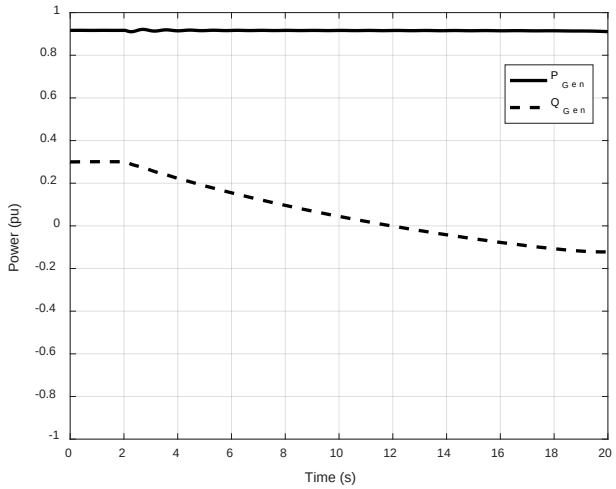

Figure 3.30 Active and reactive powers of synchronous generator following LOE- L_1 loading condition

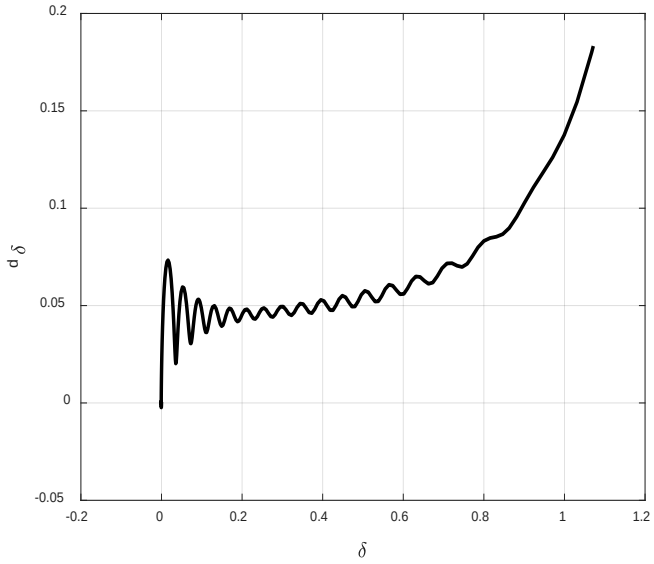

Figure 3.31 Variation of generator angle during LOE occurrence- L_1 loading condition

Also, the slip frequency for this loading condition is less than the typical swing frequency as shown in Figure 3.32, it is close to zero value.

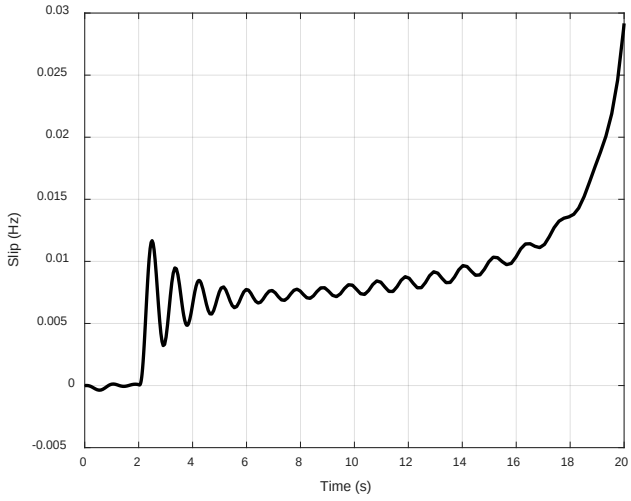

Figure 3.32 Slip frequency variation during LOE occurrence- L_1 loading condition

Based on the calculated variables, the proposed algorithm detects this contingency as LOE after half a cycle and will not block the relay. Then the apparent impedance at relay location moves toward the third quadrant of the R-X plane after loss of excitation. It enters zone2 and zone 1 of the relay at 8.56 s and 9.03 s, respectively. The typical pre-defined time delay for zone 1 LOE is 0.1 s (the breaker operating time is 0.05 s), so the generator disconnected from the grid at 9.18 s

by the zone 1 of LOE relay. The impedance locus and the trip signal instant are depicted in Figure 3.33 and Figure 3.34, respectively.

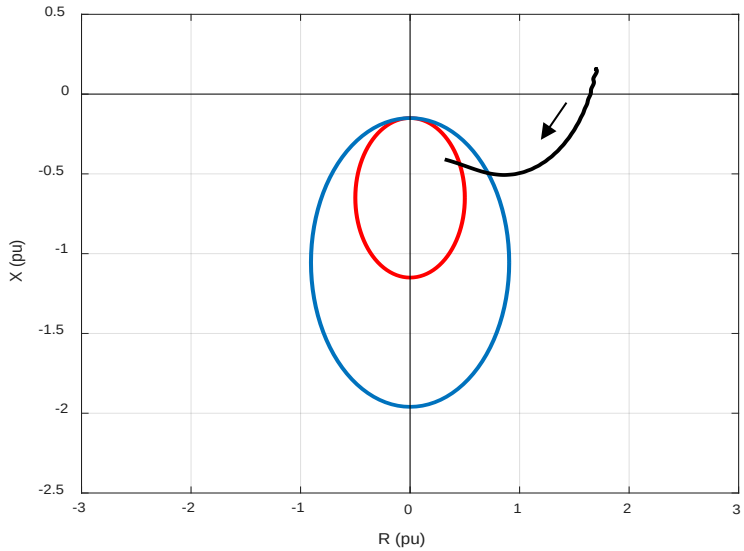

Figure 3.33 Apparent impedance locus during LOE occurrence- L_1 loading condition

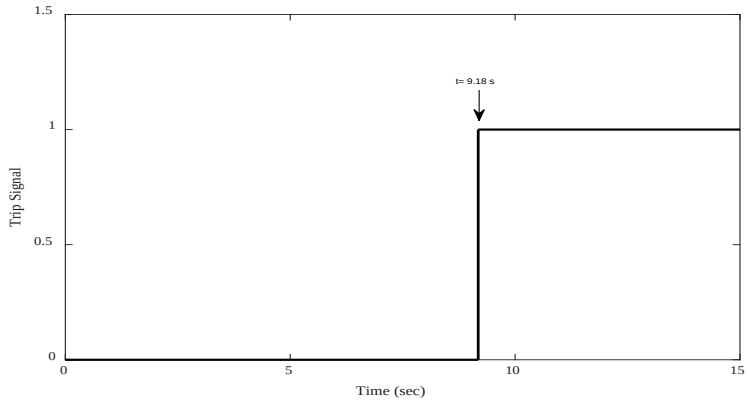

Figure 3.34 LOE Trip signal issued at 9.18 s

b. Power swing condition

If a fault occurs at the middle of the lower tie-line on the system shown in Figure 3.29, at t= 4 s and cleared after 0.1 s by tripping the faulted line, the generator oscillates to get the new equilibrium point. The active and reactive output powers of the generator are shown in Figure 3.35. The reactive power oscillates around the new positive output power. The angle (δ) is non-monotonic during the power swing and the rate of change of angle $d\delta$ changes between positive and negative values. The trajectory of the power angle variations is illustrated in the $d\delta$-δ plane in Figure 3.36. The angle locus starts from origin and rotates in the negative and positive side of this

plane to reach to the new operating point for stable power swing. The polarity of the $d\delta$ changes after every half cycle.

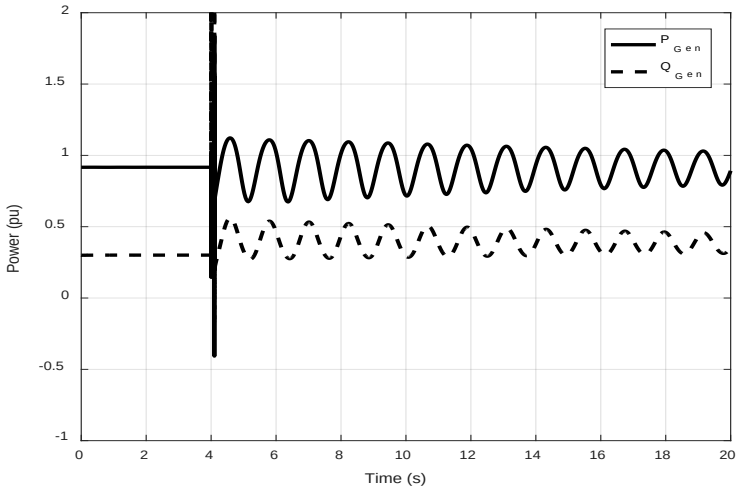

Figure 3.35 Active and reactive powers of synchronous generator during power swing- L_1 loading condition

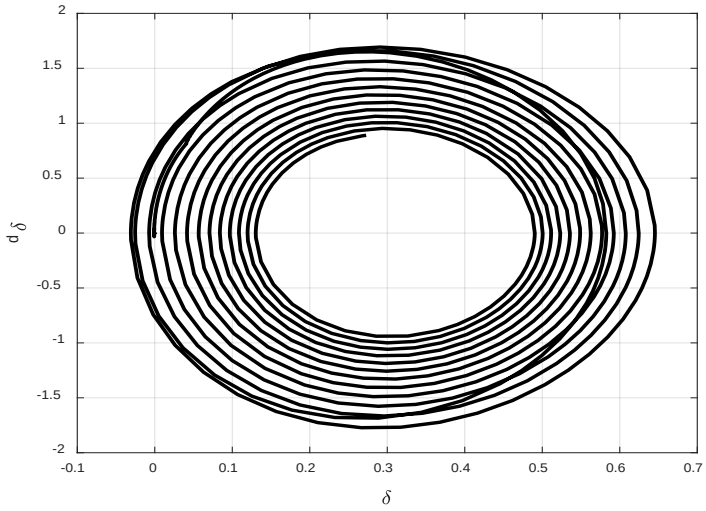

Figure 3.36 Variation of generator angle during power swing- L_1 loading condition

Besides, the slip frequency for this loading condition is more than 1 Hz and the proposed algorithm detects this condition as the power swing and blocks the relay correctly. The stable power swing is shown in Figure 3.32.

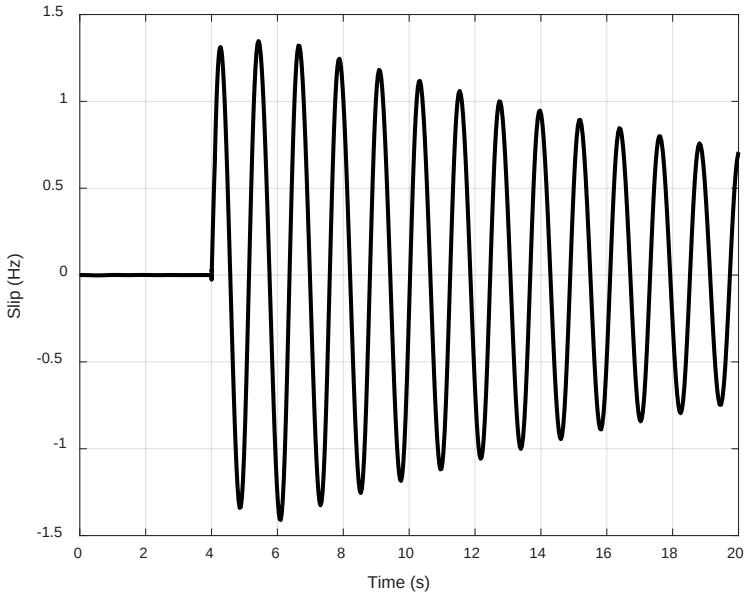

Figure 3.37 Slip frequency variation during stable power swing- L_1 loading condition

2. Generator height loading condition with leading positive PF (L_2= 0.4-j0.35 p.u.)
   a. LOE condition

Similar to tthe previous loading condition, the excitation system of the generator is short circuit at t=2 s. Since the generator lost its exciter, the output reactive power decays while the active power is still constant at its initial value. The output active and reactive powers of generator are depicted in Figure 3.38.

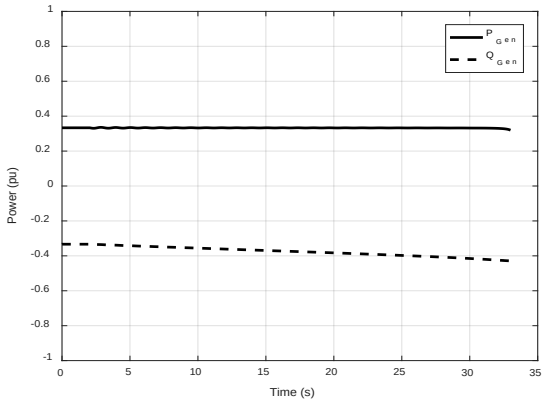

Figure 3.38 Active and reactive powers of synchronous generator following LOE- L_2 loading condition

The polarity of the rate of change of power angle (δ) is always positive during loss of excitation. The trajectory of the power angle variations is always in the first quadrant of the dδ-δ plane as illustrated in Figure 3.39.

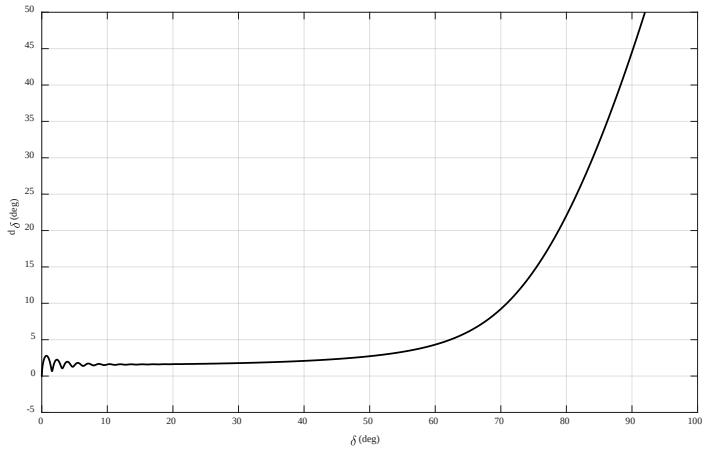

Figure 3.39 Variation of generator angle during LOE occurrence- L_2 loading condition

Also, the slip frequency for this loading condition is less than 0.05 Hz before losing the synchronism as shown in Figure 3.40.

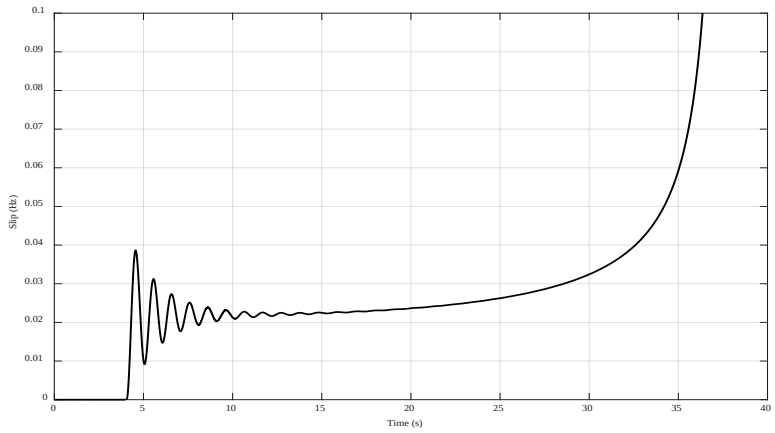

Figure 3.40 Slip frequency variation during LOE occurrence- L_2 loading condition

Based on the calculated variables, the proposed algorithm detects this contingency as LOE after half a cycle and will not block the relay. Since the generator is operated with the initial leading PF, the apparent impedance starts its trajectory from a point with negative reactance in the third quadrant of the R-X plane after loss of excitation. It enters zone2 and zone 1 of the relay at 14.24 s and 14.89 s, respectively. The typical pre-defined time delay for zone 2 LOE is 0.65 s (the breaker operating time is 0.05 s), so the generator tripped from the grid at 14.94 s by operating the zone 2 of the LOE relay. The impedance locus and the trip signal instant are depicted in Figure 3.41 and Figure 3.42, respectively.

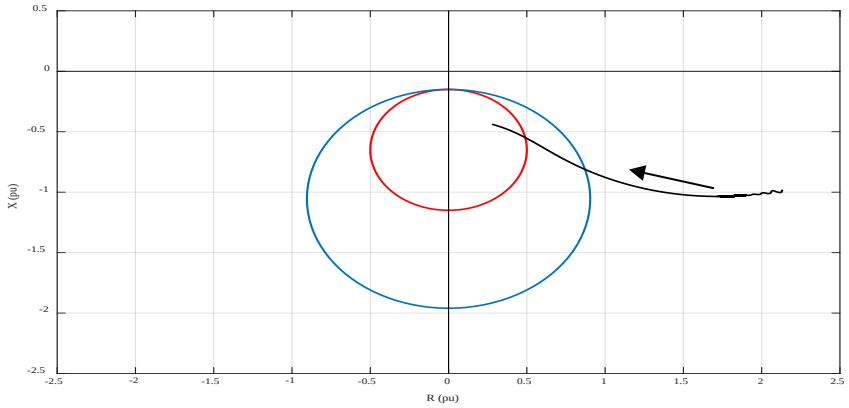

Figure 3.41 Apparent impedance locus during LOE occurrence- L_2 loading condition

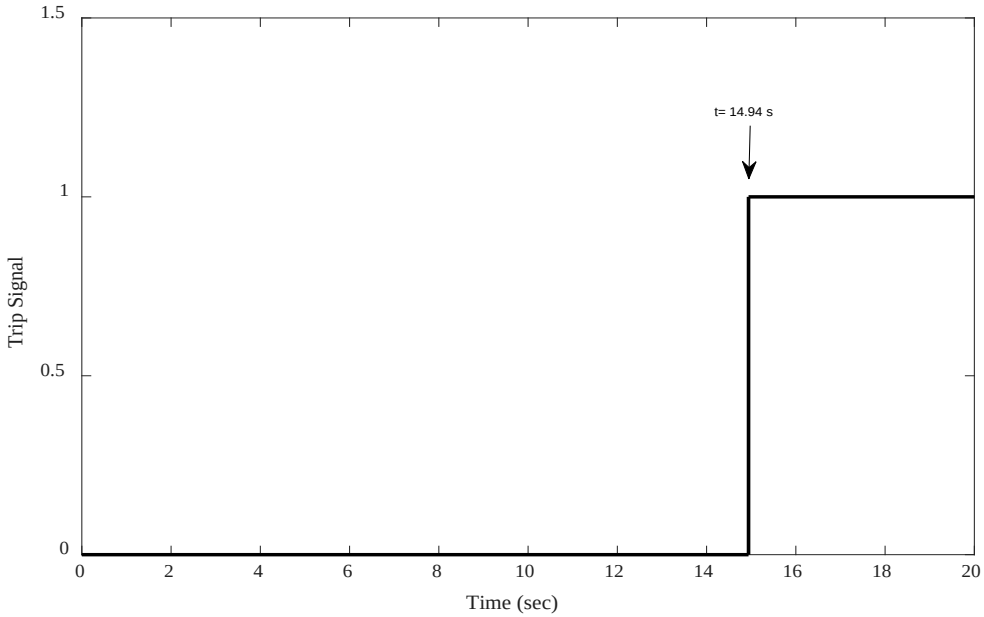

Figure 3.42 LOE Trip signal issued at 14.94 s

b. Power swing condition

A 3-phase fault applied on the lower tieline in single machine infinite bus system and cleared after 0.1 s by opening the line. The system experiences power swing. The active and reactive output powers of the generator are shown in Figure 3.43. The reactive power oscillates around the new negaticve output Var. The angle (δ) is non-monotonic during the power swing and the rate of change of angle $d\delta$ changes between positive and negative values. The trajectory of the power angle variations is illustrated in the $d\delta$-δ plane in Figure 3.44. The angle locus starts from origin

and rotates in the negative and positive side of this plane to reach to the new operating point for stable power swing. The polarity of the $d\delta$ changes in every half cycle.

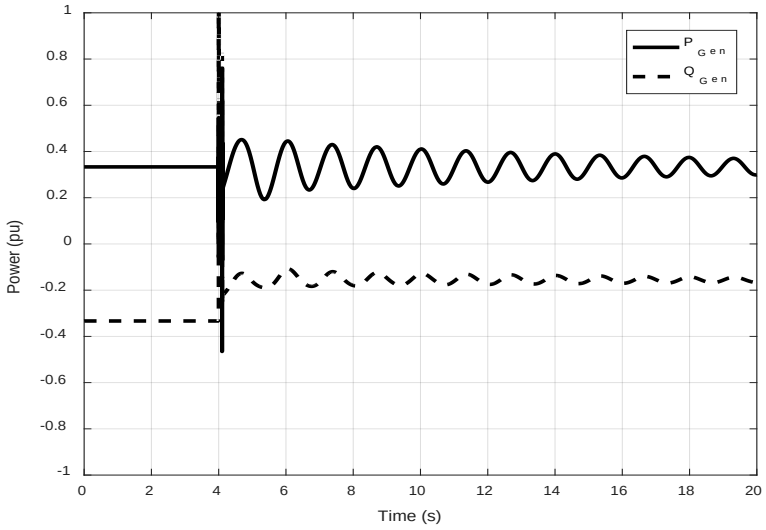

Figure 3.43 Active and reactive powers of synchronous generator during power swing- L_2 loading condition

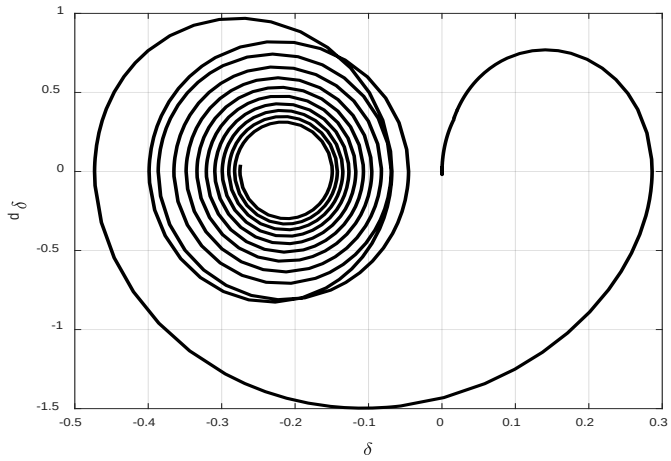

Figure 3.44 Variation of generator angle during power swing- L_2 loading condition

Besides, the slip frequency for this loading condition is more than 0.7 Hz and the proposed algorithm detects this condition as the power swing and blocks the relay correctly. The stable power swing is shown in Figure 3.45.

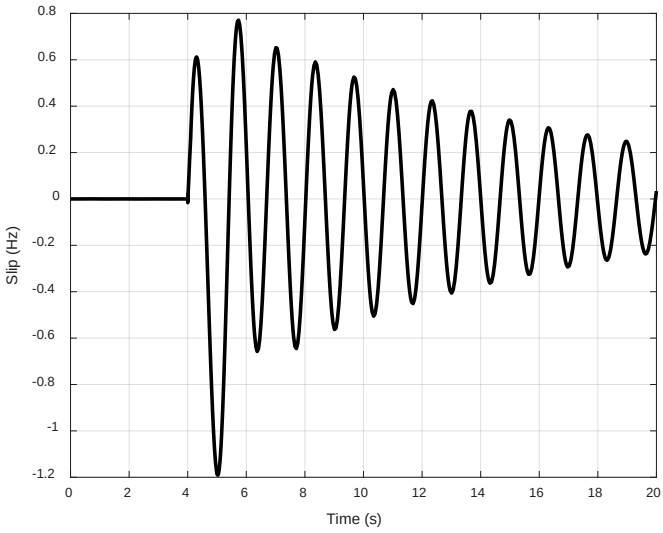

Figure 3.45 Slip frequency variation during stable power swing- L_2 loading condition

The investigated case studies with different generator initial loading conditions confirmed the accuracy of the proposed LOE strategy.

4. Conclusions

In this project, the dynamic simulation and protection model were linked in CAPE-PSS/E co-simulation platform in which all the protection devices (relays, breakers, VTs, and CTs) were modelled precisely. Mis-operation conditions of impedance elements of distance relay and loss of excitation (LOE) relay were investigated in the co-simulation platform. The simulation results demonstrated that under certain conditions these relays with the typical time delay and blocking settings may mis-operate.

The response of the distance relays in the WECC system model after the critical outages was examined. It can be concluded that failure in detecting mis-operating relays may result in a system-wide collapse.

Moreover, to prevent the LOE relay mis-operation during power swing a novel method was proposed. The rate of change of rotor angle and the machine slip frequency magnitude were utilized to distinguish the LOE from power swing. Conventional LOE relays can be enhanced by adding a logic block which is designed based on the proposed method to differentiate power swing from LOE condition. As a result of using the proposed method, LOE relays become more secure as mis-operation of the relays are prevented during power swing conditions.

The performance of the proposed method were evaluated using numerous test cases with different generator loading levels and the power factors active power some of which are reported in the case study results section.

The test system was simulated in CAPE-PSS/E co-simulation platform and the obtained results demonstrated that the proposed method can detect power swing conditions in half a cycle and block the relay from mis-operations.

Appendix:

The parameters of the test system used for co-simulation (Figure 2.4) are as follows:

Generator 1:

600MVA, 22 kV, 60 Hz, Inertia constant 4.4 MW/MVA

Xd= 1.8 pu, X'd=0.3 pu, X"d=0.23 p.u., T'd0= 8 s, T"d0=0.03 s, Ra= 0.003 p.u.

Transformer:

600 MVA, 22/400 kV Δ/Y, X=0.163 pu.

The transmission lines parameters are reported in Table. A. 1.

Table A.1 Transmission lines resistance and reactance

From bus	To bus	R (pu)	X (pu)
2	3	0.008	0.165
3	4	0.008	0.165
2	4	0.0165	0.325

The exciter is modelled by IEEE ESST1A type in PSS/E.

Table A.2 Parameter of exciter model

Parameter	Value	Parameter	Value
T_R (sec)	0.1	$V_{A\,MAX}$	4.6
$V_{I\,MAX}$	5	$V_{A\,MIN}$	-4.6
$V_{I\,MIN}$	-5	$V_{R\,MAX}$	3.4
T_C (sec)	0.01	$V_{R\,MIN}$	-3.4
T_B (sec)	240	K_C	0.01
T_{C1} (sec)	0.01	K_F	0.1
T_{B1} (sec)	0.1	T_F (sec)	0.1
K_A	1	KLR	1
T_A (sec)	0.01	ILR	2

CTs and VT with the CTR and VTR 120 and 1000 are located at the relays' locations, respectively. According to the CT and CT ratios, and impedance of the lines, the zone 1 and zone 2 of the line distance relays are defined as follows:

$$X_{Secondary} = \frac{kV^2 \times X_{primary}}{MVA} \times \frac{CTR}{VTR} \tag{4.1}$$

The typical time delays are used for the distance relays time settings. The LOE relay time delay is set 0.1 s for zone 1 and 0.75s for zone 2. Breaker operating time is 50 ms (3 cycles).

References:

[1] U.S.-Canada Power System Outage Task Force, "Final report on the August 14, 2003 blackout in the United States and Canada: Causes and Recommendations", April 5, 2004. [Online]. Available: http://www.nerc.com.

[2] J. J. Bian A. D. Slone, P. J. Tatro "Misoperations Report:Protection System Misoperations Analysis" *NERC Planning Committee*, April, 2013.

[3] "Standard PRC-004-3 — Protection System Misoperation Identification and Correction".

[4] D. Tziouvaras, "Relay Performance during Major System Disturbances".

[5] M. A., Khorsand, and V. Vittal, "Modeling Protection Systems in Time-Domain Simulations: A New Method to Detect Mis-operating Relays for Unstable Power Swings," submitted to *IEEE Trans. power sys.*, 2016.

[6] "Protection system response to power swings" *Syst. Protec. and Cont. Subcom., NERC*, Aug. 2013.

[7] M. Kezunovic, C. Pang, J. Ren, and Y. Guan, "New Solutions for Improved Transmission Line Protective Relay Performance Analysis,".

[8] S. A. Soman, T. B. Nguyen, M. A. Pai and R. Vaidyanathan, "Analysis of angle stability problems: a transmission protection systems perspective," *IEEE Trans. on Power Del.*, vol. 19, no. 3, pp. 1024-1033, July 2004.

[9] N. Zhang, H. Song and M. Kezunovic, "Transient based relay testing: a new scope and methodology," *IEEE Mediterranean Electrotechnical Conf. (MELECON)*, Malaga, pp. 1110-1113, 2006.

[10] S. A. Soman, T. B. Nguyen, M. A. Pai and R. Vaidyanathan, "Analysis of angle stability problems: a transmission protection systems perspective," *IEEE Trans. on Power Del.*, vol. 19, no. 3, pp. 1024-1033, July 2004.

[11] Q. Verzosa, "Realistic Testing of Power Swing Blocking and Out-of-Step Tripping Functions,".

[12] N. Fischer, G. Benmouyal, D. Hou, D. Tziouvaras, J. B. Finley, and B. Smyth, "Tutorial on Power Swing Blocking and Out-of-Step Tripping," 39th *Annual Western Protective Relay Conference*, Spokane, WA, Oct., 2012.

[13] U. N. Khan, and L. Yan, "Power Swing Phenomena and its Detection and Prevention," *7th EEEIC Int. Workshop on Environ. and Elec. Eng*., Cottbus, May 2008.

[14] "Generating Out-of-Step Blocking and Tripping Settings in the Computer-Aided Protection Engineering System (CAPE)," CAPE Users' Group, June, 2005.

[15] Yao Siwang, Wang Weijian, Luo Ling, Gui Lin , Qiu Arui, "Discussion on Setting Calculation of Loss-Of-Excitation Protection for Large Turbogenerator," *Int. Conf. on Elect. Mach. and Syst. (ICEMS)*, pp. 1413–1416, 2010.

[16] C. R. Mason, "New loss of excitation relay for synchronous generators," *AIEE Trans.*, vol. 68, no. 2, pp. 1240–1245, 1949.

[17] J. Berdy, "Loss of excitation protection for modern synchronous generators," *IEEE Trans. Power Appar. Syst.*, PAS-94, (5), pp. 1457–1463, 1975.

[18] C. J. Mozina, M. Reichard, "Coordination Of Generator Protection With Generator Excitation Control and Generator Capability," *IEEE Gen. Meeting* , 2007.

[19] E. Pajuelo, R. Gokaraju, M. S. Sachdev, "Identification of generator loss-of-excitation from power-swing conditions using a fast pattern classification method," *IET Generation, Transmission & Distribution*, Vol. 7, Iss. 1, pp. 24–36, 2013.
[20] IEEE Power System Relaying Committee working group, "Performance of Generator Protection During Major System Disturbances," *IEEE Trans. Power Delivery*, vol. 19, no. 4, pp. 1650–1662, October 2004.
[21] "PSS®E 33.5 Program operation manual" Siemens Oct. 2013.
[22] "CAPE Series CAPE-TS LinkTM Module User's Guide," Electrocon International, Inc, March 2015.
[23] S. M. Brahma, "Distance Relay With Out-of-Step Blocking Function Using Wavelet Transform," *IEEE Trans. Power Delivery*, vol. 22, no. 3, July 2007.
[24] T. E. Baker, " Electrical Calculations and Guidelines for Generating Station and Industrial Plants," Taylor and Francis Group, 2012.
[24] California ISO, "Transmission Plan" 2010-1011.
[26] G. Xu, V. Vittal, A. Meklin, and J. E. Thalman, "Controlled islanding demonstrations on the WECC system," *IEEE Trans. Power Syst.*, vol. 26, no. 1, pp. 334-343, Feb. 2011.
[27] Major WECC remedial action schemes (RAS), WECC, Available: https://www.wecc.biz/Reliability/TableMajorRAS4-28-08.pdf.
[28] "Power swing and out-of-step considerations on transmission lines," *report Power System Relaying Committee (PSRC)- IEEE PES*, July, 2005.
[29] Y. Siwang, W. Weijian, L. Ling, G. Lin and Q. Ami, "Discussion on setting calculation of loss-of-excitation protection for large turbo generator," *Int. Conf. Elect. Mach. and Sys.*, pp. 1413-1416, Incheon, 2010.
[30] A. P. de Morais, G. Cardoso and L. Mariotto, "An Innovative Loss-of-Excitation Protection Based on the Fuzzy Inference Mechanism," *IEEE Trans. on Power Del*, vol. 25, no. 4, pp. 2197-2204, Oct. 2010.
[31] M. Amini, M. Davarpanah and M. Sanaye-Pasand, "A Novel Approach to Detect the Synchronous Generator Loss of Excitation," *IEEE Trans Power Del.*, vol. 30, no. 3, pp. 1429-1438, June 2015.
[32] B. Mahamedi, J. G. Zhu and S. M. Hashemi, "A Setting-Free Approach to Detecting Loss of Excitation in Synchronous Generators," *IEEE Trans. on Power Del.*, vol. 31, no. 5, pp. 2270-2278, Oct. 2016.
[33] A. Hasani; F. Haghjoo, "A Secure and Setting-Free Technique to Detect Loss of Field in Synchronous Generators," *IEEE Trans. Energy Conv.*, vol.PP, no.99, pp.1-1, 2017.
[34] *IEEE Guide for AC Generator Protection*, *IEEE* Standard C37.102- 2006, Nov. 2006.
[35] D. Reimert, "Protective Relaying for Power Generation Systems," 3rd edition, Taylor & Francis, 2006.
[36] G. Benmouyal, D. Hou, and D. Tziouvaras, "Zero-setting power-swing blocking protection,"[Online].Available: http://www.selinc.com/ techpprs/6172_ZeroSetting_ 20050302.pdf